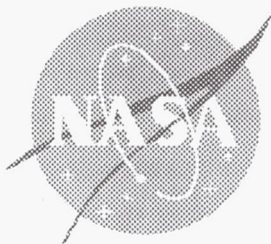NASA Contractor Report 191194

Fiber Optic Control System Integration for Advanced Aircraft

Electro-Optic and Sensor Fabrication, Integration, and Environmental Testing for Flight Control Systems

Daniel W. Seal, Thomas L. Weaver, Bradley L. Kessler,
Carlos A. Bedoya, and Robert E. Mattes
McDonnell Douglas Aerospace
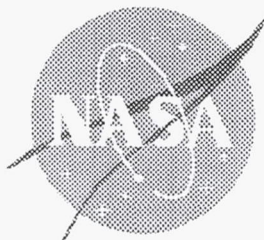*St. Louis, Missouri*

November 1994

Fiber Optic Control System Integration for Advanced Aircraft

Electro-Optic and Sensor Fabrication, Integration, and Environmental Testing for Flight Control Systems

Daniel W. Seal, Thomas L. Weaver, Bradley L. Kessler,
Carlos A. Bedoya, and Robert E. Mattes
McDonnell Douglas Aerospace
St. Louis, Missouri

November 1994

REPORT DOCUMENTATION PAGE

1. AGENCY USE ONLY (Leave blank)	2. REPORT DATE	3. REPORT TYPE AND DATES COVERED
	November 1994	Final Contractor Report

4. TITLE AND SUBTITLE

Fiber Optic Control System Integration for Advanced Aircraft

5. FUNDING NUMBERS

WU–505–62–50
C–NAS3–25796

6. AUTHOR(S)

Daniel W. Seal, Thomas L. Weaver, Bradley L. Kessler, Carlos A. Bedoya, and Robert E. Mattes

7. PERFORMING ORGANIZATION NAME(S) AND ADDRESS(ES)

McDonnell Douglas
P.O. Box 516
Saint Louis, MO 63166–0516

8. PERFORMING ORGANIZATION REPORT NUMBER

E–8151

9. SPONSORING/MONITORING AGENCY NAME(S) AND ADDRESS(ES)

National Aeronautics and Space Administration
Lewis Research Center
Cleveland, Ohio 44135–3191

10. SPONSORING/MONITORING AGENCY REPORT NUMBER

NASA CR–191194

11. SUPPLEMENTARY NOTES

12a. DISTRIBUTION/AVAILABILITY STATEMENT

Unclassified - Unlimited
Subject Category 35

This publication is available from the NASA Center for Aerospace Information, (301) 621–0390.

12b. DISTRIBUTION CODE

13. ABSTRACT (Maximum 200 words)

This report describes the design, development and test of passive optical sensors and a multiplexing architecture for installation and test on the NASA F-18 systems research aircraft. A variety of sensor types (rotary position, linear position, temperature, and pressure) incorporating a broad range of sensor technologies (WDM analog, WDM digital, analog microbend, and fluorescent time rate of decay) were obtained, integrated with the multiplexing architecture, and laboratory tested prior to installation in the F-18 for flight test.

14. SUBJECT TERMS

Fiber optics; Optical sensors; Optical multiplexing; Fly-by-light; Flight control

15. NUMBER OF PAGES

125

16. PRICE CODE

A06

17. SECURITY CLASSIFICATION OF REPORT	18. SECURITY CLASSIFICATION OF THIS PAGE	19. SECURITY CLASSIFICATION OF ABSTRACT	20. LIMITATION OF ABSTRACT
Unclassified	Unclassified	Unclassified	

Table of Contents

Table of Contents

Table of Contents

List of Pages

ii through viii
1 through 117

List of Illustrations

List of Illustrations

List of Tables

List of Abbreviations and Acronyms

ACA	Associate Contractor Agreement
ATR	Air Transport Ratio
B&W	Babcock & Wilcox
CCD	Charge Coupled Device
DAC	Data Acquisition Card
EMI	Electromagnetic Interference
EMP	Electromagnetic Pulse
EOA	Electro-Optic Architecture
FIFO	First In First Out
FOCSI	Fiber Optic Control System Integration
FWHM	Full Width Half Maximum
GE	General Electric
GRIN	GRaded INdex
I/O	Input/Output
ICD	Interface Control Document
KHz	Kilohertz
LED	Light Emitting Diode
LEF	Leading Edge Flap
LVDT	Linear Variable Differential Transducer
MDA	McDonnell Douglas Aerospace
MDC	McDonnell Douglas Corporation
MTBF	Mean Time Between Failure
N.A.	Numerical Aperture
NASA	National Aeronautics and Space Administration
NAWC	Naval Air Warfare Center
NWS	Nose Wheel Steering
OTDR	Optical Time Domain Reflectometer
PBL	Power-By-Light
PLC	Power Lever Control
PWB	Printed Wiring Board
RFI	Request For Information
RFP	Request For Procurement
RVDT	Rotary Variable Differential Transducer
SEM-E	Standard Electronic Module, size "E" format
SHARP	Standard Hardware Acquisition and Reliability Program
SRA	Systems Research Aircraft
SRAM	Static Random Access Memory
TDM	Time Division Multiplex
TEF	Trailing Edge Flap
TI	Texas Instruments
TRD	Time Rate of Decay
VMS	Vehicle Management System
WDM	Wavelength Division Multiplex

Summary

This report describes the design, development, and testing of passive fiber optic sensors and a multiplexing Electro-Optic Architecture (EOA) for installation and flight test on a NASA-owned F-18 aircraft. This hardware was developed under the Fiber Optic Control Systems for Advanced Aircraft program, part of a multi-year NASA initiative to design, develop, and demonstrate (through flight test) "Fly-by-light" systems for application to advanced aircraft flight and propulsion control. This development included the design and production of 10 passive optical sensors and associated multiplexed EOA hardware based on Wavelength Division Multiplexed (WDM) technology. A variety of sensor types (rotary position, linear position, temperature, and pressure) incorporating a broad range of sensor technologies WDM analog, WDM digital, Analog Microbend, and Fluorescent time rate of decay) were obtained from different manufacturers and functionally integrated with an independently designed EOA. The sensors were built for installation in a variety of aircraft locations, placing the sensors in a variety of harsh environments. The sensors and EOA were designed and built to have the resulting devices be as close as practical to a production system. The integrated system was delivered to NASA for flight testing on a NASA-owned F-18 aircraft. Development and integration testing of the system provided valuable information as to which sensor types were simplest to design and build for a military aircraft environment and which types were simplest to operate with a multiplexed EOA. Not all sensor types met the full range of performance and environmental requirements. EOA development problems provided information on directions to pursue in future Fly-by-light flight control development programs. Lessons learned in the development of the EOA and sensor hardware are summarized below:

Electro-Optic Architecture Lessons Learned:

- Need a Flexible EOA Interface Specification, But a Rigid Optical Sensor Interface Specification
- Use a Linear Charge Coupled Device (CCD) Detector Array to Optimize EOA Receiver Speed, Sensitivity, and Decoding Accuracy
- An Optical Spectrum Analyzer with a Digital Signal Processor (DSP) is the Most Efficient and Versatile EOA Approach
- Maximize the Use of "Off-The-Shelf" Hardware

Fiber Optic Sensor Lessons Learned:

- Rotary Optical Sensors are Easier to Build and Use Than Linear Sensors.
- Digital Optical Sensors are Easier to Manufacture Repeatably and Decode Than Analog Sensors
- Repackaging Commercial Sensors for a Military Aircraft Environment is Non-Trivial

1. Introduction

This report describes the design, development, and testing of passive fiber optic sensors and a multiplexing Electro-Optic Architecture (EOA) for installation and flight test on a NASA-owned F-18 flight test aircraft. The Fiber Optic Control Systems for Advanced Aircraft program is part of a multi-year NASA initiative to design, develop, and demonstrate (through flight test) "Fly-by-light" systems for application to advanced aircraft flight and propulsion control. This initiative is commonly referred to as Fiber Optic Control Systems Integration (FOCSI). MDA was awarded a contract for the development of fiber optic sensors and associated multiplexed Electro-Optic Architecture (EOA) hardware for aircraft flight control application. General Electric (GE) was awarded a similar contract for the development of an EOA and sensors for engine control applications.

1.1 Background

Over the last 20 years, flight control technology has evolved from the original concept of mechanical control linkages with autopilot aiding to that of multi-disciplinary control integration technology. Control integration technology now encompasses several functional elements including flight control, propulsion control, weapons delivery, and displays. The concept of integrated control is to automate the coordination of these functional control elements to allow optimal coupling of the subsystems thereby reducing pilot workload, increasing aircraft performance, and enhancing overall mission effectiveness. Recent avionic architecture studies defined the fundamental concept of a Vehicle Management System (VMS) architecture as a means of achieving the required level of control integration for advanced aircraft.

Integration of interrelated functions such as flight and propulsion control would unlock significant performance, reliability, maintainability, and supportability benefits for emerging digitally controlled systems. Digital Fly-By-Wire technology combines sensors, effectors, and communications to provide a level of integration and performance not possible with mechanical flight control systems. Advanced digital Fly-By-Wire flight control systems can dramatically increase the operational flight envelope through faster control system response and increased number of active control surfaces. This increase in active control surfaces brings about a corresponding increase in sensor resources and the need for innovative management of these resources. Reliability of these systems becomes increasingly important as mechanical linkages are removed and buses, networks, and protocols are relied upon to provide the physical integration of functional elements.

Requirements for increased levels of control integration coupled with the increased use of composite materials in advanced airframes will impose stringent electromagnetic susceptibility requirements on Fly-By-Wire systems as shown in Figure 1-1. Meeting these stringent requirements may mandate the use of Fly-By-Light avionic systems. Fiber optic technology offers numerous well known benefits including: high bandwidth, low weight, and immunity to man made threats such as Electromagnetic Interference (EMI), and Electromagnetic Pulse (EMP) generated by nuclear blasts. Commercial fiber optic research activities have led to the development of flight qualified fiber optic data networks but have not yet produced optical sensors acceptable for advanced aircraft.
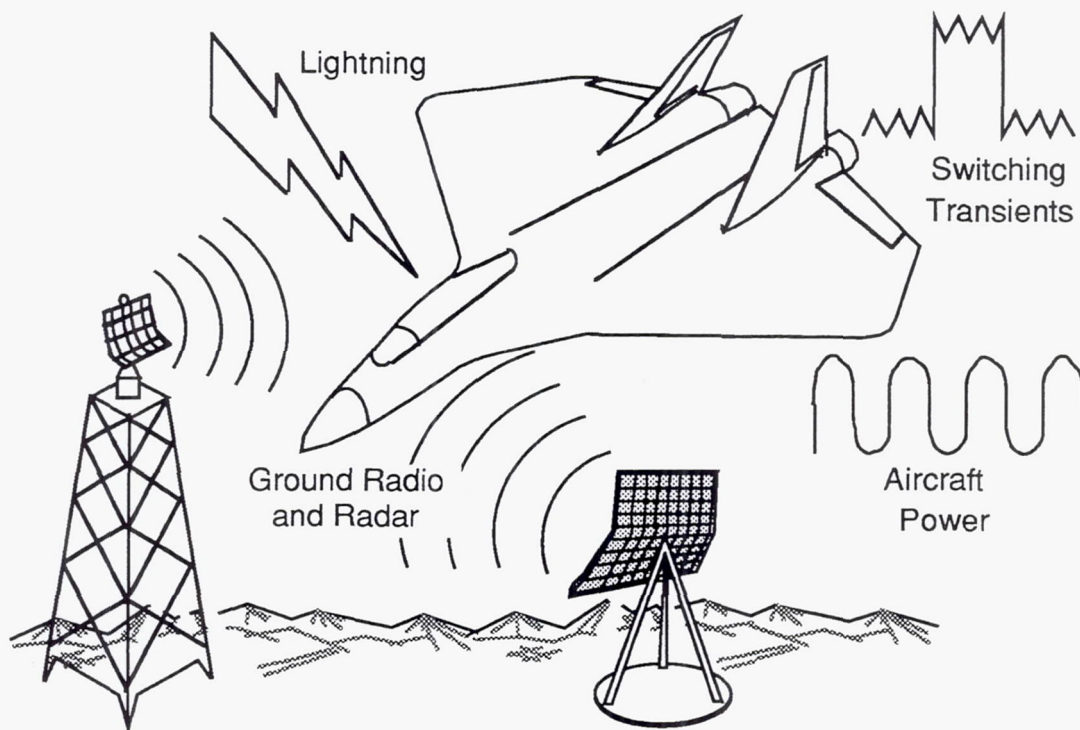
Figure 1-1. Aircraft External Environment

Fly-by-light is appealing in concept; but, the concept must be developed and demonstrated. The 1960s and 1970s were the period of intense development of the electric technologies that eventually led to Fly-By-Wire systems. Electrical cables were tested to learn which worked in aircraft, and which did not. Sensor concepts were built and tested, and eventually mated to hydraulic actuators. The result of that effort was an eventual standardization of cables, sensors, sensor excitation, controllers, and actuators, around which a major industry developed.

The goal of the Fly-by-light program is to duplicate that process for optic and fiber optic control systems, with one major difference. By having a planned, directed program, it is hoped that progress toward optical standards will be rapid and inexpensive. The reason the difference is necessary is that aircraft of the 1990s are larger, more expensive, and there are fewer types of them than there were half a century ago. Thus there are fewer opportunities for the "I have an idea, Let's build it and try it" approaches which were fruitful in the past. Figure 1-2 shows a representative fly-by light aircraft control system with major components identified.
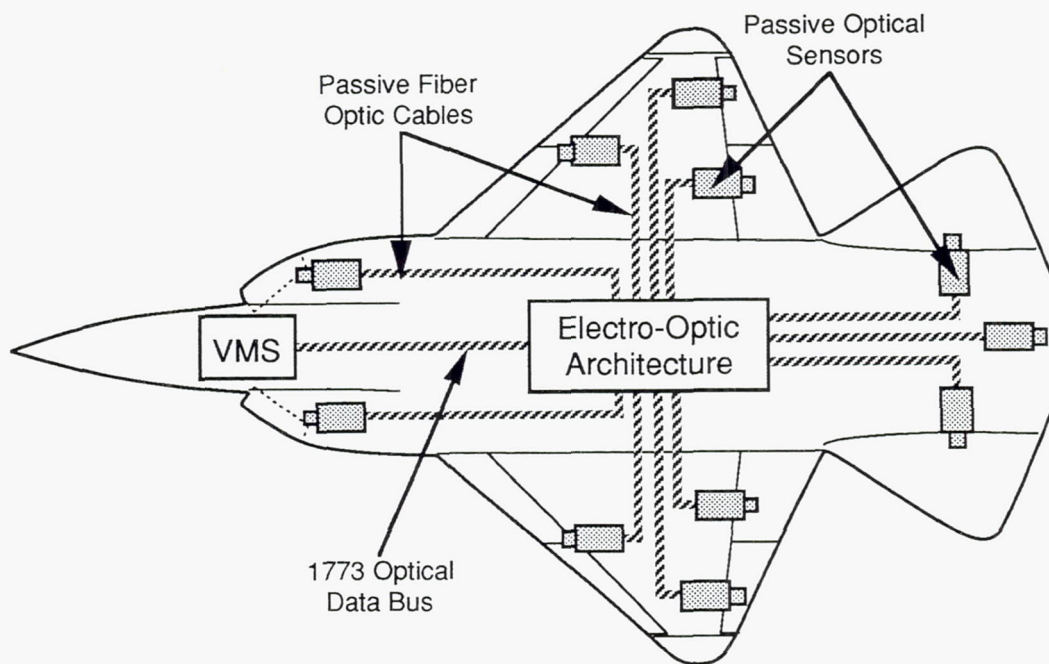
Figure 1-2. Fly-By-Light Flight Control System Block Diagram

DOD and NASA have recently sponsored several programs to promote research and development in the area of aircraft optical sensor technologies. Since 1985, representatives of all these groups have been working together on a program under the heading of Fly-by-light for the application of optic technologies to the flight control aspects of aircraft.

The Fly-by-light program began as a tri-service (NASA, Navy, and Air Force) initiative to design, develop, and demonstrate a totally integrated fiber optic flight/propulsion control system for advanced aircraft. The program has had several phases over the years since its inception in 1985, each building on the results of the previous phases. Figure 1-3 shows the major Fly-by-light program phases. Each of these program is described briefly in the following paragraphs.
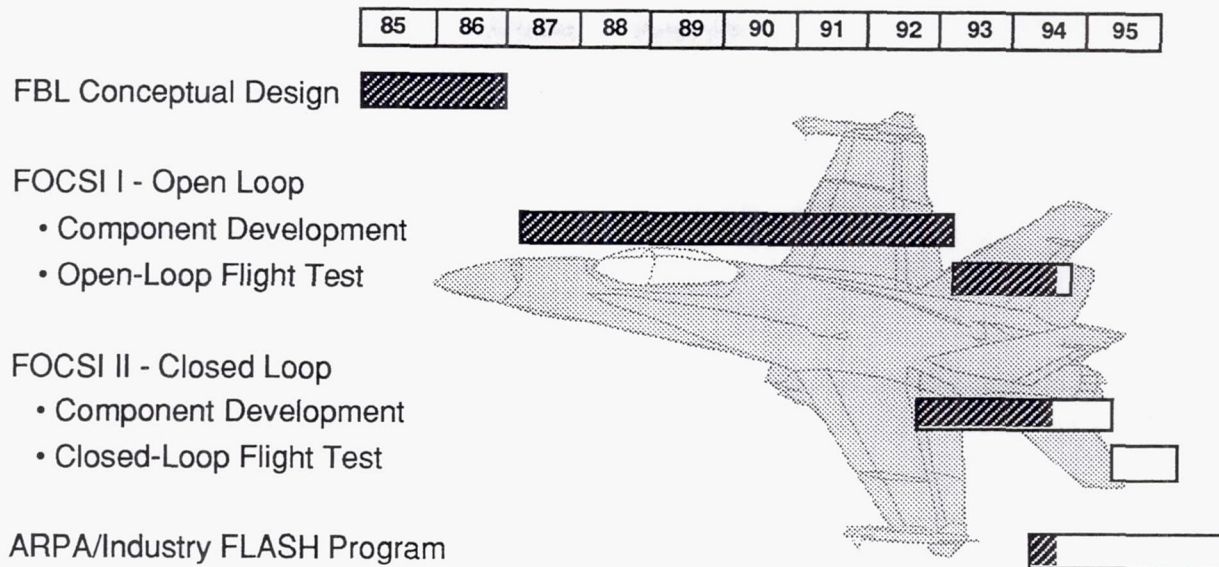
Figure 1-3. Fly-By-Light Development Schedule

The first phase, Fly-by-light Conceptual Design, defined Fly-By-Light system concepts, completed technology trade studies, and prepared hardware development plans for use in later phases. This phase concentrated primarily on the definition of Fly-By-Light systems for propulsion control and was awarded to General Electric and Pratt & Whitney. MDA was involved as a subcontractor to support Pratt & Whitney with airframe information.

The second phase, FOCSI I - Open Loop, focused on the design, development, and test of optical sensors and EOAs for application to Fly-By-Light control systems. Evaluation of optical sensor technologies and associated multiplexing EOA designs for flight control systems was performed under a previous NASA contract NAS3-25345 - "Optimizing Electro-Optic Architectures for Advanced Aircraft Flight Control". Similar contracts were awarded to General Electric and Pratt and Whitney for evaluation of Fly-By-Light concepts for propulsion control systems. NASA subsequently awarded two follow-on contracts for the development and test of Fly-By-Light hardware for aircraft flight and propulsion control systems. MDA was awarded a contract for the development of fiber optic sensors and associated multiplexed Electro-Optic Architecture (EOA) hardware for aircraft flight control application. General Electric (GE) was awarded a similar contract for the development of an EOA and sensors for engine control applications. Development of the FOCSI I - Open Loop hardware for flight control is described in this final report. Flight test of the hardware developed under the FOCSI I - Open Loop program is currently underway at on the NASA Systems Research Facility (F-18 #845) at the NASA-Dryden Flight Research Facility located in Edwards, California.

The third phase, FOCSI II - Closed Loop (referred to as the Fly-by-light Aircraft Closed-loop Test (FACT) program) will develop an optical control system for closed-loop flight control of the aircraft. The program will build on optical sensor and EOA developments in the previous FOCSI I (Open Loop) program. The primary focus of the FACT program is the development of redundant optical sensors for installation internal to hydraulic actuators. FACT will also develop a multiplexed EOA module with faster speed, higher accuracy, and smaller size than in previous phases.

Future Fly-By-Light development efforts include the Fly-by-Light Advanced Systems Hardware (FLASH) program (sponsored by the Advanced Research Products Agency), and the Fly-By-Light/Power-By-Wire program (sponsored by NASA). These programs will demonstrate key Fly-By-Light technologies and system concepts to minimize the risk for transition of these technologies to future commercial and military aircraft.

1.2 Scope

The scope of the FOCSI flight control development program was to develop and evaluate optical sensors and multiplexed EOAs for advanced aircraft integrated flight control systems. The sensors and EOA were designed for open-loop testing on test benches and eventually on an aircraft. Open-loop in this case meant the optical sensors were to be paired with standard electrical sensors and operated by the EOA; however, the optical outputs were only recorded for comparison with the outputs from the standard sensors. The aircraft did not use the outputs of the optical sensors for its flight control.

As illustrated in Figure 1-4, a total of 10 passive optical sensors were developed for an optically implemented version of the feedback side of an F-18 aircraft flight control system. This development included the design and production of passive optical sensors, optic cables, and the necessary optoelectronics to excite the sensors and interpret the returned optical signals. Sensors with different methods of operation were obtained from different manufacturers and functionally integrated with independently designed optoelectronics. The sensors were built for installation in a variety of aircraft locations, placing the sensors in a variety of harsh environments. The sensors and optoelectronics were designed and built according to a plan to have the resulting devices be as close as practical to a production system. The integrated system was delivered to NASA for flight testing on a NASA-owned F-18 aircraft.

SRA Fly-By-Light Hardware Development

- Air Data Pressure Sensor
- Electro-Optic Architecture Mechanical Chassis
- Leading Edge Flap Position Sensor
- Nose Wheel Steering Position Sensor
- Rudder Pedal Position Sensor
- Rudder Position Sensor
- Stabilator Position Sensor
- Trailing Edge Flap Position Sensor
- Pitch Stick Position Sensor
- Air Data Temperature Sensor
- Power Lever Control Position Sensor
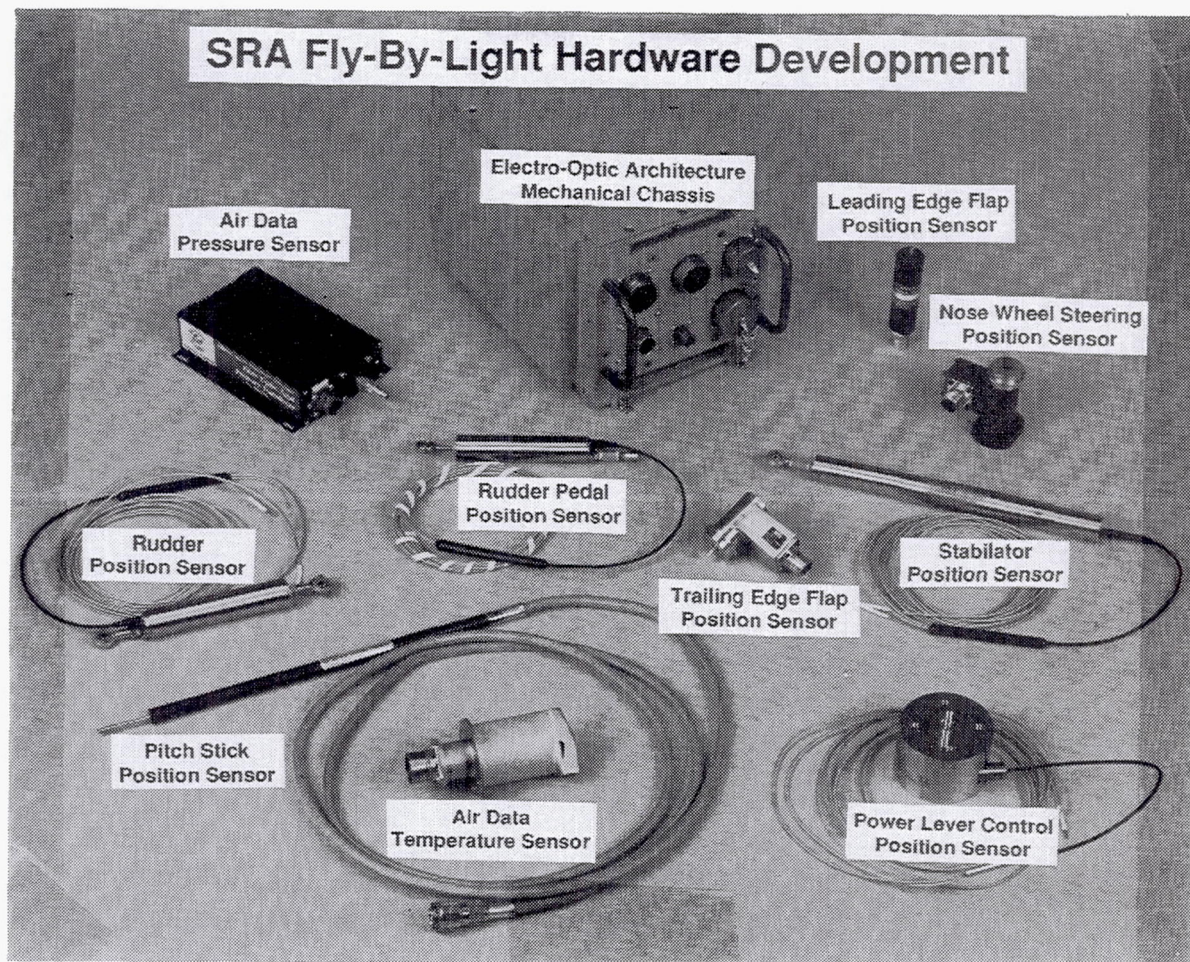
Figure 1-4. FOCSI Fly-By-Light Hardware Configuration

This final report for FOCSI flight control development contains results of FOCSI hardware development, integration, and environmental test activities funded by NASA Lewis. Preliminary results of aircraft installation and flight test activities, funded by NASA-Dryden, have also been included for technical completeness.

2. Program Description

The Fiber Optic Control Systems for Advanced Aircraft program is part of a multi-year NASA initiative to design, develop, and demonstrate (through flight test) "Fly-By-Light" systems for application to advanced aircraft flight and propulsion control. This initiative is commonly referred to as Fiber Optic Control Systems Integration (FOCSI). MDA was awarded a contract for the development of fiber optic sensors and associated multiplexed Electro-Optic Architecture (EOA) hardware for aircraft flight control application. General Electric (GE) was awarded a similar contract for the development of an EOA and sensors for engine control applications.

The overall roadmap for the FOCSI program is shown in Figure 2-1. Hardware development, integration, and environmental test activities (shown in the solid boxes in Figure 2-1) were funded through NASA Lewis Contract NAS3-25796. Aircraft installation and flight test activities (shown in the dotted box in Figure 2-1) were funded through NASA Dryden Contract NAS2-13311.
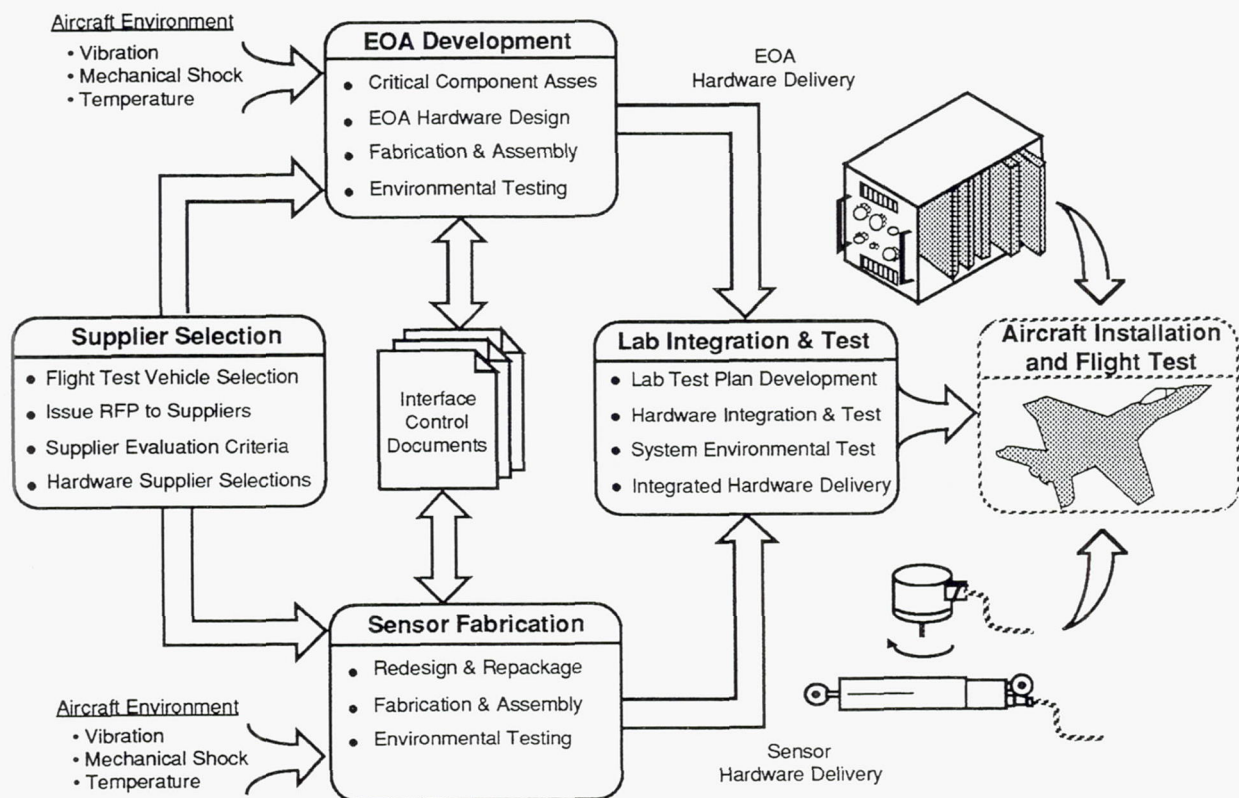
Figure 2-1. FOCSI Program Roadmap

2.1 Supplier Selection

The first step in the FOCSI program, as highlighted in Figure 2.1-1, involved the selection of qualified hardware suppliers. The supplier selection process was specifically tailored so that NASA program goals could be met within the available program budget constraints.

Aircraft Environment
- Vibration
- Mechanical Shock
- Temperature

EOA Development
- Critical Component Asses
- EOA Hardware Design
- Fabrication & Assembly
- Environmental Testing

EOA Hardware Delivery

Supplier Selection
- Flight Test Vehicle Selection
- Issue RFP to Suppliers
- Supplier Evaluation Criteria
- Hardware Supplier Selections

Interface Control Documents

Lab Integration & Test
- Lab Test Plan Development
- Hardware Integration & Test
- System Environmental Test
- Integrated Hardware Delivery

Aircraft Installation and Flight Test

Sensor Fabrication
- Redesign & Repackage
- Fabrication & Assembly
- Environmental Testing

Aircraft Environment
- Vibration
- Mechanical Shock
- Temperature

Sensor Hardware Delivery

Figure 2.1-1. FOCSI Program Roadmap - Supplier Selection

The overall goals of the FOCSI program were to develop and multiplex optical sensors into a flyable system, and to expand the industrial and government experience base with optical sensors and multiplexing. To achieve these goals, the selection of suppliers for the FOCSI program were based on the following goals:

- **Maximize the number of optical sensor technologies.**
- **Maximize the number of optical sensor suppliers.**

Meeting these often conflicting goals within available budget constraints required the development of a supplier selection process specifically tailored to these unique requirements of the FOCSI program.

Supplier selection for the FOCSI program was accomplished using the approach shown in Figure 2.1-2. Supplier selection entailed a number of tasks including: 1) flight test vehicle selection, 2) preparation and issuance of Request For Proposal (RFP) packages to potential suppliers, 3) definition of supplier proposal evaluation criteria, 4) selection of the most qualified suppliers, and 5) award of FOCSI hardware development contracts. Selection of suppliers was closely coordinated with NASA to ensure that program objectives were met.
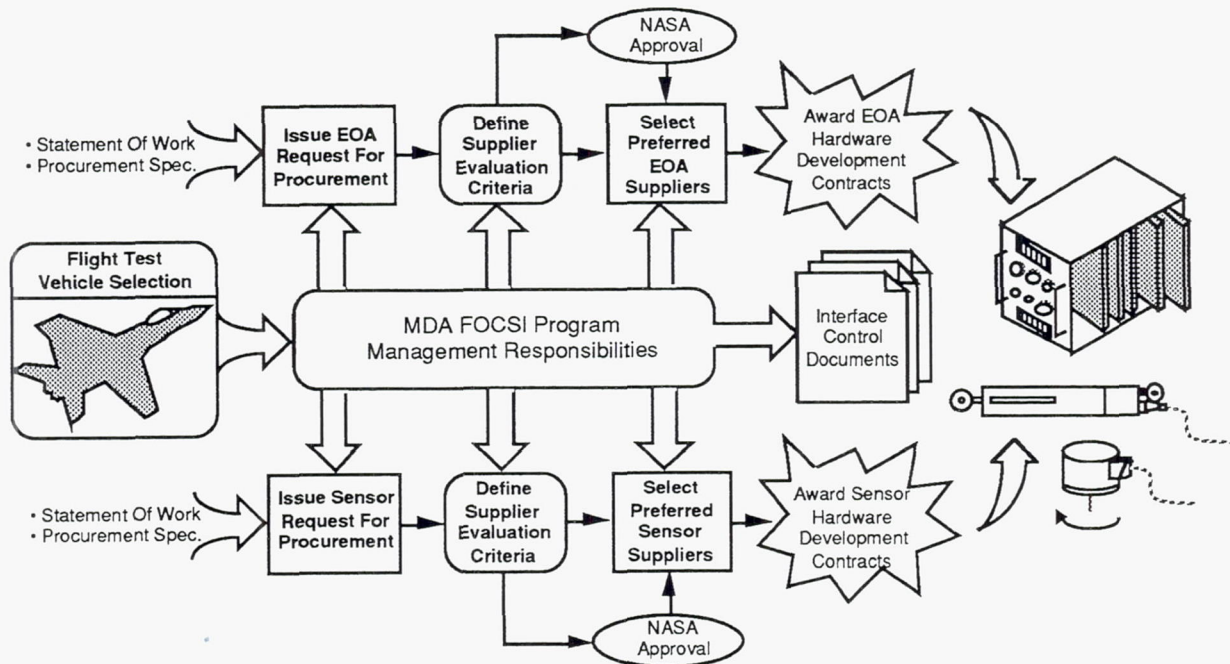
Figure 2.1-2. FOCSI Supplier Selection Process

Each of these steps in the supplier selection process is described in the following paragraphs.

2.1.1 Flight Test Vehicle Selection

As the first step in the supplier selection process, MDA worked closely with NASA Lewis and NASA Dryden to identify a suitable flight test aircraft for the FOCSI program. After evaluating a number of F-15 and F-18 aircraft in the NASA Dryden inventory, a suitable flight test aircraft was identified. The flight test vehicle selected for FOCSI was the F-18 Systems Research Aircraft (SRA). The F-18 SRA was the most logical choice for the FOCSI "Fly-By-Light" flight test because in contains an electrical "Fly-By-Wire" flight control system providing a basis for direct comparison of Fly-By-Light sensor performance with Fly-By-Wire sensor performance. The F-18 flight control system installation is shown in Figure 2.1-3.
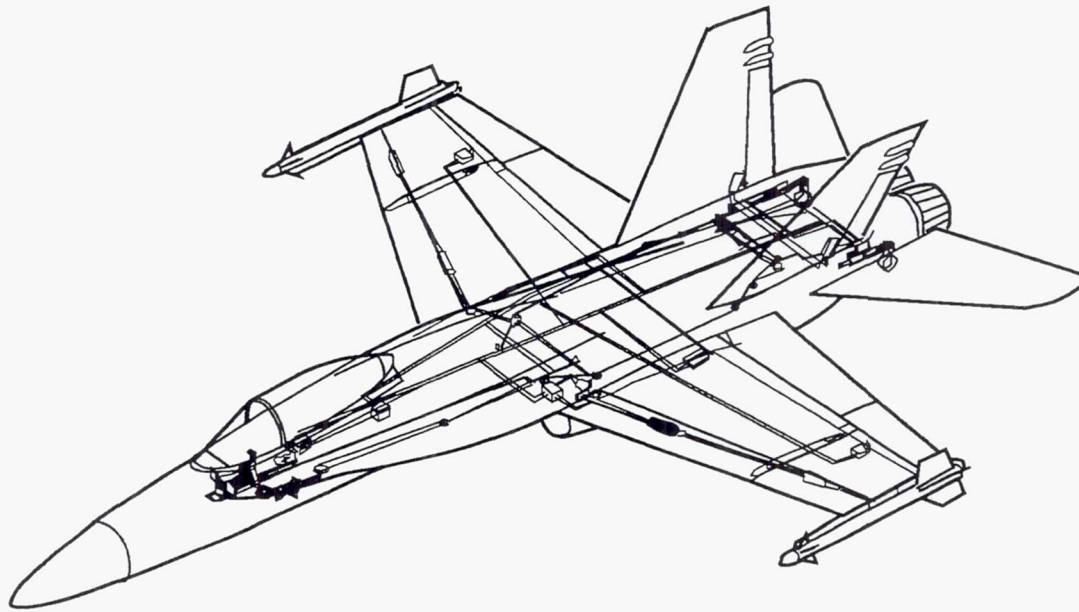
Figure 2.1-3. F-18 "Fly-By-Wire" Flight Control System

After selection of the flight test vehicle, MDA identified 14 suitable F-18 flight control and air data sensors as candidates for replacement with optical sensors. These sensors and their operating characteristics are shown in Figure 2.1-4.

SENSOR		SIGNAL			
TYPE	NAME	RANGE	RESOLUTION	LINEARITY	NULL OFFSET
Linear Position	Pitch Stick Position	+2.02 to -1.01 inches	0.00098 in	+/-0.0202 in	+/-0.0120 in
	Roll Stick Position	+/- 1.01 inches	0.00049 in	+/-0.0051 in	+/-0.0060 in
	Rudder Pedal Position	+/- 0.750 inches	0.00037 in	+/-0.0019 in	+/-0.0045 in
	Aileron	+/- 2.19 inches	0.00137 in	+/-0.0197 in	+/-0.0088 in
	Stabilator	+/- 3.56 inches	0.00174 in	+/-0.0356 in	+/-0.0178 in
	Rudder	+/- 0.665 inches	0.00032 in	+/-0.0033 in	+/-0.0033 in
	Trailing Edge Flap	+/- 4.05 inches	0.00200 in	+/-0.0405 in	+/-0.0202 in
Rotary Position	Nose Wheel Steering	+/- 75 degrees	0.0366 deg	(see Note 1)	+/-0.9380 deg
	Leading Edge Flap Asym	+/- 67.5 degrees	0.0330 deg	+/-0.675 deg	+/-0.3198 deg
	Power Lever Control	+/- 65 degrees	0.0168 deg	(see Note 2)	+/-0.4065 deg
Pressure	Total Pressure	1.25 to 80 inches Hg	0.007 in Hg	(see Note 3)	N/A
	Static Pressure	1.0 to 38 inches Hg	0.003 in Hg	(see Note 4)	N/A
	Throttle Force	+/- 44.0 lbs	0.0370 lbs.	+/-0.44 lbs	+/-0.4202 lb
Temperature	Air Data Temp	-100 to +450 deg F	0.20 deg	+/-1 deg F	N/A

Note 1:
Linearity = +/- 0.188 deg for +/- 0 to 15 deg
Linearity = +/- 0.75 deg for +/- 15 to 45 deg
Linearity = +/- 1.5 deg for +/- 45 to 75 deg

Note 2:
Linearity = +/- 0.175 deg at 0 deg
Linearity = +/- 0.80 deg for +/- 10 deg
Linearity = +/- 1.5 deg for +/- 55 to 65 deg
linear variation between specified values.

Note 3:
Resolution = 0.0009 in Hg for 1 in Hg
Resolution = 0.0005 in Hg for 5 in Hg
Resolution = 0.0005 in Hg for 20 in Hg
Resolution = 0.002 in Hg for 70 in Hg
linear variation between specified values.

Note 4: Accuracy = 20 ft or 0.2% Hp, whichever is greater

Figure 2.1-4. F-18 Aircraft Sensor Characteristics

2.1.2 Request for Proposal

After selection of the flight test vehicle and identification of candidate aircraft sensors, MDA prepared RFP packages to solicit competitive bids from potential sensor and EOA hardware suppliers. Evaluation criteria were developed for use in comparing responses to this RFP. Each RFP package included a statement of work and a procurement specification which contained pertinent information including operational characteristics, aircraft environment (temperature, vibration, etc.), and mechanical envelopes for each of the candidate sensors identified in Figure 2.1-4.

The procurement specifications for the FOCSI sensor and EOA flight test hardware were derived primarily from the trade studies conducted under a previous NASA contract NAS3-25345 - "Optimizing Electro-Optic Architectures for Advanced Aircraft Flight Control". This effort surveyed over 100 manufactures of optical sensing technologies and identified the most promising technologies for potential application to advanced aircraft Fly-By-Light control systems. Figure 2.1-5 illustrates the preferred sensor and EOA technologies identified under the previous effort. The technologies shown in Figure 2.1-5 can be generally grouped into three EOA classifications: Time Division Multiplexed (TDM) digital, TDM analog, and Wavelength Division Multiplexed (WDM). The EOA RFP included hypothetical architectures for all three technology approaches. A more detailed discussion of these technologies can be found in the final report for the "Optimizing Electro-Optic Architectures for Aircraft Flight Control" program (NASA CR-182268).

	Rotary Position	Linear Position	Angular Velocity	Tachometer/ Shaft Speed	Linear Acceleration	Temperature	Pressure	Sensor Classification	EOA Classification
TDM Digital Optical Code Plate	●	●					●	TDM Digital	TDM Digital
Beam Interrupt/Pulse Count	●	●		●					
Analog Gradient Filter Plate	●	●						TDM or WDM Analog Self-Referenced Intensity Modulated	TDM Analog
Microbend Modulated				●			●		
Reflective Diaphragm						●	●		
Photo-Elastic							●		
Absorption Edge Shift						●			WDM Optical Spectrum Analyzer
Fabry-Perot Interferometer						●	●		
WDM Digital Optical Code Plate	●	●						WDM Optical Spectrum Analyzer	
Moving Diffraction Grating							●		
Phosphorescent						●		WDM Optical Spectrum TRD	WDM Optical Spectrum Analyzer
Fluorescent						●			

▨ = Sensors in the shaded regions are not suitable for use in an Aircraft Multiplexed Flight Control System

Figure 2.1-5. Candidate Optical Sensor & EOA Technologies

The completed RFP packages were issued to the suppliers shown in Figure 2.1-6. These suppliers had been identified under the previous NASA Optimizing Electro-Optic Architectures Contract (NAS3-25345) as manufacturers of products having potential application to military aircraft.

EOA Suppliers	Sensor Suppliers		
• Allied Signal (Bendix) South Bend, IN	• Allied Signal (Bendix) South Bend, IN		• Optical Technologies, Inc. Herndon, VA
• BEI Motion Systems Carlsbad, CA	• Aster Corporation Milford, MA	• Lear Seigler Astronics Santa Monica, CA	• Rosemount, Incorporated Bridgeton, MO
• ELDEC Corporation Bothell, WA	• Aurora Optics Blue Bell, PA	• Litton Poly-Scientific Blacksburg, VA	• Simmonds Precision Prod. Vergennes, VT
• Lear Seigler Astronics Santa Monica, CA	• Babcock & Wilcox Alliance, OH	• Luxtron Corporation Mountain View, CA	• Singer Kearfott Black Mountain, NC
• Litton Poly-Scientific Blacksburg, VA	• BEI Motion Systems Carlsbad, CA	• Metricor Woodinville, WA	• Teledyne Ryan Electronics San Diego, CA
• Teledyne Ryan Electronics San Diego, CA	• ELDEC Corporation Bothell, WA	• Optelecom, Incorporated Gaithersburg, MD	• Teledyne Microelectronics Chicago, IL
• Teledyne Microelectronics Chicago, IL			

Figure 2.1-6. Potential FOCSI Suppliers

Supplier proposals in response to the FOCSI RFP packages were evaluated against the supplier selection criteria described in the following section.

2.1.3 Supplier Selection Criteria

The overall goals of the FOCSI program were to develop and multiplex optical sensors into a flyable system, and to expand the industrial and government experience base with optical sensors and multiplexing. To achieve these goals, the selection of suppliers for the FOCSI program were based on the following goals:

- **Maximize the number of optical sensor technologies.**
- **Maximize the number of optical sensor suppliers.**

Furthermore, to reduce program risk, it was decided that no new optical sensor technologies would be considered. Only those manufacturers with demonstratable prototype sensors at the time of supplier selection were considered for selection.

Finally, supplier selection was constrained by the available funds for sensor development, and the constraints of available flight control sensors on the F-18 flight test aircraft which could be used for comparison with the optical sensor system. Using the above program goals and constraints as guidelines, MDA prepared a list of supplier selection criteria which was approved by NASA and used to select suppliers for FOCSI. Candidate supplier proposals were evaluated in four separate categories: 1) specification compliance, 2) development capabilities, 3) delivery and business issues, and 4) cost. The actual supplier selection process is described in the following section.

2.1.4 Hardware Supplier Selection

2.1.4.1 EOA Supplier Selection

Candidate EOA supplier proposals were evaluated in four separate categories: 1) specification compliance, 2) development capabilities, 3) delivery and business issues, and 4) cost. Evaluation scores in each of these four areas were used to determine an overall weighted grade for each proposal. All suppliers with a weighted proposal grade above a particular limit were considered technically qualified to participate in the FOCSI program. Suppliers were selected from among those technically qualified, starting first with the supplier having the lowest overall EOA cost. Additional suppliers were ranked in ascending order of cost. After evaluating all EOA technical and cost proposals, it was determined that available funding could only support development of one EOA technology. An EOA based on WDM technology was selected based on compatibility with the majority of optical sensor types specified in the FOCSI RFP (Figure 2.1-5). Litton Poly-Scientific, was subsequently selected as the WDM EOA supplier for FOCSI; a purchase order was issued, completing the EOA supplier selection process. Figure 2.1-7 shows a functional block diagram of the WDM EOA proposed by Litton Poly-Scientific. Functional operation of the FOCSI EOA modules is described in paragraph 2.3.2.1
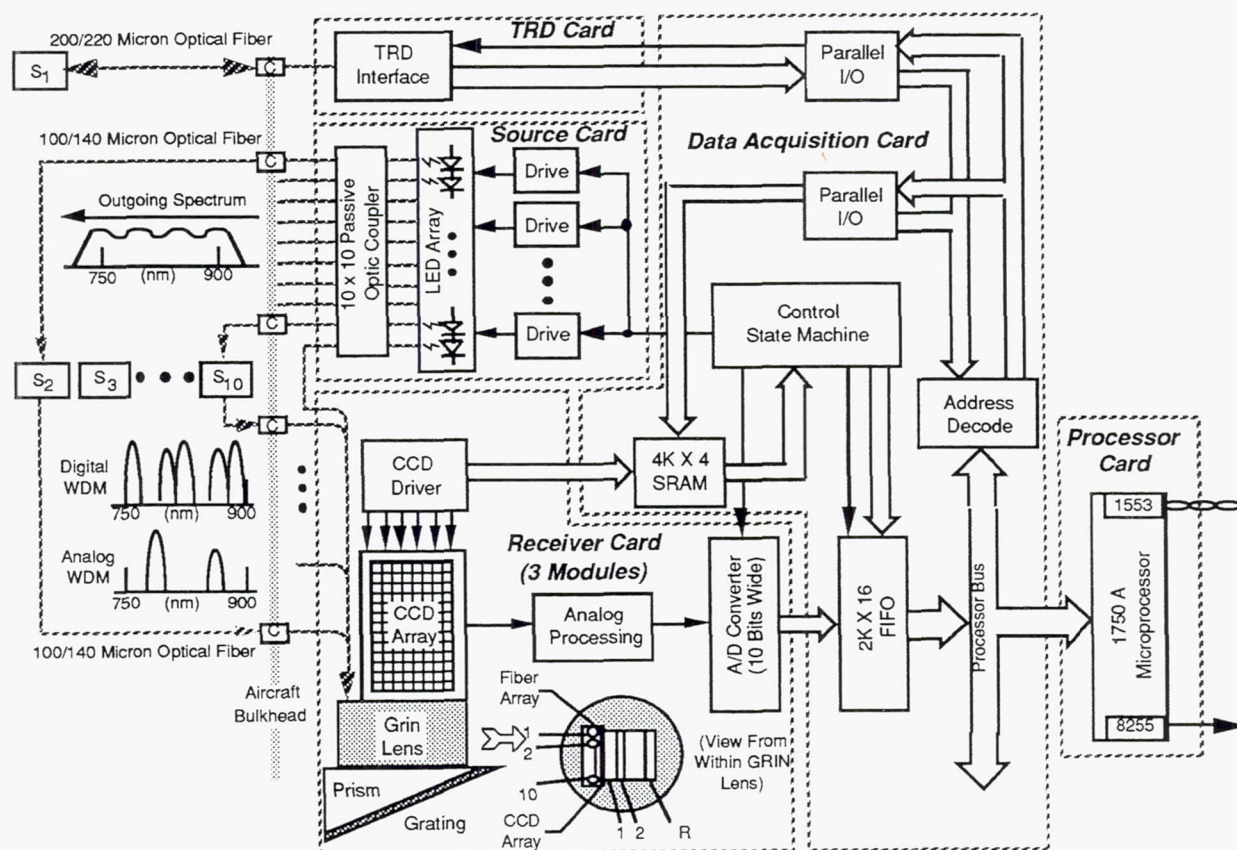
Figure 2.1-7. Litton WDM EOA Functional Block Diagram

2.1.4.2 Sensor Supplier Selection

Once the decision was made to develop an EOA based only on WDM technology, selection of sensor suppliers began. Candidate WDM sensor supplier proposals were then evaluated in four separate categories: 1) specification compliance, 2) development capabilities, 3) delivery and business issues, and 4) cost. Evaluation scores in each of these four areas were used to determine an overall weighted grade for each proposal. All suppliers with a weighted proposal grade above a particular limit were considered technically qualified to participate in the FOCSI program. In order to maximize the number of optical sensor vendors selected, and to maximize the number of individual WDM optical sensor technologies developed, all technically qualified suppliers were considered as equals during the actual supplier selection process. Available program funding allowed the selection of 10 WDM compatible sensors from a total of five different suppliers (Litton Poly-Scientific, BEI Motion Systems, AlliedSignal, Babcock & Wilcox, and Rosemount). A total of four different WDM optical sensor modulation schemes were selected. After procurement selection results were approved by NASA, purchase orders were issued to the five sensor suppliers, completing sensor supplier selection process. Figure 2.1-8 shows the EOA and 10 aircraft sensors selected for FOCSI flight test.
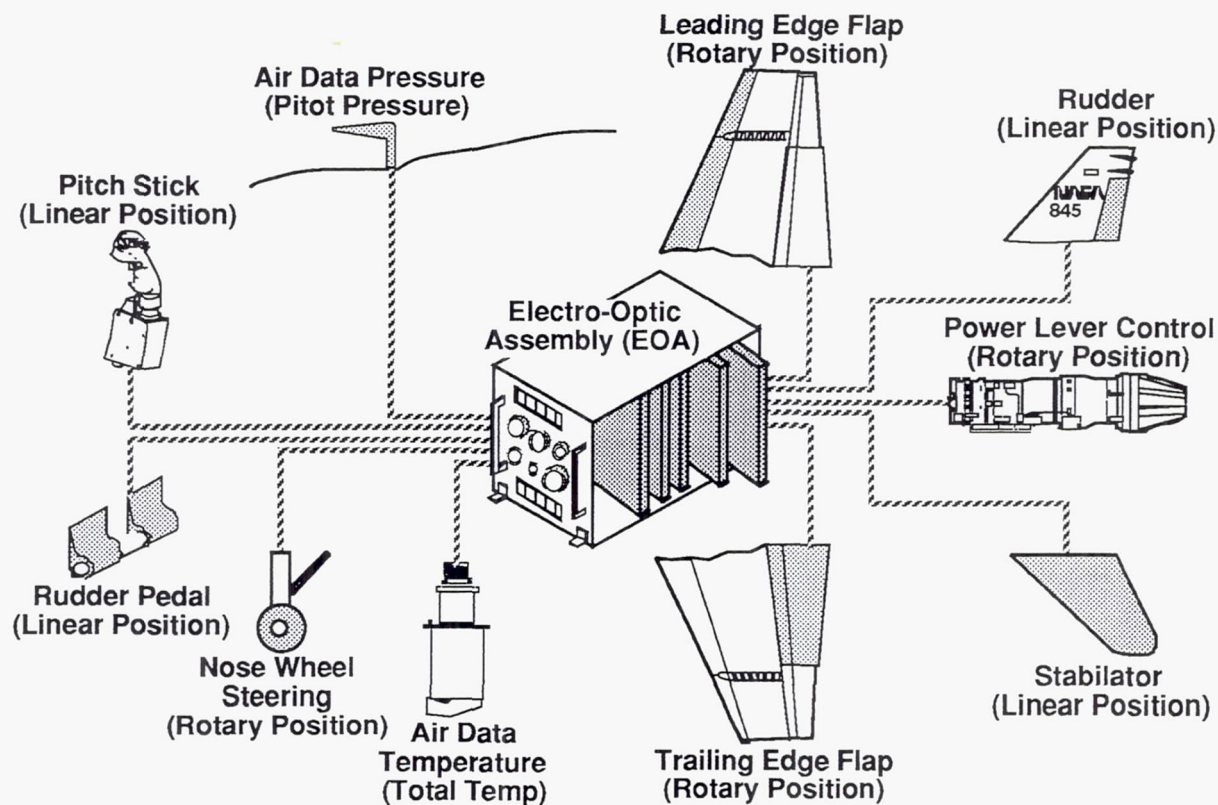
Figure 2.1-8. FOCSI Flight Test Hardware Configuration

FOCSI procurement goals were successfully met with the selection of 10 WDM compatible optical sensors from a total of five different suppliers, and implementing a total of four different WDM optical sensor modulation schemes. Figure 2.1-9 shows the relationship between FOCSI suppliers, technologies, and aircraft sensors.
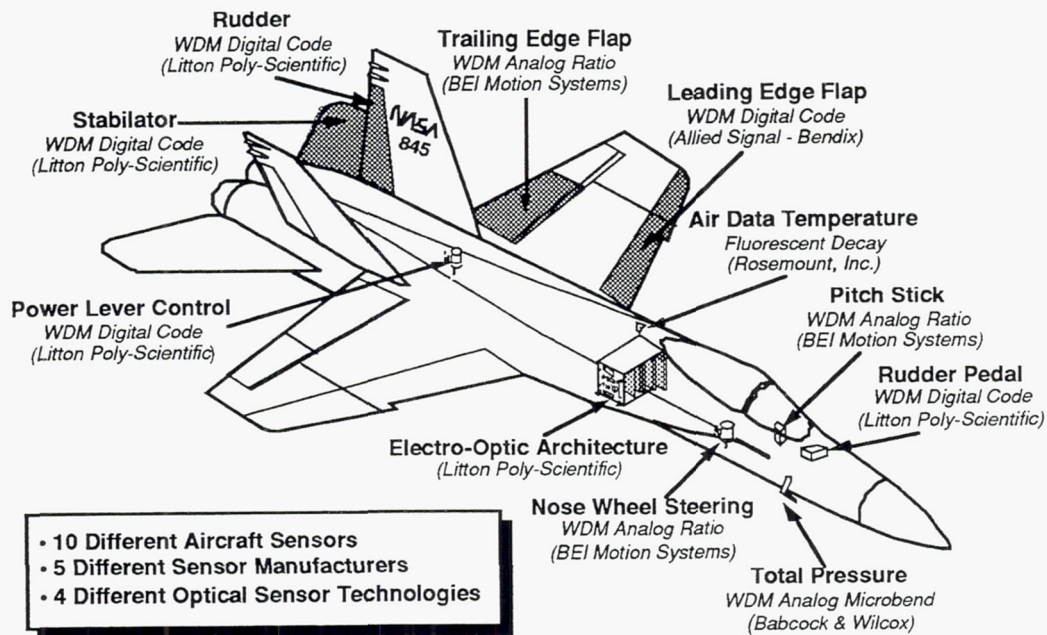
Figure 2.1-9. FOCSI Flight Control Hardware Configuration

The overall FOCSI flight test configuration is shown in Figure 2.1-10. Where possible, the optical sensors were installed in parallel with the production F-18 aircraft sensors in order to provide an operational reference point. Some sensors could not be directly monitored with existing electrical aircraft sensors and required the addition of separate electrical instrumentation reference sensors to be installed by NASA-Dryden.
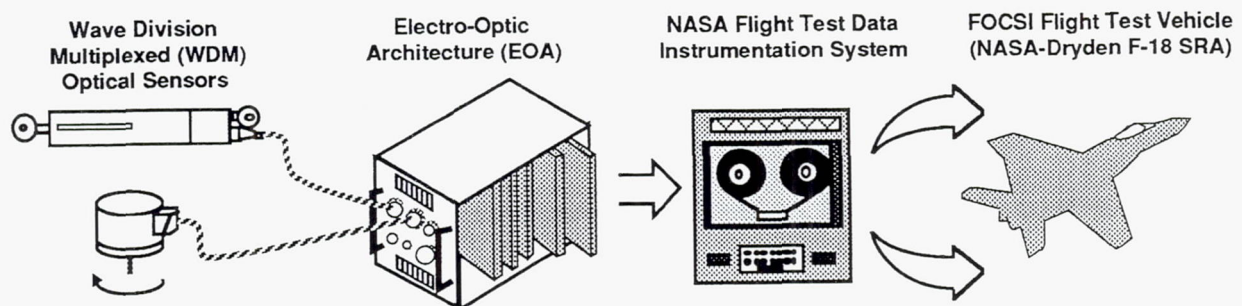
Figure 2.1-10. FOCSI SRA Flight Test Configuration

2.2 Interface Control Documents

Once qualified sensor and EOA suppliers were selected, the process of hardware development began. Perhaps the most challenging problem to overcome was not in actually developing the hardware, but in integrating the efforts of the five different sensor suppliers with the EOA supplier. To control the development of hardware from numerous suppliers, two approaches were considered. Either all the suppliers could work together as a single integrated design team; or, the suppliers could each design their own unique hardware to meet the requirements of a mutually agreed upon system interface specification. Since all of the suppliers selected were fierce competitors in a very unique market, it was apparent that the integrated design team approach would not work. Instead MDA decided to develop an Interface Control Document (ICD) to control all parameters at the interfaces between the suppliers' devices.

The purpose of the ICD was to facilitate liaison, coordination, and data exchange between suppliers to ensure interoperability between the EOA and optical sensors from different suppliers. As a result, the ICD became the primary technical interface between the sensor and EOA suppliers (Figure 2.2-1).
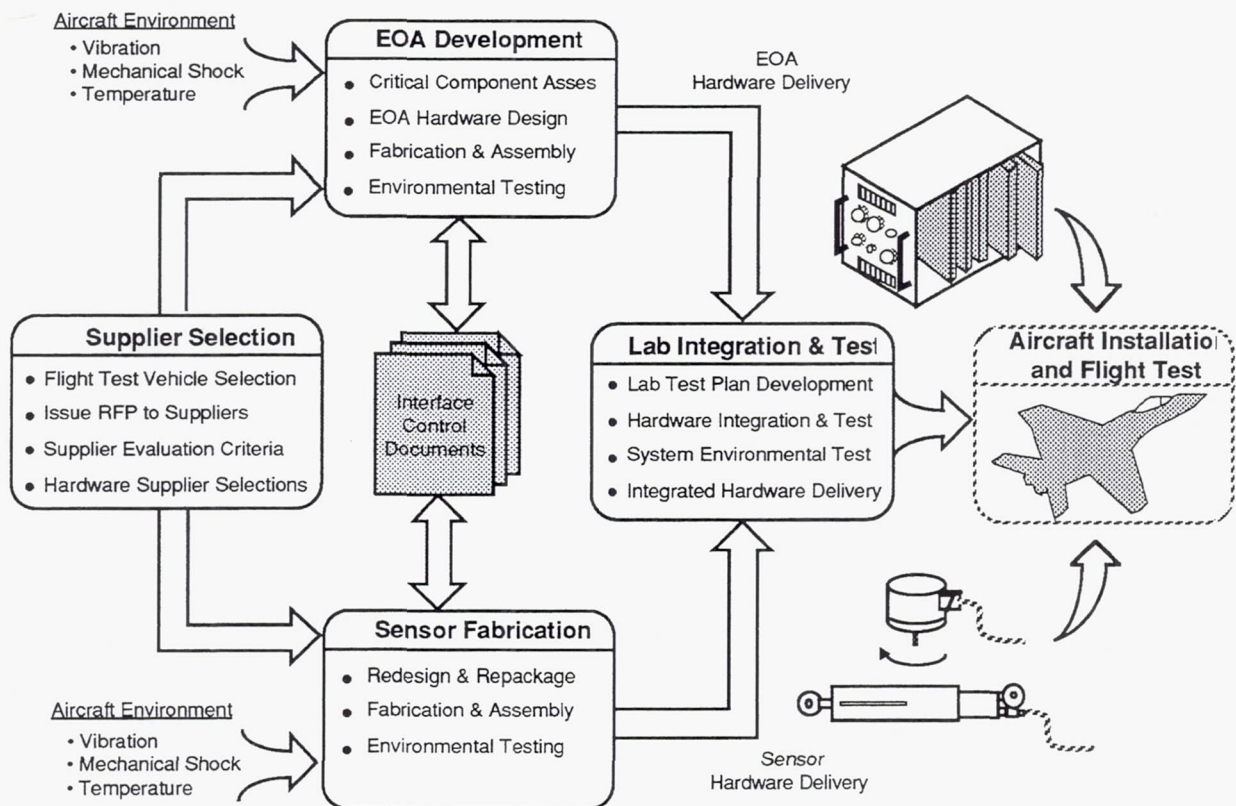
Figure 2.2-1. Interface Control Document Development

The ICD defined the optical, mechanical, electrical, and environmental interfaces between the sensors and EOA. MDA took responsibility for the development and maintenance of the ICD. Because of the number of suppliers involved, and the complexity of the EOA interface, MDA insisted that a standard ICD be developed and agreed upon by all suppliers **before** beginning hardware development. This approach worked for most of the sensors. However, in some cases, the ICD required significant modifications to reflect the actual sensor performance.

In order to facilitate the development of the ICD, all sensor suppliers agreed to enter into an Associated Contractor Agreement (ACA) with the EOA supplier for the purpose of ICD development. The ACA was a legally binding contract between the sensor suppliers and the EOA supplier which allowed the transfer of proprietary information related to sensor operation required to develop sensor decode algorithms in the EOA.

2.2.1 Sensor ICD Development

Using the information derived from the individual sensor supplier proposals, MDA developed a draft sensor ICD for review by the suppliers. However, because of the original procurement constraint of "no new technology development" which was levied upon the sensor suppliers, it was nearly impossible for the individual suppliers to agree upon a common ICD format.

Another problem in developing the sensor ICD was the reluctance of many suppliers to provide proprietary data in a public format, even with the ACAs in place. This problem was exacerbated by the fact that the sensor suppliers would not enter into ACAs between themselves, only with the EOA supplier. As a solution to this problem, it was decided to develop separate ICDs for the EOA and for each of the sensors. MDA agreed to include any supplier proprietary data in an appendix to the individual sensor ICDs. In order to provide maximum protection of supplier proprietary rights, individual sensor ICDs and proprietary appendices were established and maintained solely by the parties to the applicable ACA and MDA. MDA and Litton jointly accepted the responsibility for assuring that the individual sensor ICDs were compatible with the EOA ICD.

A final problem encountered in the sensor ICD process was that the aircraft electrical and optical sensors each possess unique operating characteristics. Specifications from the production F-18 flight control system sensors were originally used to establish optical sensor parameters such as linearity, repeatability, accuracy, null offset, etc. As the program unfolded, it was discovered that many of these sensor parameters were unique to electrical sensor technologies and therefore did not map directly to optical sensors.

2.2.2 EOA ICD Development

It was nearly impossible for the individual suppliers to agree upon a common ICD format. The result was an EOA ICD that was extremely broad in scope in order to accommodate the various existing sensor technologies.

The use of broad parameter ranges had both benefits and problems. The benefit was that an EOA which could meet these wide ranges would be usable with a large variety of sensors in the future. The main problem is that the major part of the effort for designing to meet the wide parameter ranges falls on the EOA supplier. Design of the EOA was expected to be the most difficult part of the FOCSI program, because the EOA was the only part which did not exist in some form prior to the advent of the FOCSI program. The requirement that it deal with wide parameter value ranges greatly increased the difficulty of the EOA development process.

2.2.3 ICD Conclusions:

The original procurement constraint of "no new technology development" which was levied upon the sensor suppliers, made it impossible for the individual suppliers to agree upon a common ICD format. This resulted in an EOA ICD that was extremely broad in scope in order to accommodate the various existing sensor technologies. The EOA ICD was so broad that it almost impossible to develop a common EOA implementation using today's technology.

In summary, the ICD was ultimately limited by the flexibility of the EOA interface. In future development programs, the EOA operating parameters should be established **first** and then used to define a single interface specification. Sensor manufacturers have demonstrated great flexibility in tailoring their manufacturing process to accommodate a variety of different optical interfaces.

In spite of the failure to establish a single common ICD for WDM sensor and EOA technologies, the ICD process did prove to be an invaluable tool for the technical management of sensor and EOA suppliers on the FOCSI program.

2.3 EOA Development

The next step in the FOCSI program was the development of an EOA suitable for multiplexing the selected optical sensors. As highlighted in Figure 2.3-1, EOA development was accomplished concurrently with sensor development.
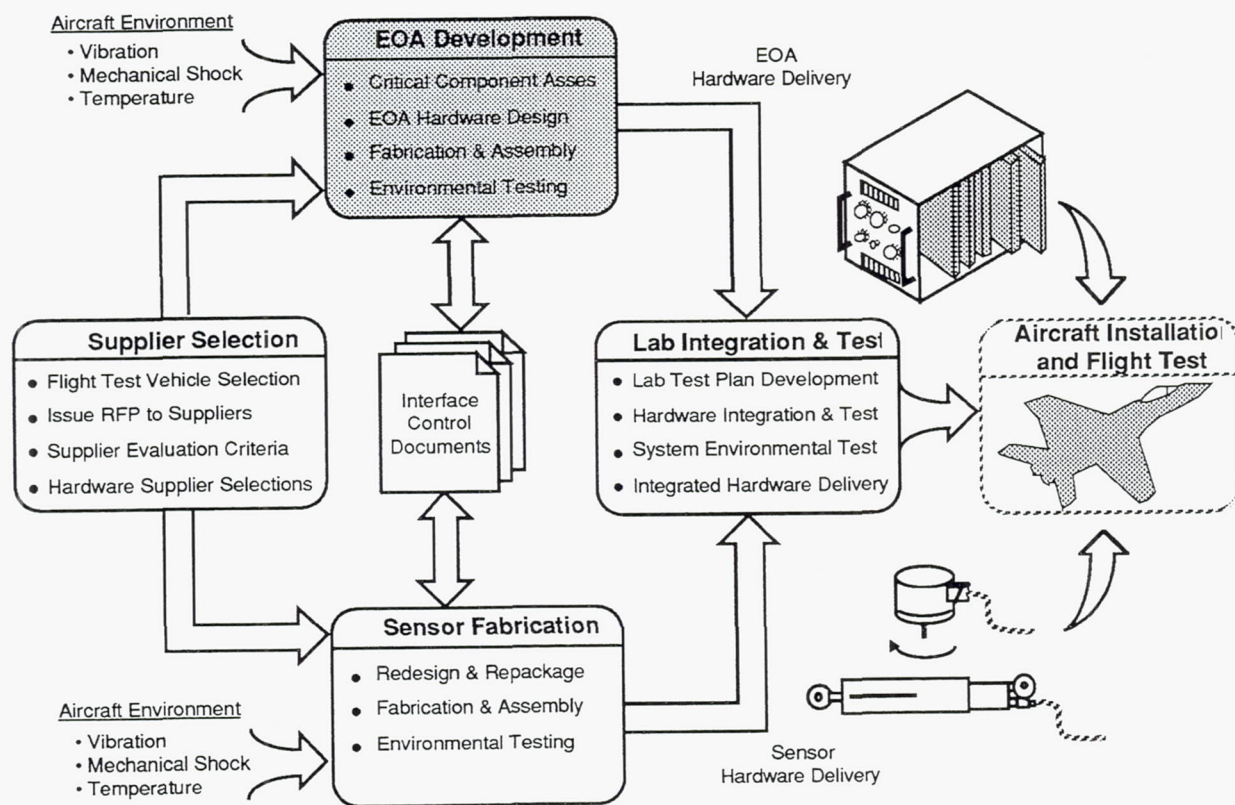
Figure 2.3-1. FOCSI Program Roadmap - EOA Development

One of the goals of the FOCSI program was to develop a common multiplexing EOA which incorporated "advanced avionic" packaging concepts. The reason for this was to eliminate the need to repackage the EOA for future transition of this technology into advanced aircraft. This goal was accomplished. The FOCSI EOA uses a standard 3/4 Air Transport Ratio (ATR) electronics enclosure and modules conforming to the Standard Electronic Module size-E format (SEM-E). The SEM-E module format is the standard adopted by the Department of Defense for all future avionics developments, including the F-22 fighter aircraft. To further promote technology transition, several of the key FOCSI hardware components were developed by the Naval Air Warfare Center (NAWC) as part of the Navy's Standard Hardware Acquisition and Reliability Program (SHARP). SHARP is a Navy initiative to develop a standard family of avionics enclosures, modules, power supplies, and batteries to order reduce life cycle costs. The FOCSI program used SHARP enclosures, SEM-E power supply modules, SEM-E 1750 processor modules with 1553 interface, and SEM-E 1773 optical data bus modules.

The completed FOCSI flight test EOA unit is shown in Figure 2.3-2.
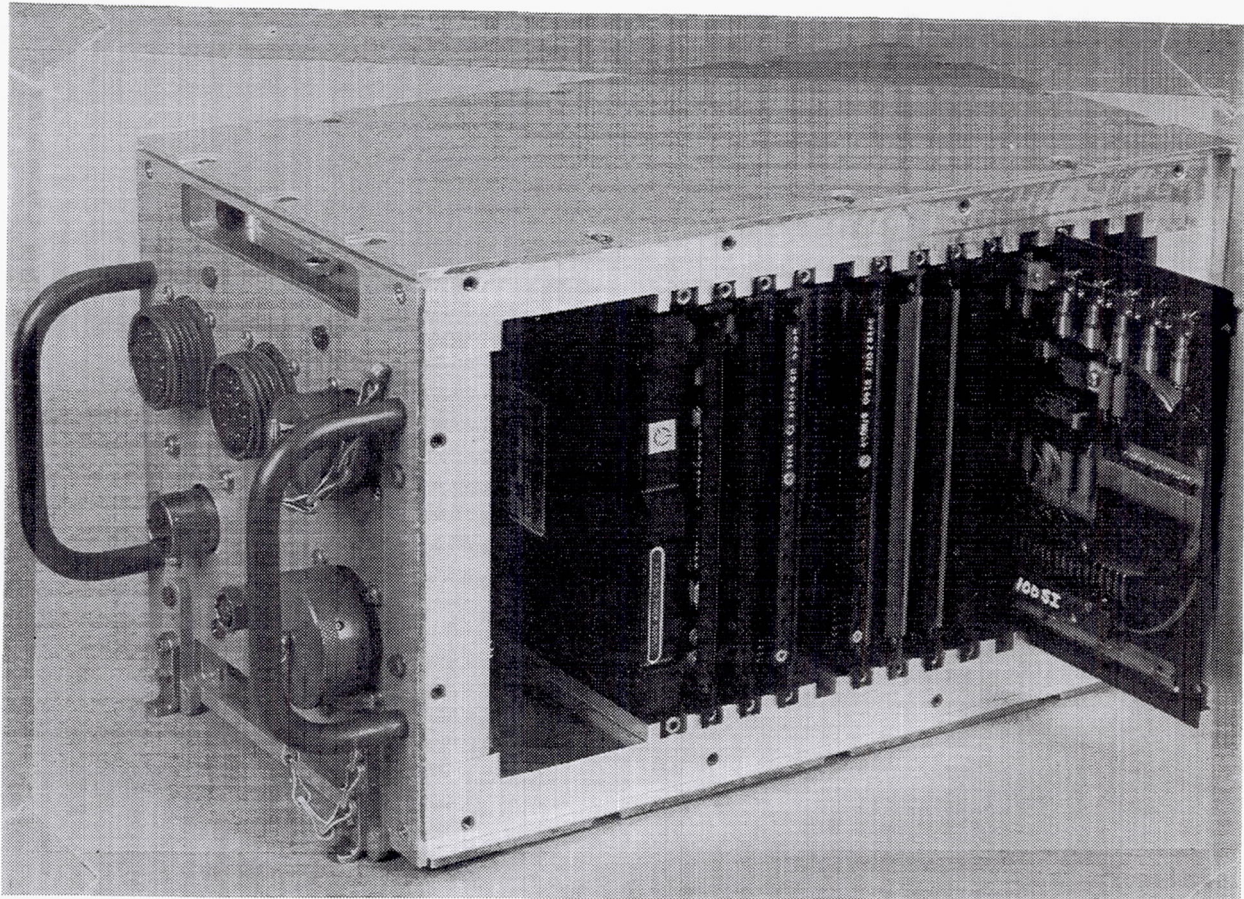
Figure 2.3-2. FOCSI Flight Test EOA

To ensure effective transition of the FOCSI EOA technologies, FOCSI EOA suppliers were asked to identify requirements for critical components. A "critical component" is defined as any component which could reduce risk, increase performance, or reduce cost of the overall system implementation. Much of the FOCSI flight test EOA was based on low risk SHARP standard hardware. Because this equipment is currently qualified by the Navy for fleet applications, these technologies were considered "low risk" and required no critical component development. The WDM EOA core modules were considered a new technology development item with a potential requirement for critical components as described in the following paragraphs.

2.3.1 Critical Component Assessment

As the first step in the EOA design, critical components required for development of the WDM EOA modules were identified. Based on EOA designs developed under the previous contract (NAS3-25345), no critical component development effort was anticipated. However, two items were identified as potential critical components; a single element broadband LED optical source, and a CCD detector array. These components are discussed in the following paragraphs.

2.3.1.1 Broadband LED Optical Source

A search of available single element broadband optical sources showed that none existed which would cover the entire 150 nm spectral range (from 750 - 900 nm) required for the FOCSI WDM sensors. As a substitute for a single element broadband source, Litton decided to evaluate the feasibility of constructing a multiple element broadband optical source from several narrowband LEDs.

A broadband optical source was initially constructed and evaluated using four narrowband LEDs, having individual Full Width Half Maximum (FWHM) outputs of 40 nm each, and an optical coupler. A single element Plessey broadband LED with a FWHM output of 115 nm was subsequently evaluated. Test results indicated that the broadband LED launched about the same amount of power as the prototype multiple LED source built of four narrowband LEDs. All the LEDs operated well during temperature tests. The Plessey LEDs were subsequently selected for the FOCSI WDM EOA module design.

To achieve the entire 150 nm spectral range required for FOCSI, one narrowband LED (with 40 nm FWHM at 900 nm) was combined with the Plessey broadband LED (120 nm FWHM), to produce a broadband source containing only two LEDs and an optical coupler.

A single broadband source could improve the EOA optical power budget and reliability, while decreasing system complexity and electrical power consumption. However, given the unknown development cost and schedule for a single LED source, the two LED source appeared to be a preferable device for FOCSI.

Preliminary operating specifications for the broadband LED optical source are provided in Table 2.3-1.

Spectral Width =	150 nm (FWHM)
Power Spectral Density =	-25 dBm/nm
Temp Range =	-55°C to +125°C
Development Cost =	Unknown

Table 2.3-1. Broadband LED Optical Source Characteristics

2.3.1.2 CCD Detector Array

The primary issue for the EOA detector was to determine if a commercial CCD detector array could meet FOCSI program requirements for sensitivity, dynamic range, temperature, update rate, etc.

Upon review of the requirements on CCD arrays for FOCSI, we concluded that the Litton and AlliedSignal optical sensor resolution requirements were the major constraints. Two CCD array suppliers, EG&G and Thomson-CSF, were contacted regarding standard CCD arrays, and custom arrays with pixels sized to meet FOCSI needs. Litton also evaluated the published temperature tolerance of standard arrays.

Preliminary operating specifications for the CCD detector array are provided in Table 2.3-2.

Dynamic Range (@-70 dBm) =	>10 dB
Update Rate =	1 KHz
Temp Range =	-55°C to +125°C
Development Cost =	$100K-$500K

Table 2.3-2. CCD Detector Array Characteristics

As an alternative to a custom CCD array, A commercial CCD array (from Thomson-CSF) is available which appeared to meet the FOCSI needs. The array was originally designed for commercial video camera applications. It had a larger number of rows of pixels than was required for the number of sensors to be multiplexed in the FOCSI program. The CCD array was designed for a camera and has one serial video output. The number of rows of pixels controlled the read-out time, limiting the FOCSI sensor update rate. The need for a blanking period to shift out data forced the FOCSI optical source to be pulsed to provide short dark periods for data read-out.

A custom CCD array designed for EOA applications could provide faster cycle times, improved optical sensitivity, increased optical dynamic range, smaller size, and operation over full military temperature range. However the likely $500K cost and unknown development schedule made a commercial array preferable despite the constraints it placed on EOA design.

2.3.1.3 Critical Component Summary

Although the development of a single element broadband LED optical source and a custom CCD detector array could have greatly enhanced the operation of the EOA, they were not required for development of the EOA. Therefore, use of the alternative approaches was recommended for the FOCSI flight test program.

2.3.2 EOA Hardware Design

In order to accomplish the FOCSI flight test mission, the EOA contained several unique hardware items, as shown in Figure 2.3-3. The EOA consisted of hardware developed by a number of different sources including Litton, MDA, and NAWC. The mechanical enclosure, including backplane and connectors, was the responsibility of MDA. The WDM EOA core modules were the responsibility of Litton. EOA support modules such as the power supply and bus interface modules were the responsibility of MDA. NAWC had responsibility for the 1773 converter modules. Functional integration of all hardware elements into a single operational system was the responsibility of MDA.

EOA Electro-Optic Backplane

EOA Mechanical Chassis

28V Aircraft EMI Filter

Miscellaneous Components:
- Fiber Optic Cables
- Fiber Optic Couplers
- MIL-C-38999 Connectors
- MIL-T-29504 Inserts

EOA Core Modules:	Qty
• TRD Interface	1
• Data Acquisition	1
• Receive Electronics	1
• Receive Optics	1
• Optical Source	1

EOA Support Modules:	
• Power Supply	1
• 1773 Converter	2
• 1750 Processor	2
TOTAL MODULES	**10**

Figure 2.3-3. FOCSI EOA Hardware Components

At the heart of the FOCSI EOA is a set of WDM EOA core modules which provide sensor excitation and decoding. Development of these WDM EOA core modules was subcontracted to Litton. The FOCSI EOA also contains several additional supporting electronics modules. These modules were supplied by both MDA and NAWC, and were based on Navy/SHARP standard avionics modules. Photographs of the WDM EOA Core modules and Support Modules are shown in Figures 2.3-4 and 2.3-5 respectively.
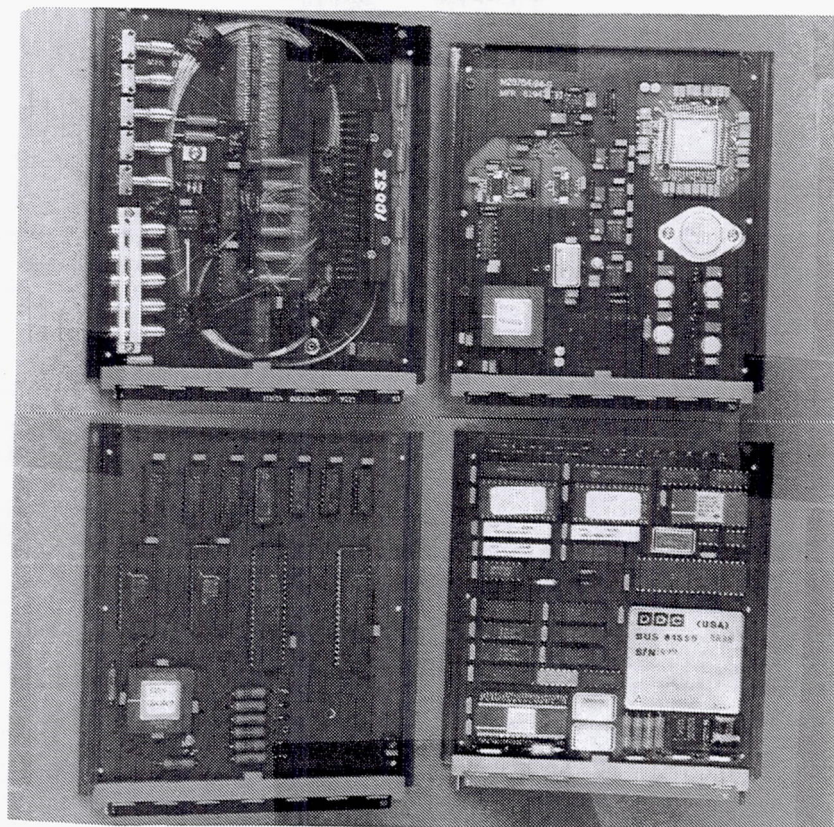
Figure 2.3-4. WDM EOA Core Modules
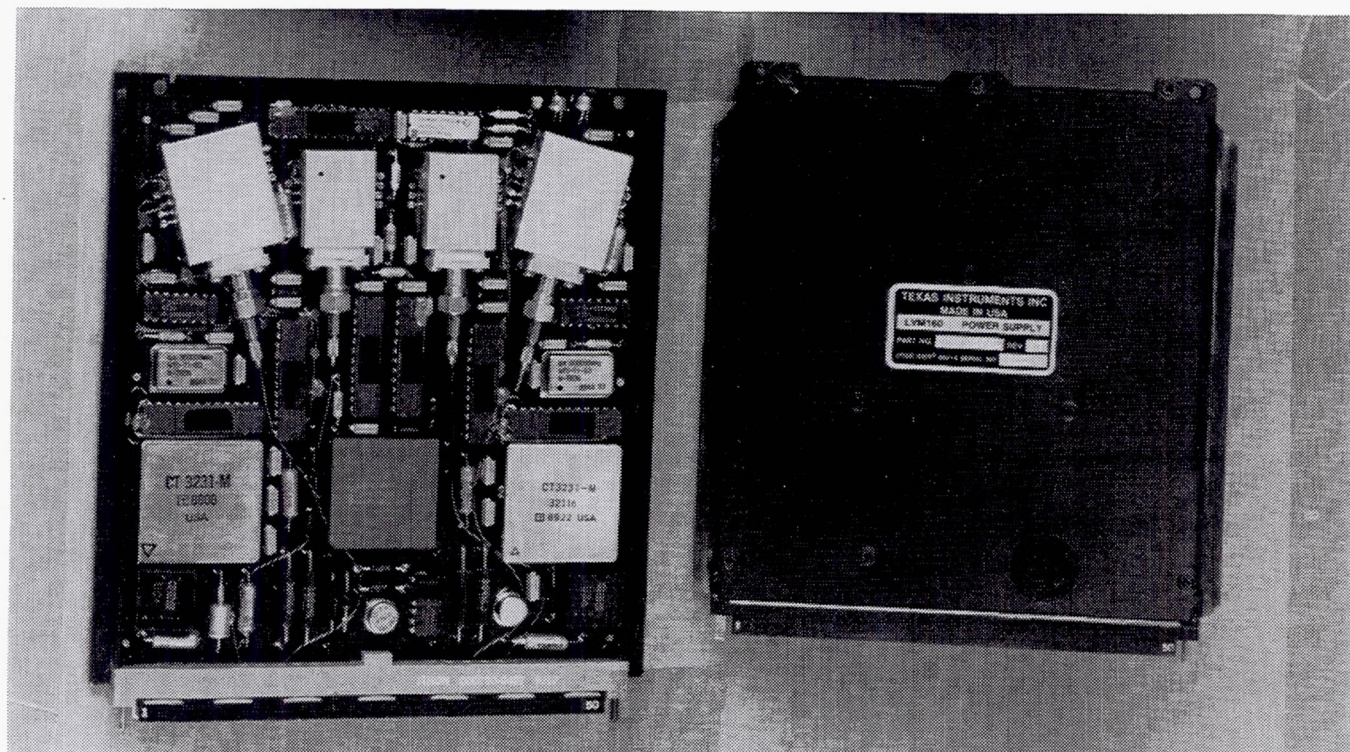
Figure 2.3-5. Navy/SHARP EOA Support Modules

2.3.2.1 Design of WDM EOA Core Modules

The heart of the FOCSI EOA, the WDM EOA core modules, was subcontracted to Litton. Since the WDM sensor characteristics fell into three operational categories: digital, analog, and Time Rate of Decay (TRD), one set of EOA parameter values was generated to work with all three categories of sensors. This was thought to make possible the development of an EOA with only two modules; a processor/output module, and a sensor module which interfaces to analog, digital, and TRD sensors. This was later found not to be possible, and separate TRD and analog/digital modules became necessary because the wavelength characteristics of the TRD sensor made operating it with the same source and receiver set as the other sensors impractical.

For the final EOA design, the team settled on a WDM EOA design requiring a total of 5 SEM-E modules. These five modules were: 1) TRD EOA module, 2) WDM EOA optical source module, 3) WDM EOA receiver module, 4) Data Acquisition Card (DAC) module, and 5) EOA processor module. The relationship between these modules is shown in Figure 2.3-6. The EOA receiver module is a triple-wide SEM-E module to accommodate the large volume required for the CCD detector array and supporting electronics. A total of 7 SEM-E module slots in the EOA mechanical chassis were assigned to the WDM EOA core modules.
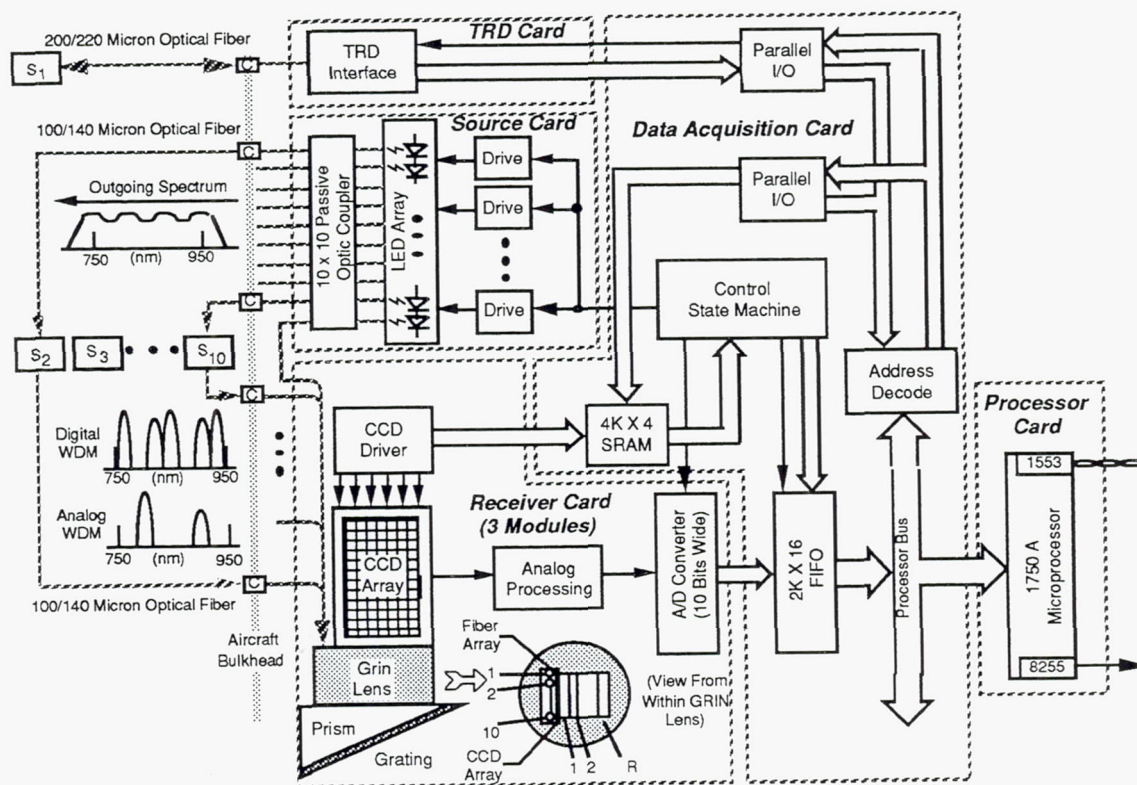
Figure 2.3-6. WDM EOA Functional Block Diagram

Functional operation of the EOA modules is described in the following paragraphs.

The EOA Source Card consists of a single width SEM-E module containing arrays of broadband and narrowband Light Emitting Diodes (LEDs) and a passive coupler to produce broadband optical pulses over the wavelength range from 750 nm to 900 nm on each of ten separate outputs. Nine of the outputs are used to excite the nine WDM optical sensor channels. The tenth output consists of an optical feedback signal to the optical source for use in stabilization of the EOA optical source power. This feature was added later in the program to aid in decoding the analog sensors.

The Receiver Card consists of three SEM-E modules (Two for receiver optics and one for electronics) which function as an optical spectrum analyzer to decode incoming optical sensor signals. The ten incoming optical signals (nine sensor channels plus one feedback channel) are collimated through a GRaded INdex (GRIN) lens and focused onto a diffractive optics assembly which separates each broadband optical signal into discrete optical wavelength bands. From here the optical signals illuminate a two-dimensional Charge Coupled Device (CCD) detector array which converts the ten optical signals into a single serial analog electrical signal stream. The low-level analog CCD output is then amplified and sent to an on-board analog-to-digital converter where it is digitized. The serial digital sensor signal stream is then sent to the Data Acquisition Card (DAC).

The DAC consists of a single width SEM-E module containing all of the EOA timing and control electronics. Digitized sensor data is sent to the 1750 processor on the Processor Card and compared to data "look-up" tables to determine the sensor reading. Sensor readings are sent from the 1750 processor module to the NASA data acquisition system via the 1553 data bus port. Sensor data is also converted from 1553 electrical to 1773 optical data via the 1773 data bus module (not shown in figure). The DAC is also responsible for controlling EOA optical output power by monitoring the optical power levels on the source-to-receiver feedback channel.

The TRD Card consists of a single width SEM-E module which interfaces to the Time Rate of Decay (TRD) temperature sensor. Original plans were for the TRD sensor to be operated by the same source and receiver modules as the other sensors. However, the characteristics of the TRD sensor made it impossible to multiplex it with the others; therefore, a separate module was designed for the TRD sensor.

The design of the WDM EOA modules is described in the following paragraphs.

2.3.2.1.1 TRD EOA Module Design
After reviewing the optical parameters of the TRD sensor, it became evident that separate TRD and Analog/Digital modules would be necessary within the EOA. The unique wavelength characteristics of the TRD sensor made operating it with the same EOA source and receiver as the other WDM sensors impractical.

The TRD EOA module was designed to act as a stand alone module containing optical source and detector circuitry. The TRD EOA would work independently of the other EOA modules. Operation of the TRD module was controlled by the DAC and processor modules.

For TRD sensor decoding, a phase-based decoding method which is widely discussed in open literature on TRD sensors was selected. In this approach, decoding the TRD signal is based on the phase of the response to a pulsed excitation.

Since the EOA supplier had no previous experience in the development of TRD sensor interfaces, they decided to construct a breadboard unit before committing to a specific module design. LEDs were procured for the TRD source from Honeywell and tested to quantify optical source parameters. As with the other analog signals, the accuracy of the interpreted TRD signal depended upon the strength of the signal. A preliminary optical power budget analysis indicated that the power budget had a deficit of approximately 6 dB below the level required to achieve an accuracy equivalent of 10 bits. The study indicated that 7 bit accuracy could be met. MDA re-evaluated the accuracy requirement and determined that 7 bit accuracy was not acceptable. It was believed that further improvements in accuracy could be achieved through careful board design, but the magnitude of the possible improvements that could be achieved with reasonable efforts in the time available was unknown. Based on the results of TRD breadboard testing, approval was given to proceed with fabrication and assembly of the TRD EOA module with reduced accuracy.

2.3.2.1.2 EOA Optical Source Module Design

Several candidate designs were evaluated for a EOA broadband optical source to cover the 150 nm spectral range (from 750 - 900 nm) required for the FOCSI WDM sensors. The initial optical source design used four individual narrowband (40 nm) LEDs to produce a broad spectrum for each of three sensors and one optical feedback fiber. This approach is very inefficient and resulted in higher cost, higher power consumption, and larger size.

A single element Plessey broadband LED with a FWHM output of 115 nm was subsequently evaluated. Test results indicated that the broadband LED launched about the same amount of power as the prototype multiple LED source built of four narrowband LEDs. After conducting thermal testing of the candidate LEDs, the Plessey LEDs were subsequently selected for the EOA optical source module design. To achieve the entire 150 nm spectral range required for FOCSI, one narrowband LED (with 40 nm FWHM at 900 nm) was combined with the Plessey broadband LED (115 nm FWHM), to produce a broadband source containing only two LEDs and an optical coupler.

As part of the EOA optical source design trades, the use of single large optical coupler for all sensors versus individual 2 x 2 couplers for each of the nine sensor channels was considered. The possibility of exciting several sensors with one broadband light source by means of a single large optical coupler held the potential to reduce the power, weight, and size of the EOA hardware drastically. The design change can be best understood by referring to Figure 2.3-7. The original approach used a broadband source produced by using a fused fiber optic coupler to combine light from multiple LEDs, each operating in a different wavelength range. Note that the fused coupler has the same number of inputs as outputs. Thus, if one LED set is used to excite one sensor, the light passing into the unused outputs is lost.

Original Approach   Proposed Approach
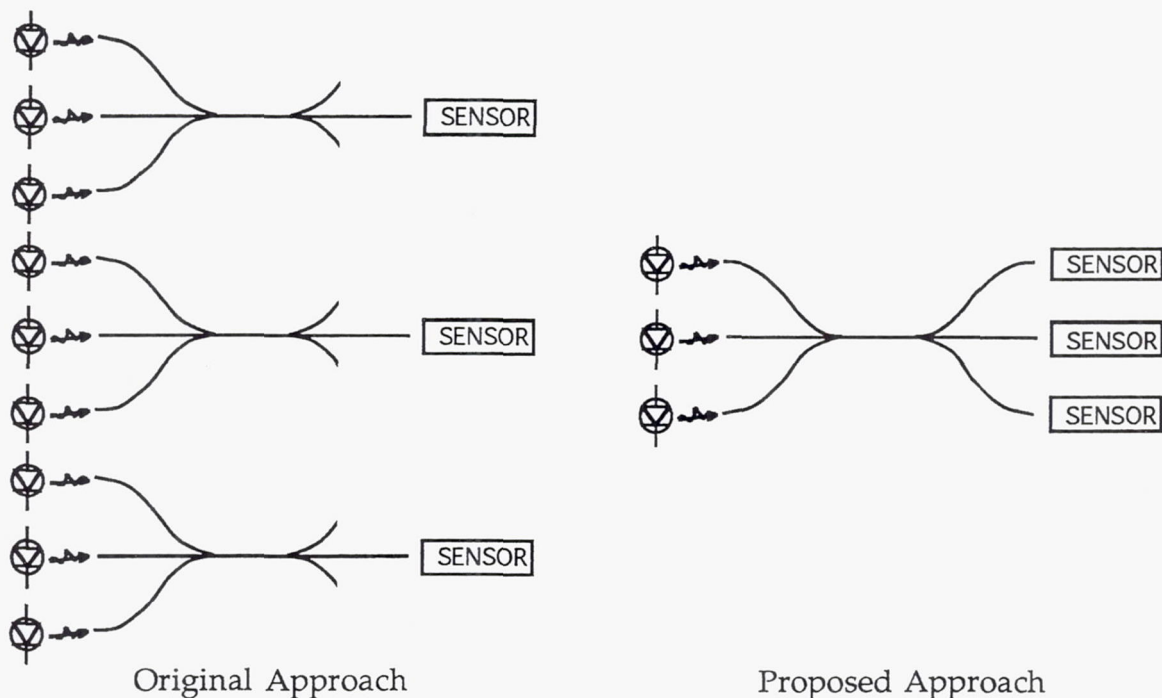
Figure 2.3-7. Candidate Sensor Excitation Approaches

The proposed approach utilized all the outputs of the fused coupler to excite sensors, thus harnessing the optical power which would have otherwise been wasted. This approach drastically reduced the number of optical sources required. Because the original receiver design did not depend upon cycling the excitation of the sensors, the optical sources could be on all the time. Since the sources could operate continuously, exciting several sensors with one source is a reasonable possibility. Furthermore, since the single source approach mixed the light from multiple sets of LEDs, the failure of one or two LEDs had only a very slight effect on the averaged output optical power reaching all the sensors. This approach was preferred by the individual sensor suppliers because it allowed all sensors to see essentially the same optical spectrum.

One concern with the single source approach, is that the fused coupler represents a potential single point failure for all the sensors connected to it. In order to address the concern of a single point failure, a failure modes and effects analysis was conducted. It was determined that the dominant failure mode appeared to be fiber failure, with a probability of about 10^{-5} per hour. The next most dominant failure mode appeared to be LED failure, with a probability of 10^{-6} per hour. From these, one could conservatively expect a Mean Time Between Failure (MTBF) of 10^4 hours for the single coupler source. Although this MTBF would be unacceptable for an EOA in a production flight control application, it was acceptable for an open loop flight test program such as FOCSI. The effect of a failure of a fiber or LED in the single source approach was estimated to be 1.0 dB/nm over the range supported by the failed fiber or LED. Failure of a second fiber or LED supporting the same band as the first will cause a change of roughly another 1.0 dB/nm. Failure of a second fiber or LED supporting the other part of the range than that affected by the first failure will reduce the other portion of the spectrum by about 1.0 dB/nm. A second failure of that type would tend to re-flatten the spectral power distribution. Based on this analysis, the design of the single source approach proceeded.

It was originally thought that the optical sources would be so simple and so stable that feedback from the source to the receiver and complicated source control circuitry would not be needed. However, early in the program it became apparent that the microbend pressure sensor would be extremely sensitive to optical source variations over time or temperature. Eventually, this was found to be a valid concern for all of the WDM analog sensors. In order to accommodate the unique characteristics of the analog sensors, the EOA was forced to include a feedback loop to monitor and correct for the effects of variations in the optical source spectrum. The incorporation of the optical feedback loop onto the EOA source module provided the ability to statically or dynamically control the optical output power.

Static source control was used to compensate for fixed but unknown system losses, such as those associated with the FOCSI optical backplane and aircraft interconnect optical cables. It was expected that the static output value would be changed very few times, if ever, during the entire FOCSI flight test program. The static source control function resided in the EOA receiver electronics module, and worked by adjusting the duty cycle of the LEDs. LED drive current would be unaffected. A value for source power level would be set once during initialization, and would remain the same value until externally altered over the EOA 1553 bus.

Dynamic source control was added to actively compensate for changes in the optical output level due to temperature or aging effects on the optical source, and was necessary to achieve the required accuracy when decoding analog sensors. The dynamic source control function resided in the EOA Source module and worked by adjusting the LED drive current to maintain the optical output at a pre-determined value. Commands for dynamic source control were issued by the EOA Data Acquisition module, based on average optical levels incident at the receiver.

2.3.2.1.3 EOA Receiver Module Design

The EOA receiver design used a 2-dimensional, or area, CCD detector array instead of a conventional linear array. This approach had the advantage that the receiver did not have to be "shared" among the various sensors connected to it by multiplexing the individual optical sources. The area array approach maximizes receiver sensitivity for each sensor channel because it is able to "stare" at each of the optical sensors for the full integration period.

As the first step in the design of the EOA receiver, trade-offs in optical demultiplexer design and CCD selection were investigated in light of the sensor ICD data and the EOA broadband optical source developments. The characteristics of several commercially available CCD arrays were evaluated before initially selecting one made by Thomson-CSF. Resolution and cost considerations forced the selection of a video camera CCD array for the EOA receiver. These arrays are read by shifting out the entire 2-dimensional image at one time by transferring each row through all the preceding rows. The EOA optical sources must be off during this process, or signals coming in from sensors will be mixed with information from other sensors being shifted through the array, resulting in data "smearing" at the receiver. It was decided that the EOA optical source would be operated in a pulsed mode with a 96% duty factor to eliminate data "smearing" while scanning values out of the CCD array. This did not impact the operation of the sensors, since they were originally designed for operation with a multiplexed (pulsed) EOA design. Furthermore, the source design did not change because the sources would all be pulsed together, rather than being pulsed sequentially as in the original multiple source design.

After selecting the CCD array, a concern arose with the EOA in the rate at which the EOA will be able to scan the sensors. The procurement specification required the EOA to scan all the sensors (except the TRD sensor) at a 1 KHz rate. The electronic scan rate of the CCD array is determined by the amount of incident optical power available, and the desired receiver sensitivity. Based on the stringent optical power margins required for the sensors, the EOA would be limited to a maximum scan rate of 100 Hz. A 100 Hz update rate is fast enough to supply data for flight test purposes, but would not be fast enough for closed-loop control applications in the future. A custom CCD array, such as that described in the critical component assessment section, would be required to meet the faster update rate. In order to control program costs and schedule, we proceeded with the design using 100 Hz update rate.

As the Sensor ICD evolved, concerns about the magnitude of the sensor insertion losses and their compatibility with the source/receiver power budget were raised. In particular, the losses in the digital sensors were a cause for concern. Questions arose as to why the sensors from different vendors, but with similar designs, had different losses. The wide range of differences made it difficult to select the proper EOA sensitivity range. Fortunately, as the sensor designs progressed, similar sensors from different suppliers approached the same optical losses.

Detector sensitivity tests and analyses were conducted on area CCD arrays. It was determined that, when used to decode a digital sensor in 10 ms (or 100 Hz update rate) at a Bit Error Rate (BER) of 10^{-6}, the EOA would have a sensitivity for a logical one (light present) of -71 dBm/nm and a dynamic range of 11 dB. Those values would be compatible with all the digital sensors, as -69 dBm/nm was required for the highest loss sensor. An important point about the receiver sensitivity with a digital sensor was the signal margin. The value of -71 dBm/nm included all corrections for pixel size and optical losses in the demultiplexer. It also included 8 dB of power margin between the zero signal (no light) level and the noise floor. Further, the analysis assumed an 8 dB difference between the one signal level and the zero signal level, to provide the 10^{-6} BER. Therefore, an optical one at the limit of -71 dBm/nm is 8 db above an optical zero at -79 dBm/nm and 16 dB above the noise limit (signal equals noise) at -87 dBm/nm. The relationship between EOA and sensor dynamic range for digital sensors in shown in Figure 2.3-8.
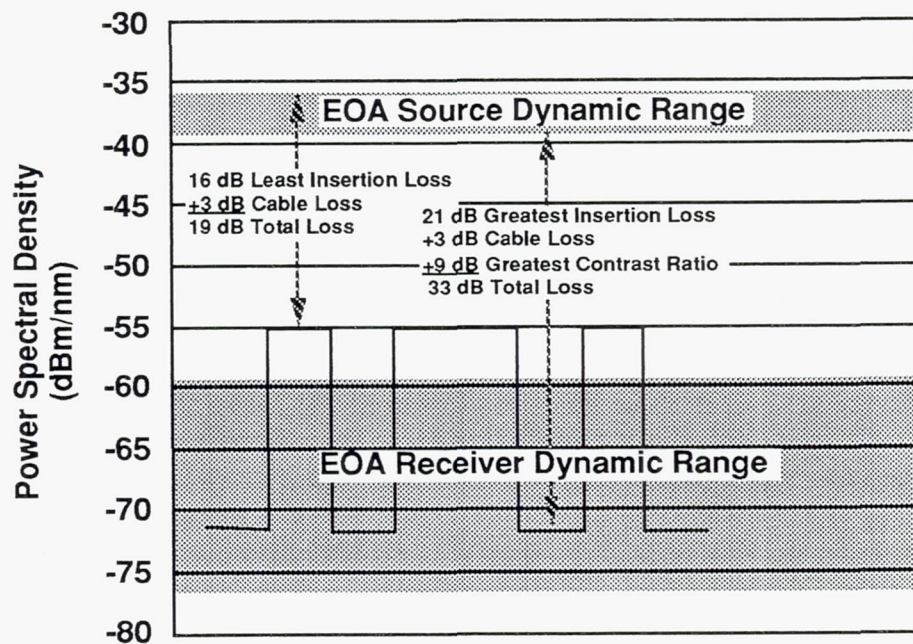
Figure 2.3-8. EOA Receiver Sensitivity Range for Digital Sensors

For decoding analog sensors with an area CCD array, the EOA noise limit was calculated to be -90 dBm/nm. Based on the sensor ICDs, the worst case need was for -76 dBm/nm to account for the fixed sensor and cable losses and the sensor dynamic range. The dynamic range of the receiver when used with an analog sensor was calculated to be 27 dB. Unlike the calculation of dynamic range for a digital sensor, the dynamic range for operation with an analog sensor did not include a margin. The range given was the range from the noise floor to the saturation limit.

The relationship between EOA and sensor dynamic range for analog sensors in shown in Figure 2.3-9.
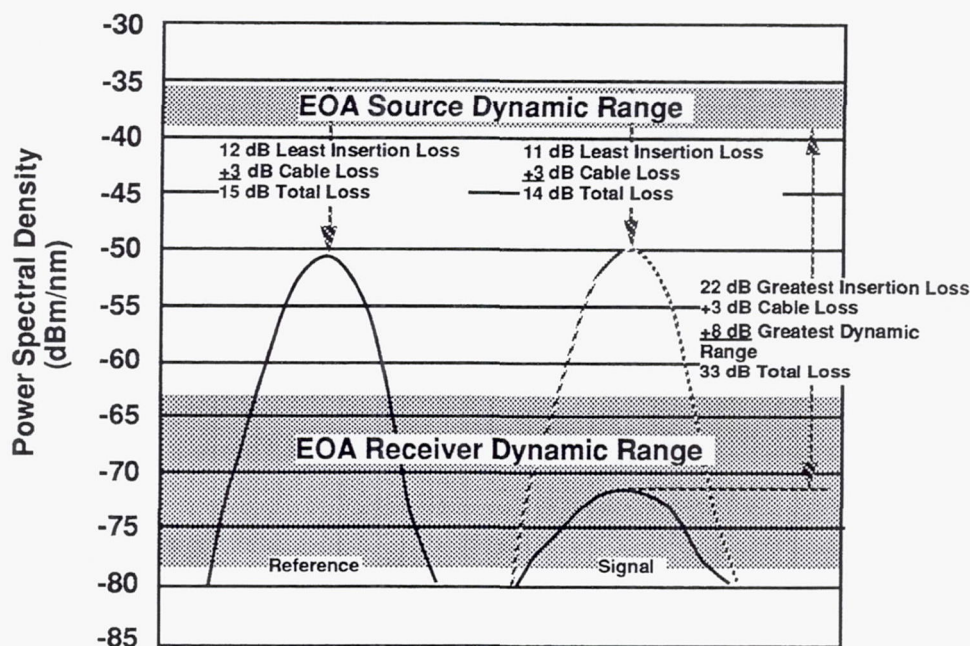
Figure 2.3-9. EOA Receiver Sensitivity Range for Analog Sensors

Two potential problems existed with the behavior of the CCD array receiver when decoding analog sensors. The first problem is that the receiver was too sensitive. The sensor and cable losses for the analog sensors were sufficiently small that the receiver would saturate, leading to errors in the measured values. Since adding loss into an optical system is not difficult, this was not viewed as a great problem. The second problem was the presence of shot noise in the CCD array. Shot noise is always present in CCD arrays, and is troublesome if analog sensors are being decoded, because it limits the resolution of the decoding process.

To decode analog sensors, the range of power which is returned from the sensor must be divided into a number of elements equal to the resolution required for the system. For FOCSI, an analog resolution equivalent to the 10 bit resolution of the digital sensors was desired. This led to a need to divide the returned sensor signals into 1024 (2^{10}) increments. Each increment had to be greater than the shot noise. According to the Litton analysis, if the full 27 dB range of the CCD array were to be divided into 1024 increments, the increments were **smaller** than the shot noise. Since the dynamic ranges of the analog sensors were only 6 dB for the pressure sensor and 15 dB for the position sensors, the increments for those sensors would be much smaller than the shot noise.

The EOA procurement specification called for the EOA analog sensor interface to use ten wavelength bands to maintain compatibility with the digital sensor interface. For analog sensors, ten bit resolution roughly translates into an accuracy requirement of 0.1%. While this accuracy may easily achievable with digital optical sensors, it is more difficult if not impossible to achieve with analog sensors. For the existing F-18 aircraft electrical flight control position sensors (which are being paralleled with analog optical sensors) the physical position accuracy ranges from only 2% to 5%, which is equivalent to a digital accuracy range of about 4 to 6 bits.

Decoding of analog sensors with a CCD array is summarized in Table 2.3-3. This table shows the effects of the actual sensors operating with both a perfect (noiseless) and real CCD arrays. At low signal levels ($\approx$-70 to -80 dBm), the CCD array produces less noise, and therefore more signal states, that at higher power levels. As a result, sensor accuracy at low power levels is effectively limited by the resolution.

Analog Sensor Manufacturer	Power Range	Resolution			Accuracy		
		States	Bits	%	States	Bits	%
B&W	-62 to -68 dBm	788	9.6	0.1	487	8.9	0.2
	-71 to -77 dBm	98	6.6	1.0	98	6.6	1.0
BEI	-62 to -77 dBm	997	10	0.1	630	9.3	0.2
	-70 to -85 dBm	158	7.3	0.6	158	7.3	0.6

Table 2.3-3.
Theoretical Noise Limited Accuracy
of Analog Sensor Decoding by a CCD-Based Receiver;.

In use, the CCD array is operated as a quantizer. If the array quantizes signals falling in its full dynamic range with a resolution of one part in 1024, the output of the CCD could be digitized with 10 bit accuracy. However, the FOCSI analog sensors could not use the full dynamic range of the array. The B&W sensor had a 6 dB range and the BEI sensors had 15 dB ranges. Those limited sensor ranges meant the sensor outputs would only be quantized to fewer than the maximum 1024 distinct states. The actual number of distinct states which a sensor's output could occupy depended upon the power of the signal returned by the sensor to the CCD array. Note in the Power Range column of Table 2.3-3, that the full range of a sensor's output could be anywhere in the CCD array's sensitivity range. The power of a sensor's signal depends upon such factors as source power and system losses as well as on the modulation produced by the sensor. Table 2.3-3 uses sensor powers falling at the top and bottom of the CCD array's dynamic range as examples.

Note under the "Resolution" heading in Table 2.3-3 that the number of distinct states occupied by the 6 dB B&W signal is different for signals at the top and bottom of the CCD array's sensitivity range. This is due to the fact that the relationship between power in watts and power in decibels is logarithmic. Thus the 6 dB range from -62 to -65 dBm covers more uniform size states in watts than the 6 dB range from -71 to -77 dBm.

If the numbers of states in the "States" column in Table 2.3-3 are converted into bits of digital resolution (assuming fractional bits are meaningful), the results shown in the Bits column appear. The % column contains the results, in percent, of resolving one state out of the total number of states given in the States column. (i.e. $1/788 \approx 0.1$ %).

The difference between the Resolution columns and the similar appearing Accuracy columns is that the values in the Resolution columns assume the CCD array has no inherent noise, so that its dynamic range could be divided into any number of states. In this case the total number of states was 1024. A real CCD array does have noise. For the FOCSI CCD array, the magnitude of the noise was greater than the size of one of the 1024 states generated when the CCD dynamic range was divided by 1024. If one uses the magnitude of the real noise as the size of the smallest resolvable state, the results in the Accuracy column are generated. For instance, the range from -62 to -68 dBm can only be divided into 487 distinct states when the state are the size of the real noise.

Because of concerns in EOA decoding accuracy for analog sensors, the feasibility of developing a separate EOA receiver for analog sensors was evaluated. It was concluded that a separate analog receiver, operating with the 15 dB range of the BEI sensors, could achieve the equivalent of ten bit resolution. However, the accuracy would be much less; roughly 0.5 to 0.6 % (about 7 to 8 bits), not 0.1%. Furthermore, it was not known what the accuracy of a separate analog receiver would be when operated with the 6.0 dB range B&W sensor, but it was not expected to improve. These results led to a recommenation that the CCD array-based receiver be used as a common digital and analog receiver. Its analog decoding accuracy was better than that needed for the existing sensors, it performed roughly as well as or better than a separate analog receiver was expected to perform, and using a common receiver was much simpler than having a separate receiver. Based on the results of the EOA receiver studies, MDA and Litton concluded that no receiver approach appeared to be able to decode the analog sensors to 0.1 % accuracy in the aircraft environment. However, a common CCD-based digital/analog receiver could decode the analog sensors with an accuracy good enough for flight control purposes.

Just prior to beginning fabrication of the EOA receiver module, the selected CCD array changed to a CCD array manufactured by Texas Instruments (TI) instead of the CCD array from Thomson-CSF. There were two reasons for switching CCD array suppliers. The first reason is that Thomson-CSF had been somewhat reluctant to provide certain information concerning the internal operation of their CCD array. This information was critical in designing the DAC module which controlled all critical CCD timing functions. The second reason for switching CCD arrays was that the TI CCD array had slightly larger pixels than the CCD array from Thomson-CSF.

The larger pixels provided the EOA with greater sensitivity and reduced noise to further aid in the decoding of analog sensors as verified by measurements of the noise levels on the TI CCD array operating at room temperature. These measurements indicated that the CCD array performed as predicted.

Based on the results of extensive trade studies and prototype component evaluations, the design of a combined digital/analog EOA receiver module was finalized and fabrication and assembly proceeded.

2.3.2.1.4 Data Acquisition Module Design
The design of the DAC module was originally thought to be straightforward. The DAC module contains all of the critical timing circuitry to control the flow of information between the EOA receiver and the 1750 processor module. No major problems were encountered in the design phase of the DAC module. However, numerous problems were encountered during fabrication/assembly and testing of this module, as described in later sections of this report.

2.3.2.1.5 EOA 1750 Processor Module Design
Early in the EOA design phase, Litton designers met with representatives from NAWC to discuss the application of the SHARP 1750 processor module to the FOCSI program. This module was selected as the EOA processor module and generic software drivers and decode algorithms for all the sensors were developed. However, when these algorithms were initially tested on an actual processor module, they were found to execute quite inefficiently. The decode algorithms were redesigned to match the unique processor characteristics, and much faster sensor decoding was achieved. The new algorithms allowed decoding within the ten millisecond limit (based on 100 Hz sensor update rate).

2.3.2.2 Design of WDM EOA Support Modules

In addition to the core EOA modules, the FOCSI EOA required additional support hardware to accomplish the FOCSI flight test. This support hardware included one 1553 bus controller module, two 1773 optical data bus modules, one power supply module, one EOA backplane, and one EOA mechanical chassis.

2.3.2.2.1 1553 Data Bus Controller Module Design

To minimize design costs, the SHARP 1750 processor module with on-board 1553 multiplex bus interface was selected as the bus controller module for the FOCSI flight test EOA. This was the identical module selected to act as the host processor for the core EOA modules and 1553 data interface. Since this module was a non-development item available from a Navy qualified supplier, there was no hardware design activity. Initial design activities focused on assigning 1553 remote terminal addresses to all of the FOCSI flight test hardware and software programming of the host processor on the 1553 card.

2.3.2.2.2 1773 Data Bus Module Design

Design of the 1773 optical data bus module for the FOCSI program was accomplished by the Navy as part of the SHARP activity. The SHARP 1773 module converts a 1 Mbps Manchester encoded electrical 1553 signal into an 8 MBps Manchester encoded optical 1773 signal as shown in Figure 2.3-10. Re-encoding the 1553 signal was necessary to overcome the data latency and ambiguous end of message frame typically associated with "direct conversion" type approaches. This approach also pomised a future growth path to higher speed data communications.

2.3.2.2.3 Power Supply Module Design

The power supply module selected for the FOCSI EOA was a model LVM 160, manufactured by Texas Instruments (TI) for the SHARP program. This module operates from 28 volt aircraft power and provides three regulated outputs of +5 volts (at 25 amperes) and +/-15 volts (at 1 ampere each) with a total power dissipation of 160 watts. Since this module was a non-development item available from a Navy qualified supplier, there was again no hardware design activity. SHARP agreed to develop a suitable EMI filter to use in the EOA mechanical chassis to filter the aircraft power supplied to the power supply module.

2.3.2.2.4 EOA Backplane Design

The backplane selected for the EOA was an electro-optic backplane consisting of wire-wrapped electrical connections and optical connections. A wire-wrapped backplane was selected over a printed wiring board backplane because of the number of design changes anticipated in the core EOA modules. To provide maximum flexibility in design changes, three-stage wire wrap posts were employed throughout the backplane. Optical connectors were based on SHARP qualified optical contacts manufactured by G&H Technologies Incorporated. The optical contacts are butt-coupled, lensed termini with 90° backshell extensions to control fiber bend radius and provide adequate clearance below the wire wrap pins in adjacent connectors. Figure 2.3-10 shows a side view of the EOA electro-optic backplane.
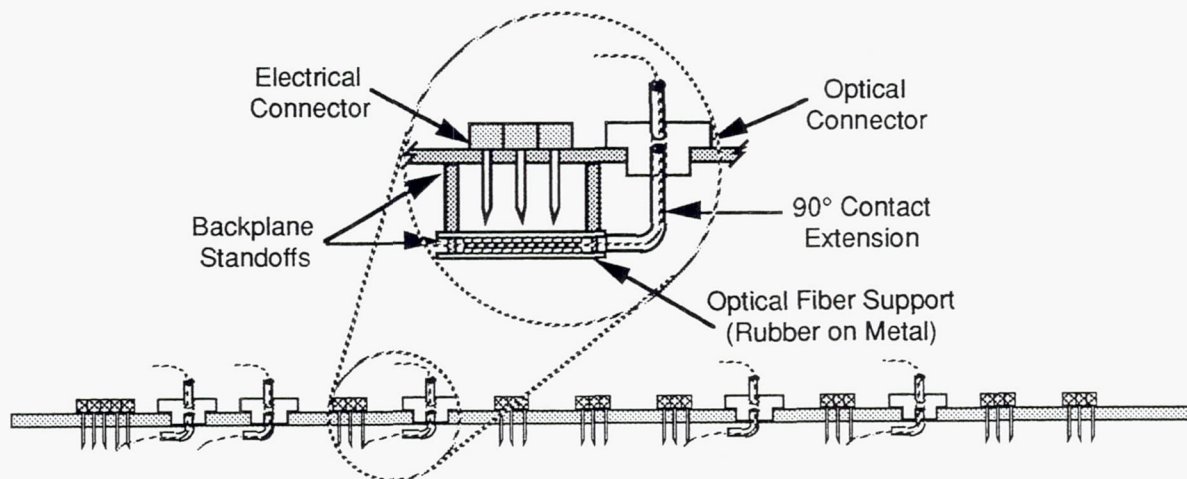
Figure 2.3-10. Side View of EOA Electro-Optic Backplane

The final backplane layout of the FOCSI EOA modules is shown in Figure 2.3-11.
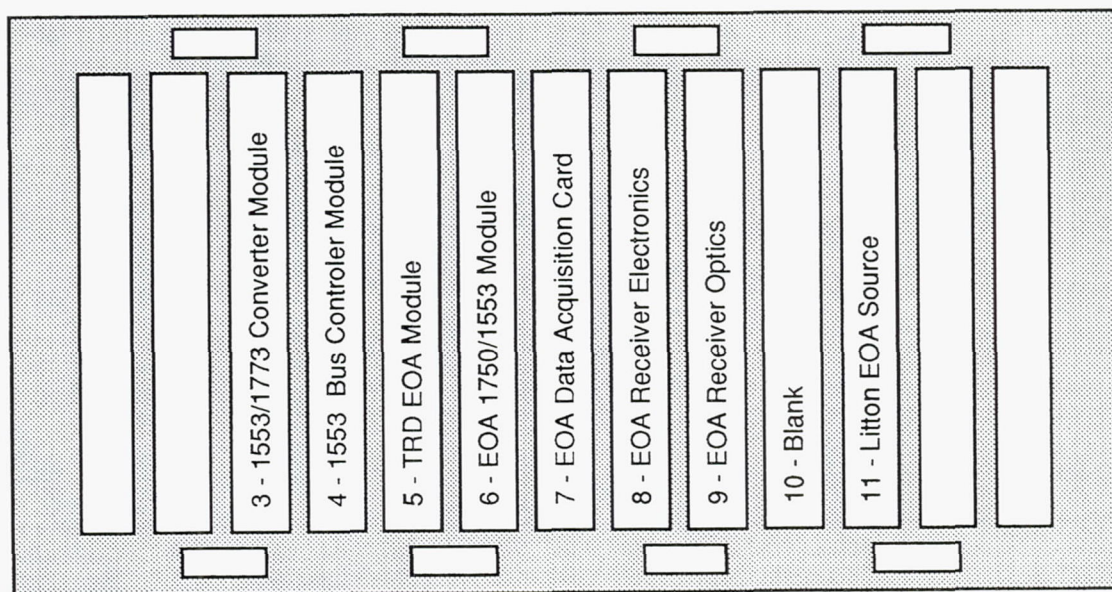
Figure 2.3-11. EOA Electro-Optic Backplane

2.3.2.3 Design of EOA Mechanical Chassis

Design of the EOA mechanical chassis was relatively straightforward. The mechanical chassis selected was an air cooled 3/4 ATR enclosure capable of holding up to 13 SEM-E modules. The enclosure was SHARP qualified, and was manufactured by MAKCO. The enclosure is compatible with forced air cooling environmental control systems, but is capable of dissipating up to 100 watts under ambient temperature conditions with no forced air. Since total power dissipation of the FOCSI EOA modules was expected to be between 50 and 60 watts, forced air cooling was not employed. The EOA mechanical chassis was delivered with a blank front panel which was modified by MDA to accommodate the connectors required for the FOCSI EOA. Figure 2.3-12 shows the EOA front panel layout.
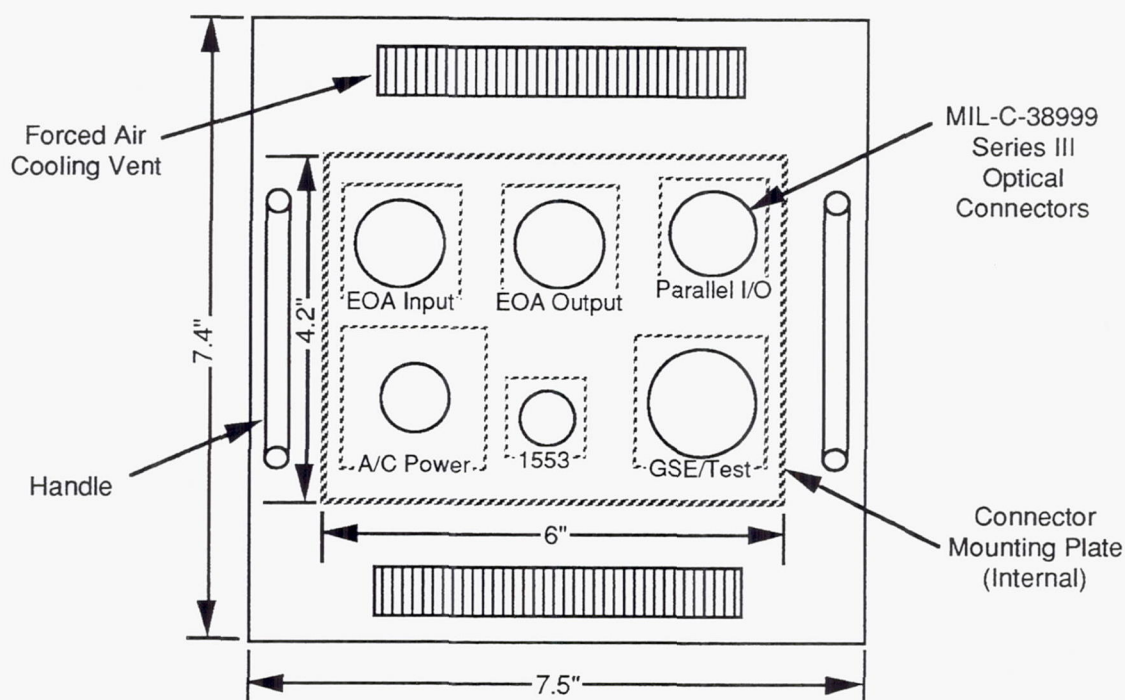
Figure 2.3-12. EOA Mechanical Chassis Front Panel Layout

2.3.3 EOA Fabrication and Assembly

2.3.3.1 Fabrication of WDM EOA Modules

Although problems were encountered in development of the WDM EOA modules, they were not entirely enexpected due to the developmental nature of the EOA. These problems or "lessons learned" resulted in redesigns and schedule slips in final delivery. To provide adequate time to complete all integration testing and still meet hardware delivery commitments to NASA-Dryden, an optically and mechanically compatible EOA prototype was used to start integration testing. Evaluation of the prototype EOA was invaluable for system checkout before final delivery of the flight test EOA.

2.3.3.1.1 TRD EOA Module Fabrication

Testing of the initial TRD module at room temperature showed that the module operated adequately, but that noise caused minor fluctuations which could be removed by signal averaging. Subsequent testing at high and low temperature extremes revealed several problems which prevented the module from operating properly. These problems required a major redesign of the TRD module, and the procurement of a new TRD Printed Wiring Board (PWB).

Fabrication of the new TRD module was completed and was tested with an actual TRD sensor. Problems during the functional integration test were traced to the LED used to excite the sensor. Although the excitation LED emitted most of its power in the proper wavelength band, it also emitted a small amount of power in the long wavelength band in which the TRD sensor fluoresces. The unwanted long wavelength optical power reflected off each connector and the sensor, and returned to the TRD module, where it passed through the optical filters and was read by the EOA as fluorescence from the sensor. The long wavelength source power was comparable in strength to the fluorescence signal from the sensor but its timing was different. Its presence with the sensor signal caused the TRD receiver to misinterpret the phase shift between the proper source signal timing and the timing of the sensor's response.

To solve the TRD optical source problem, optical filters were installed on the source to remove the unwanted wavelengths. The filters slightly increased the optical loss of the system, but the system had sufficient margin to absorb these losses.

2.3.3.1.2 EOA Optical Source Module Fabrication

The initial design of the EOA optical source module, including the optical power control, functioned properly at room temperature; but temperature cycle testing revealed a problem with the dynamic source control circuitry. When the dynamic control circuit reduced the LED drive current to compensate for increased LED brightness at low temperatures, the optical power output of the broadband LED did

not decline evenly across the output spectrum below a low current threshold. As a consequence, the only effective way to reduce the optical output of the source would be to disconnect some of the LEDs , rather than to reduce the LED drive current.

Disconnecting some LEDs became necessary after testing on the optical receiver indicated that it was more sensitive than originally expected. The tests indicated that the CCD saturated with an optical input power level at least 10 dB lower than expected. The disconnected LEDs were left in place as spares.

The completed EOA optical source module is shown in Figure 2.3-13.
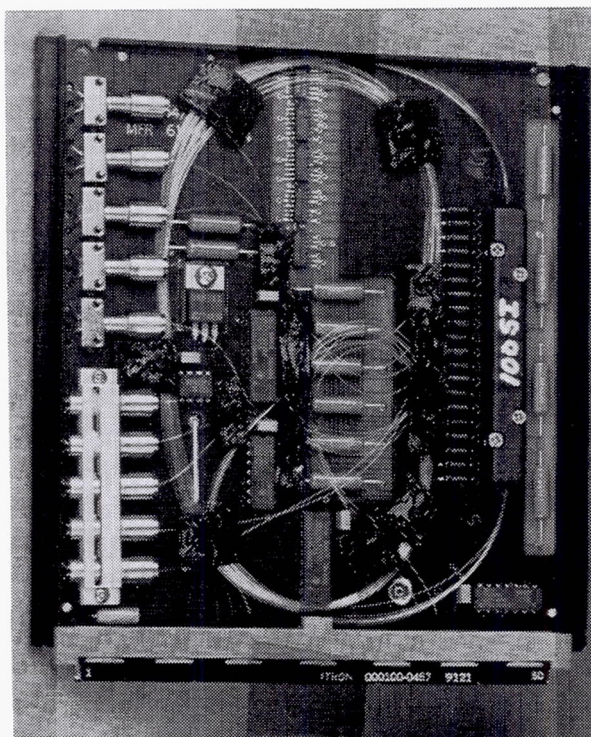
Figure 2.3-13. FOCSI EOA Optical Source Module

2.3.3.1.3 EOA Receiver Module Fabrication

EOA receiver module testing revealed problems in the optics used in the receiver and the sensor heads. The first problem was that the specified wavelengths of light were not appearing at the predicted locations on the CCD array. This was traced to a 2% to 3% shrinkage of materials in the grating/prism assembly as it cured causing the grating/prism to shift. This problem was solved with a minor tooling change. A second problem was that the fiber array holder, which aligns the fibers at an angle to compensate for some positional skewing of the optical stripes on the CCD array, was itself skewed. This resulted in higher losses than expected through the demux optics. The problem was corrected by re-aligning the fiber array holder.

Further testing of the receiver module revealed electrical signal crosstalk at the CCD array. This was corrected by shortening the CCD leads between the receiver optics module and electronics module. To compensate for the shorter electrical leads, Litton developed an active alignment method for installing the CCD array prior to locking it in place with epoxy.

Testing on the receiver to determine pixel noise levels showed that noise was close to the predicted level. However, a timing problem developed in the EOA which occasionally caused a one pixel shift in the CCD output. A correction was implemented in software by resetting the CCD buffer after reading every data frame.

Final assembly of the integrated EOA receiver module (optics and electronics) was further delayed when testing revealed a reflection in the receiver optics which caused a degradation of the receiver's performance. Since attempts to eliminate the reflection at its source were unsuccessful, the reflection was blocked externally using a beam stop. The receiver had sufficient sensitivity to operate with the slight reduction caused by the external reflection block.

The completed EOA receiver modules are shown in Figure 2.3-14.
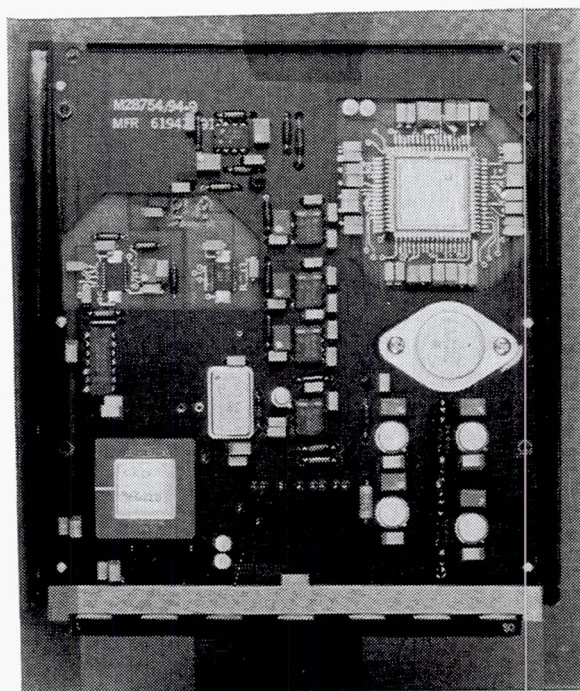
Figure 2.3-14. FOCSI EOA Receiver Modules (Optics are Underneath)

2.3.3.1.4 Data Acquisition Module Fabrication

Although design of the DAC module was relatively straightforward, technical difficulties were encountered and corrected during fabrication and checkout.

Initial inspection of the assembled DAC module revealed several missing traces which were repaired with wire jumpers. Initial testing of the DAC module over temperature revealed instability due to a timing "jitter" problem which required a major redesign of the DAC module and a second PWB layout.

Additional problems were discovered during checkout of the new DAC module. These problems included: misnumbered address lines, electromagnetic noise, and bus contention. The problem with misnumbered address lines was quickly fixed. The problem with bus contention appeared to be caused by a device attempting to talk on the bus when instructed to read from the bus. This caused a shift in pixel locations. Correcting this and the and noise problems on the DAC required a third PWB layout which successfully corrected these problems.

The completed EOA data acquisition module is shown in Figure 2.3-15.
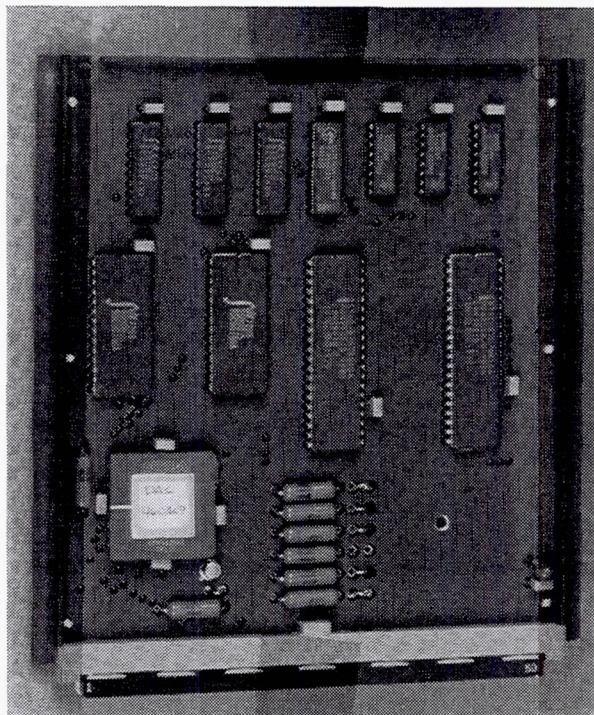
Figure 2.3-15. FOCSI EOA Data Acquisition Module

2.3.3.1.5 EOA 1750 Processor Module Fabrication

Litton purchased the 1750 processor module from DDC Incorporated, a Navy qualified supplier of SHARP 1750 processor modules. The completed EOA 1750 processor module is shown in Figure 2.3-16.
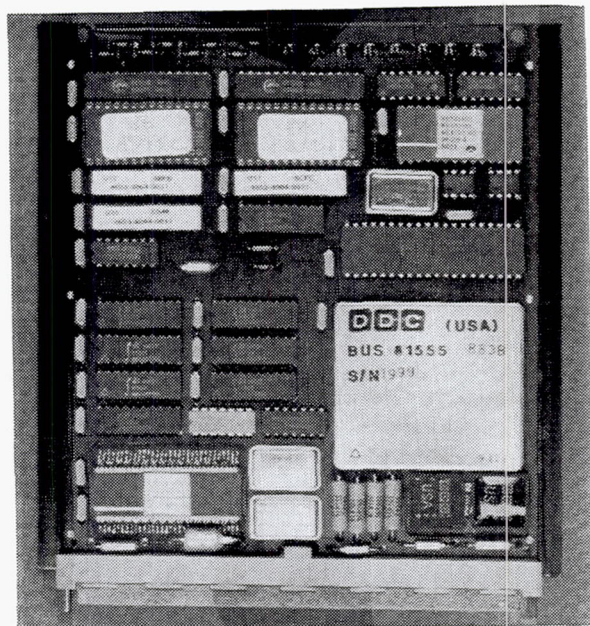
Figure 2.3-16. FOCSI EOA 1750 Processor Module

2.3.3.2 Fabrication of WDM EOA Support Modules

Fabrication of the WDM EOA support modules was accomplished by the Navy and its suppliers. This support hardware included one 1553 bus controller module, two 1773 optical data bus modules, one power supply module, one EOA backplane, and one EOA mechanical chassis. The EOA mechanical enclosure, including backplane and connectors, was the responsibility of MDA. EOA support modules such as the power supply and bus interface modules were the responsibility of MDA. NAWC had responsibility for the 1773 converter modules. Design of these support hardware elements is described below.

2.3.3.2.1 1553 Data Bus Controller Module Fabrication

Fabrication of the 1553 data bus controller was subcontracted by NAWC to DDC Incorporated, a SHARP qualified supplier of 1553 hardware. The fabrication was relatively straightforward; however, the module components were not adhesively bonded to the PWB due to a misunderstanding of the fabrication specification by DDC. This resulted in an upper vibration limit of 6 G's for the module.

After the module was received by MDA, the 1750 host processor was programmed to control the flow of data between the 1553 remote terminal addresses assigned to the FOCSI flight test hardware by MDA and GE and the NASA data acquisition equipment. Programming of the 1750 host processor was accomplished using the ADA programming language. The completed 1553 data bus module is identical in appearance to the 1553 module shown previously in Figure 2.3-18.

2.3.3.2.2 1773 Data Bus Module Fabrication

Fabrication of the 1773 optical data bus module for the FOCSI program was accomplished by the Navy as part of the SHARP activity. The 1773 transceivers were manufactured by Unisys Corporation as part of an earlier "dual-speed 1773" study completed in conjunction with NAWC. Initial fabrication of the 1773 modules revealed problems related to conducted EMI into the 1773 receiver and voltage sensitivities of the 1773 transmitter. These sections of the circuit were breadboarded to isolate the problem and identify a design solution. Both problems were eventually solved with minor design and layout changes to the 1773 module. After fabrication and functional checkout at NAWC, the 1773 modules were shipped to MDA for testing. A completed 1773 data bus module is shown in Figure 2.3-17.
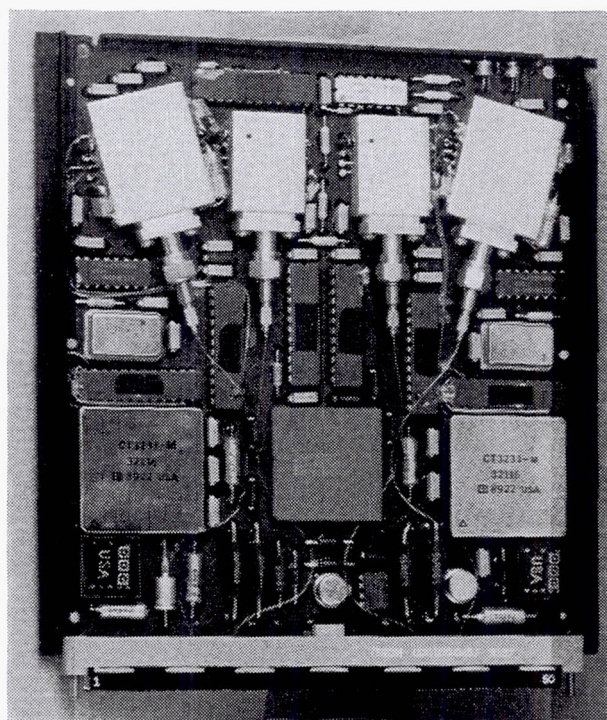
Figure 2.3-17. FOCSI EOA 1773 Data Bus Module

2.3.3.2.3 Power Supply Module Fabrication

The power supply module selected for the FOCSI program was an LVM 160 manufactured by TI, a SHARP qualified supplier of power supply modules. Fabrication of the power supply module was uneventful, as this module is a standard production item for TI. However, one minor problem did arise related to the EMI filter for the power supply module. As mentioned previously, the LVM 160 power supply module is capable of a total power dissipation of 160 watts. This was approximately three times larger than the actual power dissipation anticipated for the FOCSI modules. This resulted in a problem as the EMI filter recommended by TI for the LVM 160 power supply module was to large to be mounted internally to the EOA mechanical chassis. A smaller EMI filter design was identified and fabricated. The completed EOA power supply module is shown in Figure 2.3-18.
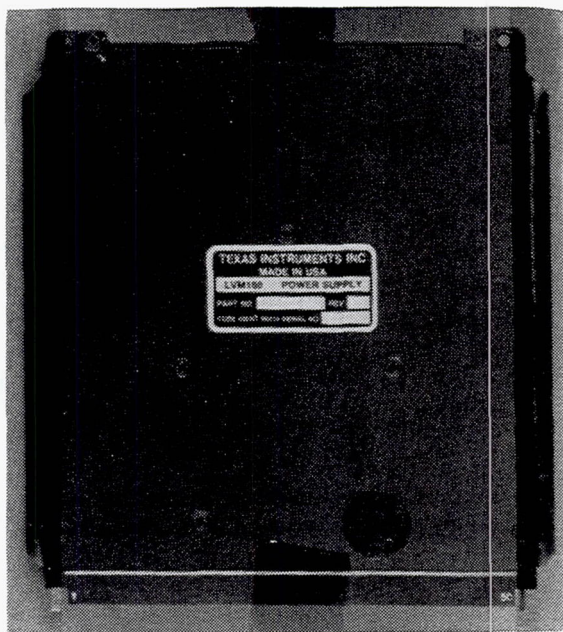
Figure 2.3-18. FOCSI Power Supply Module

2.3.3.2.4 EOA Backplane Fabrication

MDA used a hybrid electro-optic approach to fabricate of the EOA backplane, with electronic wire wrap pins used for electrical connections, and right angle butt-coupled optical contacts used for optical connections. Although fabrication of the backplane was very labor intensive, it allowed rapid modification to track the design changes which were made to the core EOA modules. A PWB backplane would have required new layouts to accommodate each design change, and would have resulted

in severe schedule slips. Ultimately the hybrid electro-optic backplane approach saved both time and money.

The completed EOA backplane is shown in Figure 2.3-19.
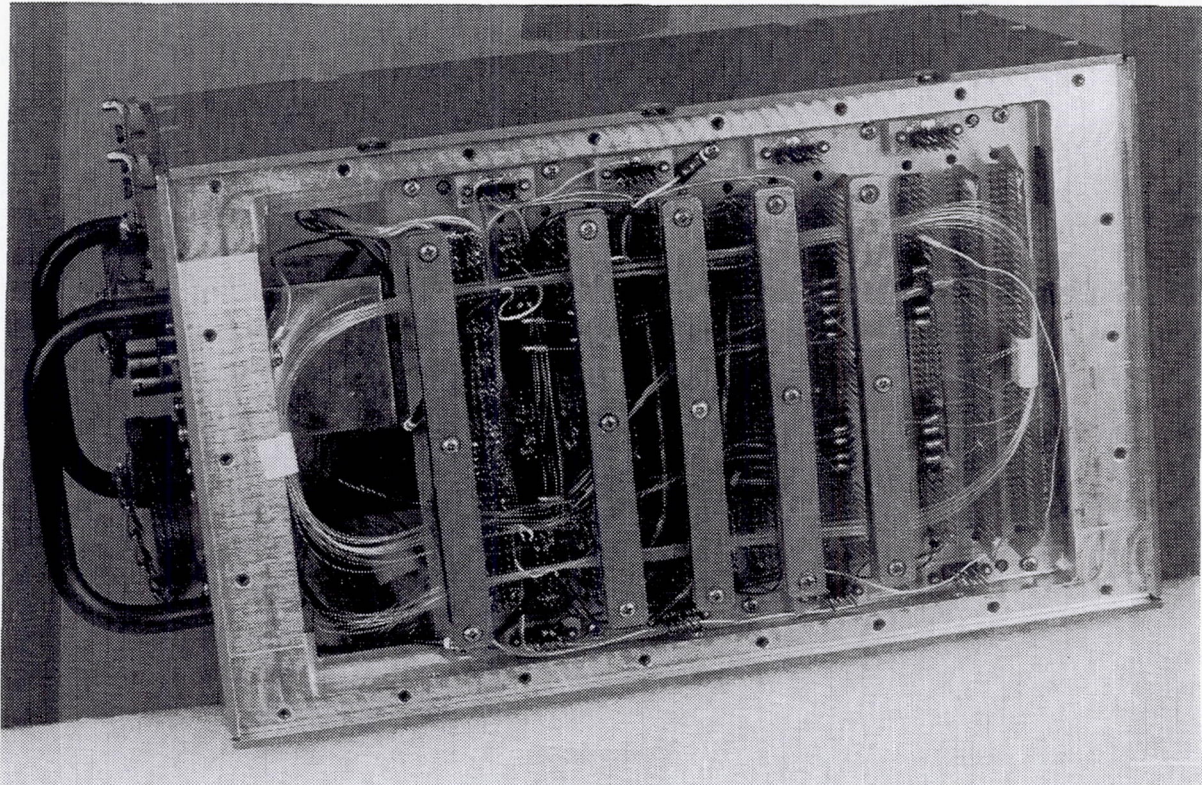
Figure 2.3-19. FOCSI EOA Backplane

2.3.3.3 EOA Mechanical Chassis Fabrication

Fabrication of the EOA chassis was accomplished by MAKCO, a SHARP qualified supplier of electronics enclosures. The EOA mechanical chassis which was delivered to MDA with a blank front panel was modified to accommodate the connectors required for the FOCSI EOA. Figure 2.3-20 shows the EOA mechanical chassis before installation of the front panel connectors.
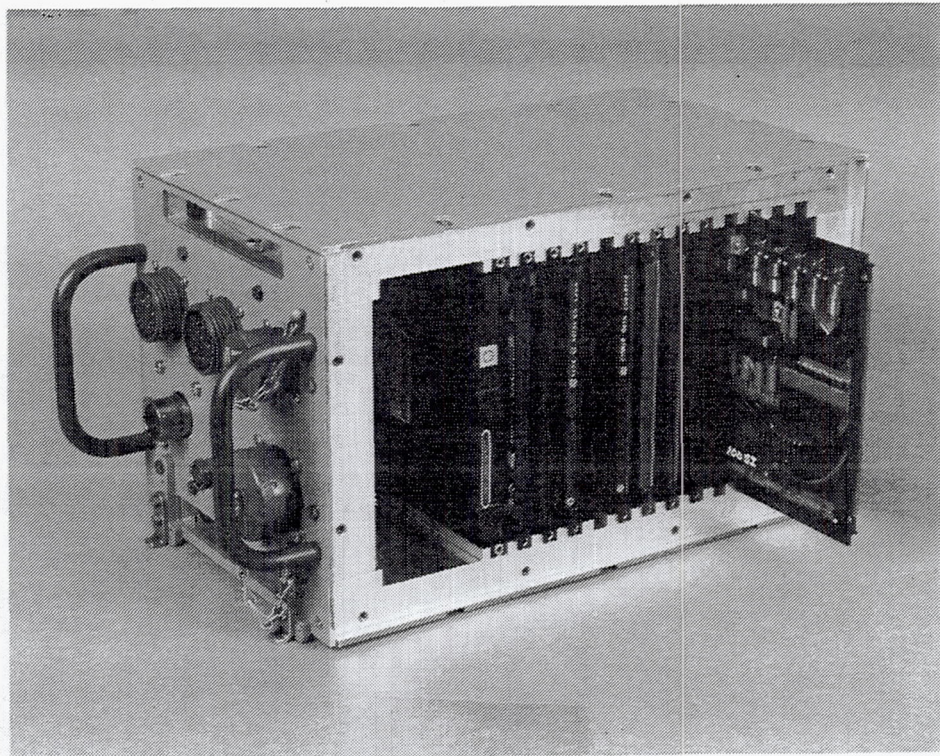
Figure 2.3-20. EOA Mechanical Chassis

2.3.4 EOA Environmental Testing

2.3.4.1 WDM EOA Module Testing

After fabrication and assembly of the individual WDM EOA modules, the five modules were integrated onto a single prototype backplane and subjected to operational, environmental (vibration and temperature), and EMI testing.

After successful functional checkout and EMI testing of the integrated WDM EOA modules, temperature testing showed that it did not perform properly over the full temperature range. At low temperatures, the information from the sensors appeared to be in the wrong places in the CCD detector. At high temperatures, the source did not always turn off for the CCD array to clock out the collected data. Temperature testing revealed that declining source power and declining CCD detector sensitivity at high temperatures caused the optical power margin for analog sensors drop to zero. At low temperatures, the increasing source power and detector sensitivity cause the same problem, but from opposite effects. At high temperatures, the signal approached the noise; at low temperatures, the receiver saturated.

The first low temperature problem was traced to the First In First Out (FIFO) data buffers in the DAC module. Those buffers were occasionally shifting the data, making the inputs appear to be on the wrong pixels. Fully correcting the problem would have required major rework on the DAC module. A work-around solution was developed by resetting the FIFOs after every frame of data was processed. The resetting corrected the problem so that no data was lost.

The high temperature problem was never solved. Fortunately, the degradation it caused in the output was too small to measure.

The lack of power margin for analog sensors at high and low EOA temperatures had no solution within the EOA. The problem did not mean that the sensors could not be decoded at high and low temperatures. What it did mean was that the optical losses in the sensors and cables must be carefully adjusted to make the power of the returned signal fall in the right range on the CCD detector. If the power does not fall in the correct range, as the source power and the detector sensitivity decrease at high temperatures, the returned signal drops into the noise floor. As part of the signal is lost, the accuracy and resolution of the decoding sufferers. At low temperatures, the increasing source power and detector sensitivity cause the signal to saturate the receiver, causing another loss of decoding accuracy and resolution. Fortunately, there was one range of power received at the detector for which the decoding of the analog sensors would not suffer at the temperature extremes; however, the optical losses had be precise for that to occur. There was no margin left for the optical losses.

The difficulties with accurately decoding the sensors were due to various causes. One cause which was not fuly accounted for was the non-linearity of the sensitivity of the CCD array to amplitude variations. A four part, piecewise-linear correction was developed which sufficiently linearized the CCD response, and yet did not overload the EOA processor. This correction allowed the EOA to correctly read the analog sensors and three of the four Litton sensors over the full temperature range. However, the EOA was still unable to read the Power Lever Control (PLC) position sensor. The reason appears to be that the block added to the demux to stop reflections strongly reduced the optical power at the long wavelength end of the spectrum; and the EOA could not identify the reference track that the PLC sensor had at that location.

The PLC sensor was vulnerable to the low power at the long wavelengths, because it had more tracks than any other sensor. The PLC sensor has a total of 15 differentially encoded tracks (30 tracks total), leaving little wavelength margin from the EOA optical source. As a result, the longest wavelength track in the PLC fell where the power was low due to the roll-off of the source and the losses caused by the optical blocking in the receiver. The PLC sensor could not be decoded without redesigning the demux optics, which the program schedule would not allow. The most efficient course was to determine the performance of the second flight test EOA and base a decision to make corrections on its performance. Therefore, the first

flight test EOA was sent to MDA. MDA began sensor/EOA integration with the understanding that the first flight test EOA would probably be declared to be a spare, and that its behavior would not be identical to that of the second flight test EOA.

Assembly of the second EOA did not take long because it was actually the prototype EOA rebuilt to meet flight requirements. Integration and environmental testing of the WDM EOA modules was successfully completed. The second EOA appeared to be better able to decode analog sensors over the full temperature range than the first EOA. This was partially due to the success with installing the optical block in the demultiplexer optics so that its effect was spread over the entire wavelength range rather than being concentrated at the long wavelength end. Testing of the second EOA was not able to show if the improved performance of the second EOA would allow it to decode the PLC temperature over the full temperature range. However, later integration testing conducted at MDA did verify better performance by EOA #2 than by EOA #1 and no further changes were made.

2.4 Sensor Fabrication

As highlighted in Figure 2.4-1, development of suitable optical sensors for application to the F-18 SRA flight control and air data systems was accomplished concurrently with EOA development.
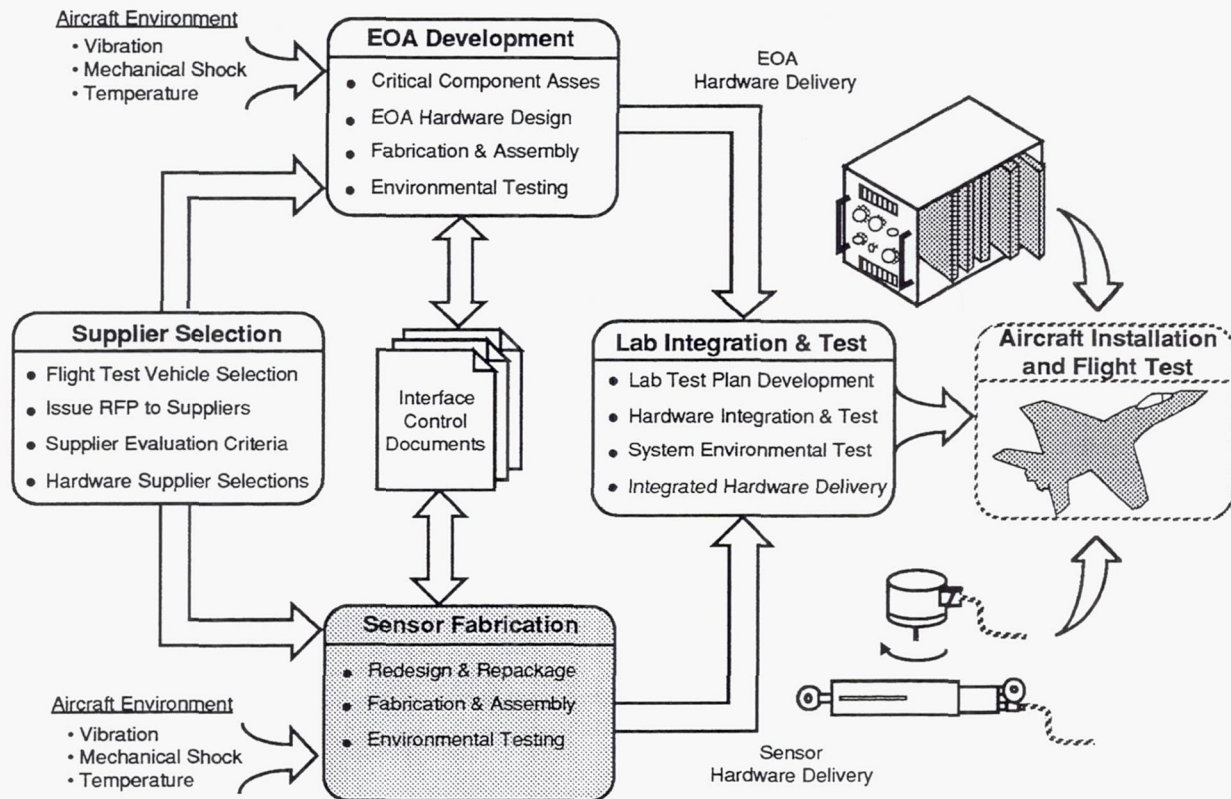
Figure 2.4-1. FOCSI Program Roadmap - Sensor Development

Selection of sensor suppliers for FOCSI was based on the following goals:

- **Maximize the number of optical sensor technologies.**
- **Maximize the number of optical sensor suppliers.**

The decision to develop an EOA based only on WDM technology drove the selection of compatible sensor suppliers. Available program funding allowed the selection of 10 WDM compatible sensors from a total of five different suppliers (Litton Poly-Scientific, BEI Motion Systems, AlliedSignal, Babcock & Wilcox, and Rosemount). A total of four different WDM optical sensor modulation technologies (WDM digital code plate, WDM analog code plate, WDM analog microbend, and fluorescent time rate of decay) were selected for FOCSI.

Figure 2.4-2 shows the relationship between FOCSI suppliers, technologies, and aircraft sensors selected.

Rudder
WDM Digital Code
(Litton Poly-Scientific)

Trailing Edge Flap
WDM Analog Ratio
(BEI Motion Systems)

Leading Edge Flap
WDM Digital Code
(Allied Signal - Bendix)

Stabilator
WDM Digital Code
(Litton Poly-Scientific)

NASA
845

Air Data Temperature
Fluorescent Decay
(Rosemount, Inc.)

Pitch Stick
WDM Analog Ratio
(BEI Motion Systems)

Power Lever Control
WDM Digital Code
(Litton Poly-Scientific)

Rudder Pedal
WDM Digital Code
(Litton Poly-Scientific)

Electro-Optic Architecture
(Litton Poly-Scientific)

Nose Wheel Steering
WDM Analog Ratio
(BEI Motion Systems)

- **10 Different Aircraft Sensors**
- **5 Different Sensor Manufacturers**
- **4 Different Optical Sensor Technologies**

Total Pressure
WDM Analog Microbend
(Babcock & Wilcox)

Figure 2.4-2. FOCSI Flight Test Hardware Configuration

The primary goal in the FOCSI sensor development effort was to redesign and repackage existing sensor technologies for application to an open-loop flight test on the F-18 SRA. Only those manufacturers with demonstratable prototype sensor technologies at the time of supplier selection were considered. The optical sensors built for FOCSI were based on one of four different mature optical sensor modulation technologies; WDM digital code plate, WDM analog code plate, WDM analog microbend, and fluorescent time rate of decay. Within each of these schemes, multiple physical implementations are possible.

FOCSI Sensor Principles of Operation

The principles of operation for each of the four different WDM optical sensor modulation technologies are described in the following paragraphs.

WDM Digital Code Plate Sensors

A total of five sensors selected for FOCSI were based on WDM digital code plate technology. These included the Rudder, Rudder Pedal, Stabilator linear position sensors from Litton; a Power Lever Control rotary position sensor from Litton; and a Leading Edge Flap linear position sensor from AlliedSignal.

An example of a WDM digital code plate linear position sensor is shown in Figure 2.4-3. The sensor operates by receiving a broadband excitation optical pulse from the EOA and using a diffractive element (usually a grating) to break the excitation into many discrete optical bands. Each optical band is physically directed do a different track on the optical code plate. The tracks may be reflective or transmissive, a reflective-type sensor is shown in the figure. The code plate alters the light intensity ("on" or "off") in each optical band according to the plate's position. It then returns the light in all the bands to the sensor optics where the light from all the bands is recombined and returned by fiber to the EOA as a wavelength encoded parallel digital bit pattern. The EOA decodes the returned wavelength pattern to determine the sensor position reading.
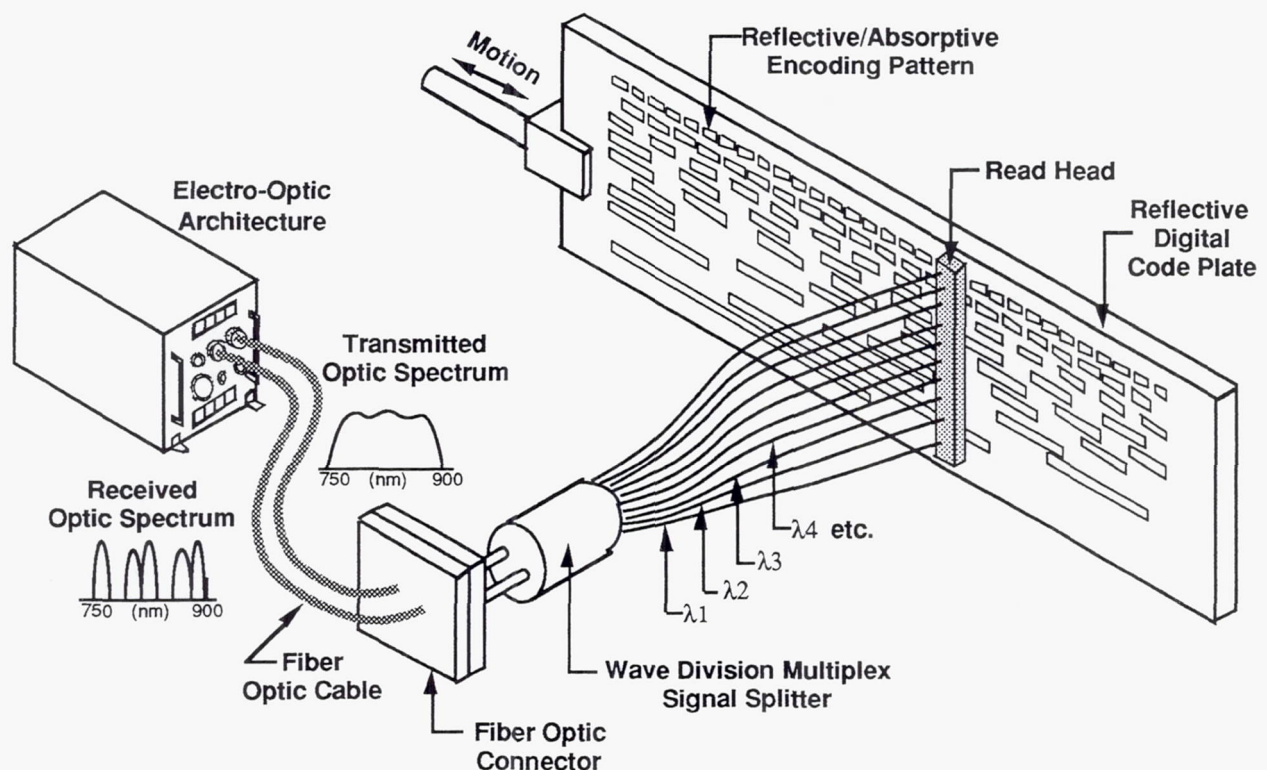
Figure 2.4-3. WDM Digital Code Plate Linear Position Sensor Operational Block Diagram

WDM Analog Code Plate Sensors

A total of three sensors selected for FOCSI were based on WDM analog code plate technology. These included the Pitch Stick linear position sensor from BEI; and the Trailing Edge Flap, and Nose Wheel Steering rotary position sensors from BEI.

An example of a WDM analog code plate linear position sensor is shown in Figure 2.4-4. In the analog sensor, the broadband light is split into only two wavelength bands. The light in the two bands is affected in the same way by all the same elements in the optical path from the EOA to the sensor and back, except that the light in one band, called the sense band, passes through a variable optical density track on the code plate and the light in the other, called the reference band passes through a track of fixed optical density. Because the optical density of the first track varies with position, the intensity of light passing through it is a function of the sensor position. Because the optical density of the second track is uniform, the intensity of light passing through it is not a function of the sensor position. Because the light in the reference band is identical to the light in the sense band except for the effect of sensor position, the light in the reference band can be used as a system reference. By taking the ratio of the two signals, the sensor output can be made insensitive to variations in the optical source, cables, or connectors.
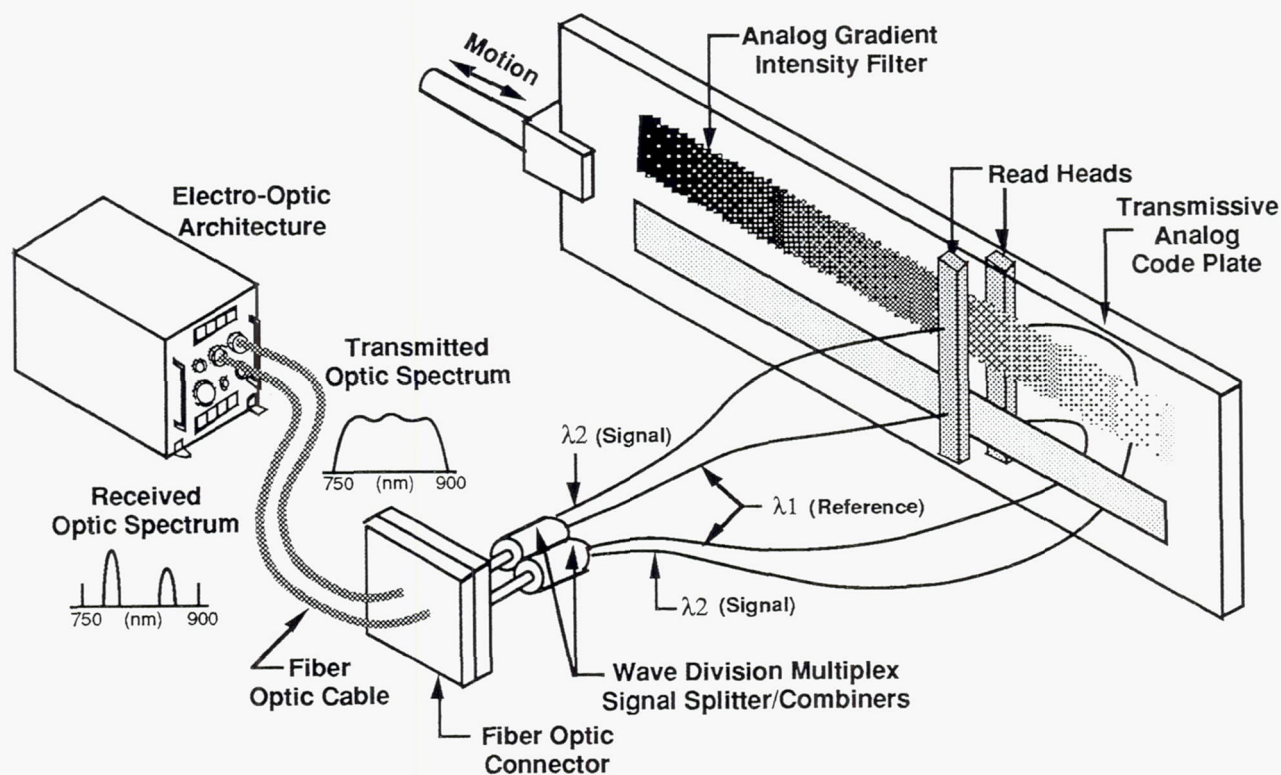
Figure 2.4-4. WDM Analog Code Plate Linear Position Sensor Operational Block Diagram

WDM Analog Microbend Pressure Sensor

The third type of sensor produced was a Microbend Optical Pressure Sensor produced by Babcock and Wilcox. This is an analog sensor, and optically its operation is identical to the operation of an analog optical position sensor. The difference, shown in Figure 2.4-5, is that the light in the sense band of a microbend pressure sensor does not leave the fiber and reach an intensity modulated code plate. Instead, the sensing light is always confined to a fiber, but the fiber is set between two sets of teeth. The fiber and the teeth serve the same purpose as the sense track on an analog optical code plate in a position sensor. In use, one set of teeth is locked in place, however, the position of the other set depends upon the pressure applied to the diaphragm. The fiber is bent between the two sets of teeth, and each bend causes some of the light in the fiber to leak out. The higher the pressure on the diaphragm, the more the movable teeth are pushed in, and the sharper the fiber is bent. The sharper the fiber is bent, the more light leaks out and the higher optical loss. Thus, the optical loss of the sense fiber is a function of the pressure on the diaphragm. Once pressure is encoded as optical loss, the optical signal can be treated the same as that from an optical position sensor.
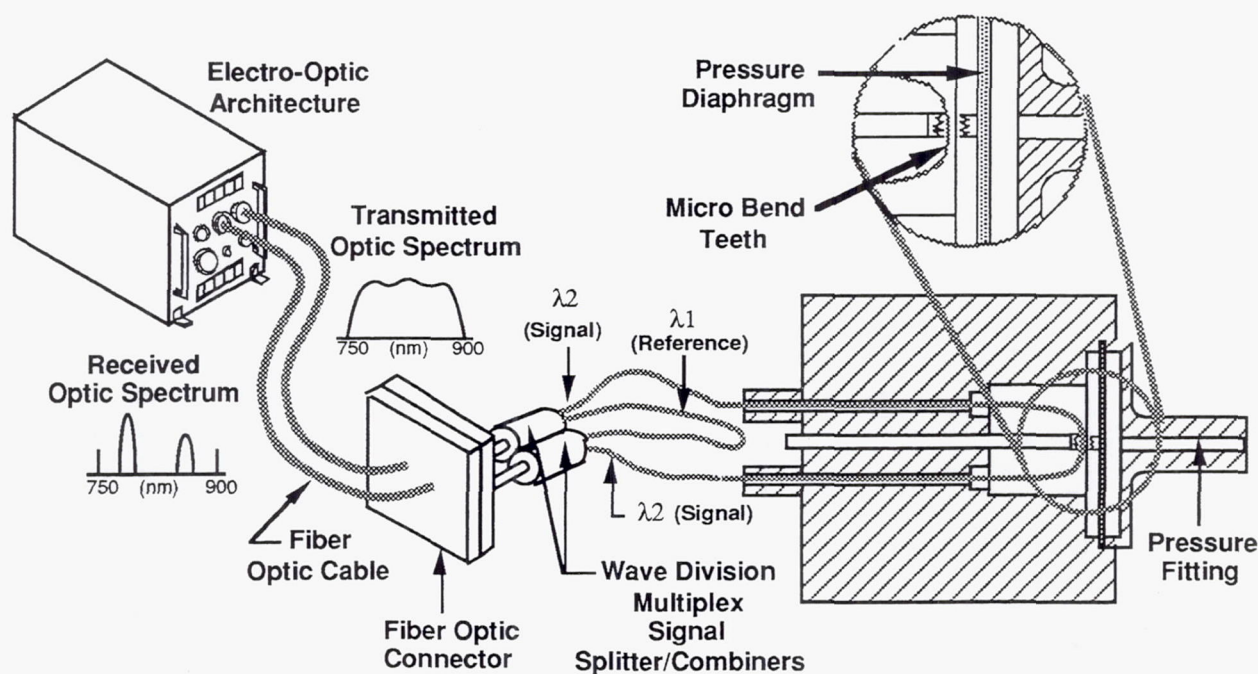
Figure 2.4-5. WDM Analog Microbend Optical Pressure Sensor
Operational Block Diagram

Fluorescent Time Rate of Decay Temperature Sensor

The operation of a Time Rate of Decay temperature sensor is illustrated in Figure 2.4-6. For the TRD sensor, the EOA produces a temporally narrow optical pulse to excite the sensor. The sensor contains a sensing element which responds to the optical excitation pulse by emitting light at a slightly longer wavelength than the excitation pulse; that is, it is photoluminescent. The intensity of the emitted pulse decays with time. The useful property of the sensing element is that the decay time of the emitted pulse is dependent upon the temperature of the sensing element. The EOA decodes the returned signal by comparing the strength of the returned signal at different times to determine the sensor signal decay time and thereby determine the sensor temperature.
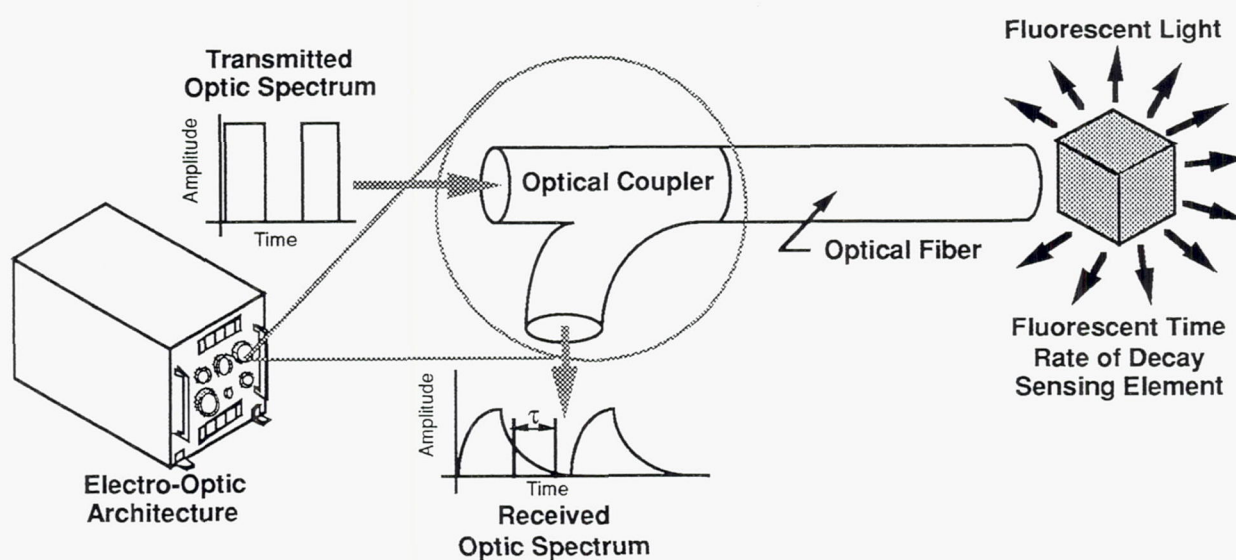
Figure 2.4-6. Time Rate of Decay Temperature Sensor Operational Block Diagram

As a general rule, the problems encountered in developing each sensor technology for FOCSI were common for a given technology, but unique among the different suppliers of that technology. As a case in point, Litton fabricated one rotary and three linear position sensors based on WDM digital code plate technology. For the most part, the lessons learned in the fabrication of the linear sensors applied directly to the fabrication of the rotary sensor and vice versa. AlliedSignal also developed a rotary position sensor based on WDM digital code plate technology. Unfortunately, the lessons learned in the development of the AlliedSignal sensor were totally different than those learned in the development of the Litton sensor. Even if the lessons learned did apply to multiple suppliers, the suppliers were generally not willing to share this information for fear of revealing proprietary technology and possibly losing a competitive advantage. Because of this fact, the discussion of FOCSI sensor development activities will be logically grouped by sensor supplier for each development activity.

2.4.1 Sensor Redesign and Repackaging

The primary goal in the FOCSI sensor development was to redesign and repackage existing sensor technologies for application to an open-loop flight test on the F-18 SRA. For the most part, this was accomplished by designing the optical sensor to be installed "piggybacked" on the existing F-18 sensors. This approach gives the benefits of allowing a direct comparison between optical and electrical sensor performances while maintaining the integrity of the production flight control system. This demanded the development of fiber optic sensors which were "non-intrusive" to the existing F-18 SRA flight control and air data systems. The result was several innovative and unique sensor design and repackaging approaches as described in the following sections.

2.4.1.1 Air Data Temperature Sensor

2.4.1.1.1 Design.

Rosemount was selected to construct an Air Data Temperature Sensor, based upon Rosemount's Time Rate of Decay (TRD) sensor proposal. As a first step, Rosemount generated detailed TRD sensor interface requirements which were submitted to the EOA supplier, Litton Poly-Scientific, for review and approval. After approval of the sensor ICD parameters, sensor mechanical design commenced. Rosemount proposed the construction of a "non-intrusive" optical air data temperature probe by installing an optical TRD element inside of a production F-18 air data probe. An outline drawing for the FOCSI Air Data Temperature Sensor is shown in Figure 2.4-7. Since Rosemount is the manufacturer of the production F-18 probe, sensor mechanical design for FOCSI primarily concentrated on the modifications necessary to incorporate the TRD sensor into the probe with the current electrical sensor and the deicing heaters.
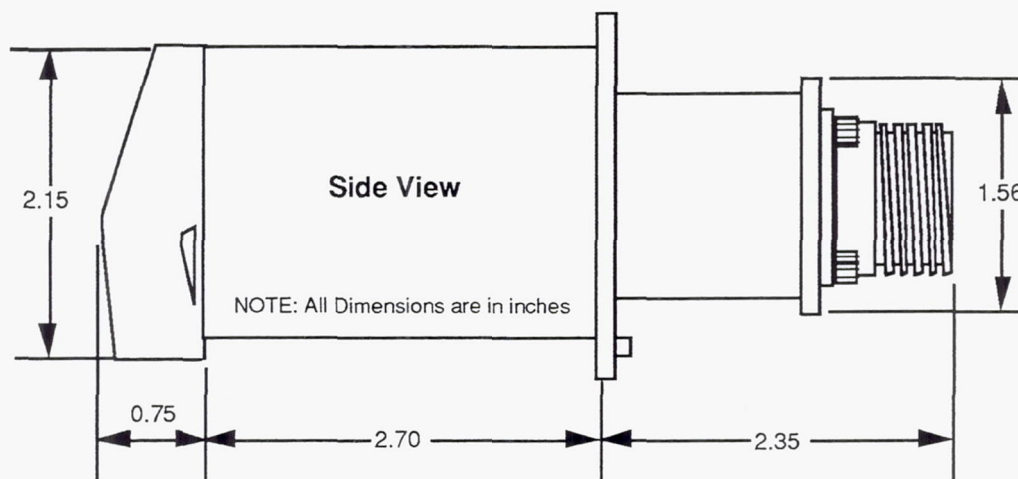
Figure 2.4-7. Air Data Temperature Sensor Mechanical Envelope

Placing of the TRD sensor inside the existing Air Data Temperature probe had advantages as well as some disadvantages. The disadvantages stemmed from the fact that the aircraft relies on data from the electrical temperature sensor inside the probe for generating flight control information. Therefore, it was critical to prove that the incorporation of the TRD sensor would not interfere with the operation of the electrical sensor; or if it did interfere, that the behavioral changes caused were predictable. To address this issue, Rosemount proposed to construct three prototype TRD sensors for wind tunnel testing. The three prototypes differed only in the physical relationship between the dual electrical sensor element and the TRD sensor element. Evaluation of the prototype probes led to the selection of an approach in which the two sensors are placed side by side within the existing probe. Two of the prototype probes constructed using this approach demonstrated only negligible effects upon the operation of the existing electrical sensor.

Next, Rosemount investigated possible approaches for connecting the fiber to the sensor. One approach was to add a fiber connector to the sensor base. This method was originally preferred; however, the sensor base was not large enough to accommodate the optical connector. Another method was to replace the existing electrical connector with a MIL-STD-38999 connector containing electrical and optical contacts. This approach would require the construction of a jumper cable to connect the 38999 connector to the existing electrical cable, and split out the optical fiber. After inspecting the flight test aircraft to verify adequate installation clearance, MDA recommended the jumper cable approach. The cable configurations without and with the optical sensor and jumper are shown in Figure 2.4-8.
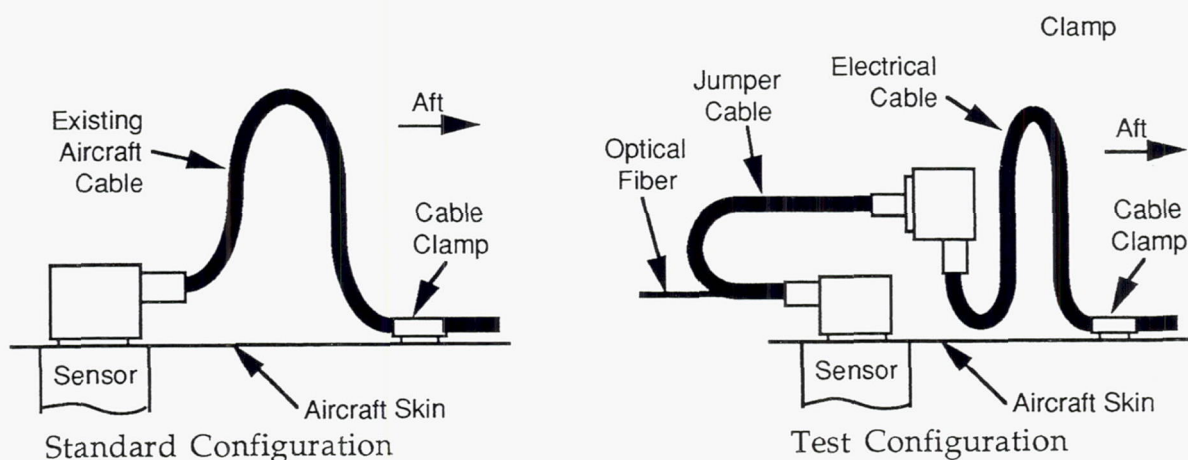
Figure 2.4-8. TRD Sensor Installation Configuration

With the optical connector issue resolved, Rosemount began the detailed design process by evaluating the process issues which could discriminate between the two approaches for locating the optical and electrical sensors inside the probe. Rosemount identified several manufacturing processes which may potentially affect sensor performance. These included brazing operations near the fiber, strain relief on the fiber, and the length of fiber from the sensing tip to the optical pin. From this effort, Rosemount determined that the side-by-side approach was superior due to manufacturing and assembly process considerations. Preparation of specifications and design drawings for such a sensor, and construction of a prototype sensor for final testing was initiated. Rosemount tested the prototype sensor in a wind tunnel to demonstrate its accuracy in comparison to the baseline electrical sensor. Wind tunnel testing showed that the prototype sensor performed well, tracking with $\pm\ 0.5°$ of the reference electrical sensor. Based on the results of prototype sensor evaluation, Rosemount was given authority to proceed with sensor fabrication.

2.4.1.1.2 Fabrication.

Rosemount initiated sensor fabrication, ordered long lead sensor hardware, and wrote software to automate sensor test evaluation. During sensor fabrication, it was discovered that the air data temperature reference, called Total Temperature, available to the NASA data acquisition system from the Air Data Computer is a function of the temperature measured by the standard electrical sensor and the Mach Number of the aircraft. Since the EOA does not receive the Static and Total Pressures, it cannot calculate the Mach Number needed to then calculate the Total Temperature. Therefore, the temperature indicated by the TRD sensor and the temperature collected from the air data computer will disagree. MDA determined that the most practical resolution to the disagreement is to assure that the NASA data acquisition system records the Mach Number (from the Air Data Computer) or records the Static and Total Pressures (from which Mach Number is calculated) along with the Total Temperature. The Mach Number correction would then be applied to the TRD sensor values in post-flight data reduction.

A potential problem arose concerning the deicing heater error compensation of the electrical sensor at very low flight speeds. To resolve questions related to deicing heater and recovery error compensations respectively, additional wind tunnel testing of the prototype sensor was conducted in the flight speed regimes below 0.3 Mach and above 0.7 Mach. Tests performed on adiabatic recovery error in the 0.7 to 0.9 Mach regime on the electrical sensor co-located with an optical sensor showed errors slightly greater than the errors seen for electrical sensors in unmodified configurations. However, the errors remained within the allowable ranges. In addition, the trend of the recovery error indicated that the error was unlikely to exceed the allowed limit at high but untested Mach numbers. The electrical sensor response did go out of tolerance at low speeds (0.2 to 0.3 Mach) due to the effect of the deicing heater. The departure from specification was found to be small and predictable; therefore, MDA notified NASA of the error in a Safety Assessment Report, so that NASA could institute the appropriate procedural changes.

After the additional wind tunnel testing, Rosemount performed vibration testing on the prototype sensor. The calibration of the two electrical elements was unchanged after successful completion of the vibration testing. The TRD element was within two degrees of the initial calibration. The two degree error was removable by re-calibration, and further drift was not seen. Rosemount believes the error was caused by compacting of the fluorescent powder used in the sensor element as a result of vibration.

The completed TRD temperature sensor is shown in Figure 2.4-9.
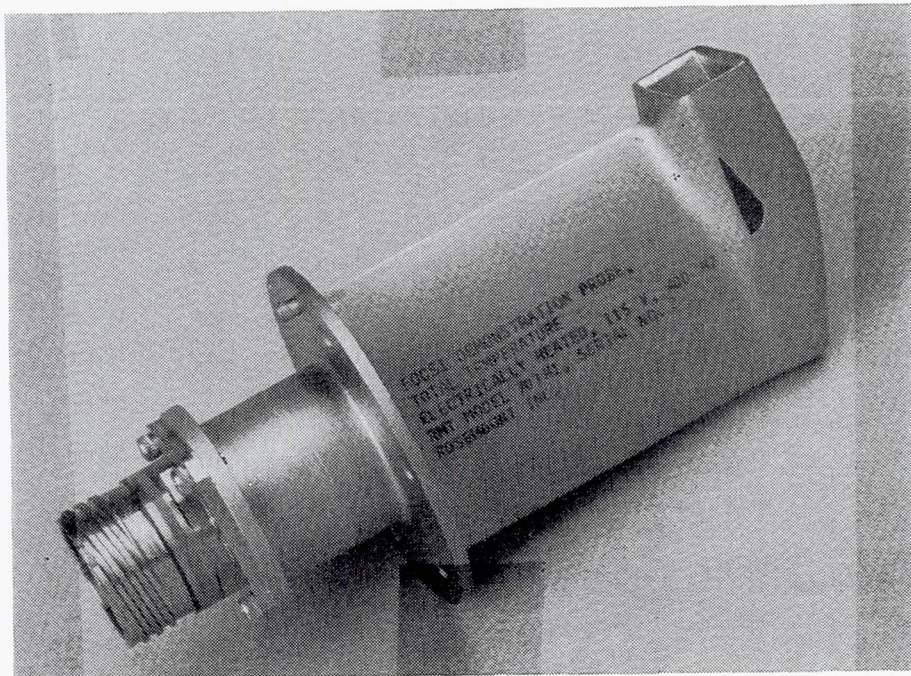
Figure 2.4-9. FOCSI Air Data Temperature Sensor
(TRD Fluorescent Decay, Rosemount Aerospace)

2.4.1.1.3 Performance Testing and Delivery to MDA.

Rosemount conducted operational and environmental testing of two FOCSI air data temperature sensors. Operational testing consisted of wind tunnel testing to demonstrate proper operation of both the optical and electrical sensors. Wind tunnel testing of the deliverable hardware verified that the de-icing heater error and recovery errors were within acceptable limits as specified by MDA. Environmental testing included temperature, altitude, and vibration testing to ensure compatibility with F-18 aircraft environments. Successful operational and environmental testing of the air data temperature sensors was witnessed by MDA, and the sensors were subsequently shipped to MDA for laboratory integration testing.

2.4.1.2 Leading Edge Flap Position Sensor

2.4.1.2.1 Design.

AlliedSignal was selected to construct a Leading Edge Flap (LEF) asymmetry detector rotary position sensor, based upon AlliedSignal's WDM digital sensor proposal. As a first step, AlliedSignal generated detailed sensor requirements which were submitted to the EOA supplier, Litton Poly-Scientific, for review and approval. After approval of the sensor ICD parameters, sensor mechanical design commenced. AlliedSignal personnel visited MDA to inspect an F-18 aircraft to obtain physical information to begin mechanical design of the LEF sensor. While inspecting an aircraft, three difficulties were identified. First, the production asymmetry detector is quite large and left little room for adding an additional "piggyback" optical sensor. Second, the sensor contained an internal reduction gear set so that the multiple rotations of the drive shaft could be translated into less than one rotation of the Rotary Variable Differential Transformer (RVDT). That meant that an optical sensor could not be placed ahead of the sensor, because in such a location it would read multiple shaft rotations. Third, the optical sensor could not be placed after the present sensor, because the electrical connectors would interfere with the operation of the optical sensor.

As a solution, it was decided to locate the LEF optical sensor at one of the leading edge flap hinges and directly connect it to the wing and flap. This approach allows direct reading of LEF flap angle and does not interfere with the existing sensor system. However, this approach has a disadvantage that aerodynamic loading forces experienced by the wing during flight cause the relationship between commanded LEF shaft position and real flap position to be unpredictable within the error imposed by twist in the LEF. Thus, the position read by the electrical position sensor on the shaft and the optical position sensor on the flap could not be directly compared. Also a sensor installed in that location would have to be designed so as not to interfere with flap motion in the event of sensor breakage or jamming. This problem was resolved by the installation of an electrical rotary position sensor on the LEF flap at the same location to be used by NASA for direct comparison with the optical position sensor. An outline drawing for the FOCSI LEF position sensor is shown in Figure 2.4-10.
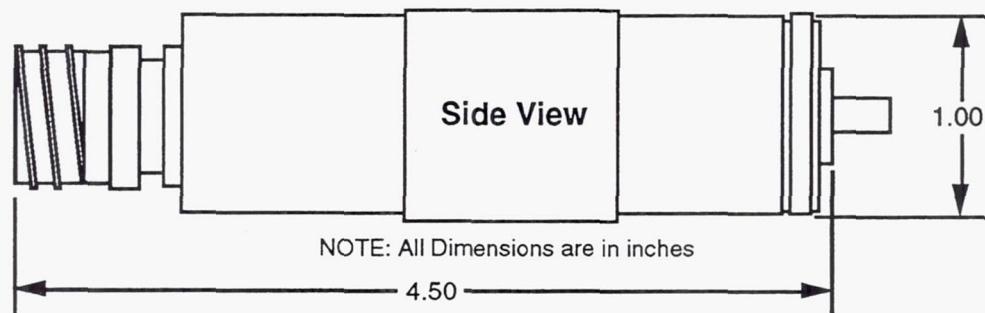
Figure 2.4-10. LEF Sensor Mechanical Envelope

While aircraft installation options were formulated, AlliedSignal proceeded with preliminary optical design of the LEF rotary sensor and design of the WDM digital code plate. AlliedSignal's WDM sensor design departed somewhat from the traditional approach usually used by WDM digital optical sensor manufacturers. Most manufacturers of WDM digital optical sensors design sensors in which the wavelength bands corresponding to particular digital optical tracks on the code plate are separated by what are called "guard bands". The guard bands are wavelength regimes which are not read by the receiver and therefore serve to reduce the cross-talk between optical bands by separating the bands. The guard band approach works well, in theory, with direct reading of the bands by an array of photo diodes or a CCD array. This assumes that the signals from particular photodiodes or particular pixels of the CCD array always correspond to particular wavelength bands.

AlliedSignal's experience with using the guard band approach was that problems with cross-talk exist despite the guard bands. Real world conditions, in which temperatures vary, linear code plates are not exactly straight, and rotary code plates do not have the axis in the exact center, contribute to decoding problems. Because of the decoding problems which AlliedSignal had previously experienced, they developed a new approach to decoding a WDM digital sensor in which the signal returned over the entire wavelength band is processed in the frequency (rather than time/amplitude) domain. AlliedSignal found that when the signal was processed in this fashion, guard bands were no longer necessary, and the requirement for large contrast ratio between high and low signals was greatly reduced.

The drawback of AlliedSignal's approach was that the EOA was being designed by Litton to work with a variety of sensors, both analog and digital, from several manufacturers. Litton was not certain that they would be able to decode the low contrast ratio, no guard band, AlliedSignal sensor.

Compounding the difficulties was the fact that the AlliedSignal sensor had the highest optical insertion loss of any of the sensors. This high optical loss was largely caused by the fact that the sensor had to be small in diameter (approximately 1.0 inch) to fit within the flight test aircraft. This small diameter forced AlliedSignal to design the sensor to use 50 μm core fiber internally. However, the aircraft cable used 100 μm core fiber, so an approximately 6.0 dB excess loss was to be expected, just due to the transition between the 100 μm and 50 μm core fibers at the sensor input.

In addition to the design issues involving optical loss and contrast ratio, AlliedSignal also determined that, regardless of the decoding approach, it was necessary to add some reference tracks to the code plate. The signal from a reference track never changes in strength, but it may vary in wavelength depending upon temperature or code plate irregularities. By finding the wavelength of the reference tracks, the receiver can locate all the signal tracks. However, this also meant that there had to be more wavelength bands, and that each band had to be narrower.

The issue was finally resolved with an agreement between AlliedSignal and Litton that if AlliedSignal could produce a sensor with no more than 28 dB of optical loss and no less that 6 dB of contrast ratio, or no more than 27 dB of optical loss and no less that 5 dB of contrast ratio, the Litton EOA would be able to decode it.

Based on the evaluations of LEF sensor detailed designs, AlliedSignal was given authority to proceed with sensor fabrication.

2.4.1.2.2 Fabrication.

After fabrication of the first FOCSI LEF sensor was completed, preliminary sensor testing found a problem with variable values for insertion loss and contrast ratio. The cause of the problem was found to be the process of making the sensor gratings from the master. The original copying process appeared to partially melt the epoxy master grating. This partial melting caused a loss of blaze angle in the copy gratings. Two new master gratings constructed of metal were ordered. However, attempts to make production gratings from these masters damaged both. New masters were ordered again.

During sensor optical testing, a question arose concerning the measurement of contrast ratio. Measured contrast ratio can be affected by the resolution of the test equipment, with higher resolutions yielding higher apparent contrast ratios. MDA stipulated that the acceptance criterion for the sensor would be to achieve the necessary contrast ratio when measured with a resolution mimicking that of the EOA, which was believed to be 0.75 nm. Since AlliedSignal did not have a spectrum analyzer with that resolution, they assembled a prototype sensor with one of the original damaged epoxy gratings and brought it to MDA to have the contrast ratio measured on the spectrum analyzer which would actually be used for sensor acceptance testing at MDA.

Tests using the available 0.5 and 1.0 nm resolution settings to bracket the 0.75 nm resolution of the EOA showed that the LEF sensor with the damaged grating was able to meet the contrast ratio requirement. AlliedSignal then used that sensor as a reference for measuring the contrast ratio of flight test sensors with the spectrum analyzer available at AlliedSignal. (Note that because of detector changes in the EOA and the characteristics of the EOA optics, the expected 0.75 nm resolution was not realized by the EOA. The actual resolution is not known precisely, but appears to be closer to 2.0 to 3.0 nm. This resolution discrepancy created some difficulties with decoding the LEF sensors. These difficulties and their resolution will be discussed later in this section.)

Following the tests, AlliedSignal assembled the two flight LEF sensors immediately upon receipt of the production gratings. Although the gratings had sub optimal optical blazing, the tests at MDA had shown that the gratings would meet the FOCSI performance requirements. The completed LEF sensor is shown in Figure 2.4-11.

Figure 2.4-11. LEF Position Sensor
(WDM Digital Code Plate, AlliedSignal)

2.4.1.2.3 Performance Testing and Delivery to MDA.

AlliedSignal conducted operational and environmental testing of two FOCSI LEF sensors. Operational testing consisted of verifying optical parameters, using the test sensor evaluated at MDA as a contrast ratio reference. Environmental testing included temperature, altitude, and vibration testing to ensure compatibility with the F-18 aircraft environments. Successful operational and environmental testing of the LEF sensors was witnessed by MDA, and the sensors were subsequently shipped to MDA for laboratory integration testing.

2.4.1.3 Air Data Pressure Sensor

2.4.1.3.1 Design.

Babcock and Wilcox (B&W) was selected to construct an Air Data Total Pressure Sensor, based upon B&W's WDM analog microbend sensor proposal. As a first step, B&W generated detailed sensor requirements which were submitted to the EOA supplier, Litton Poly-Scientific, for review and approval. After approval of the sensor ICD parameters, sensor mechanical design commenced. An outline drawing for the FOCSI Air Data Pressure Sensor is shown in Figure 2.4-12.
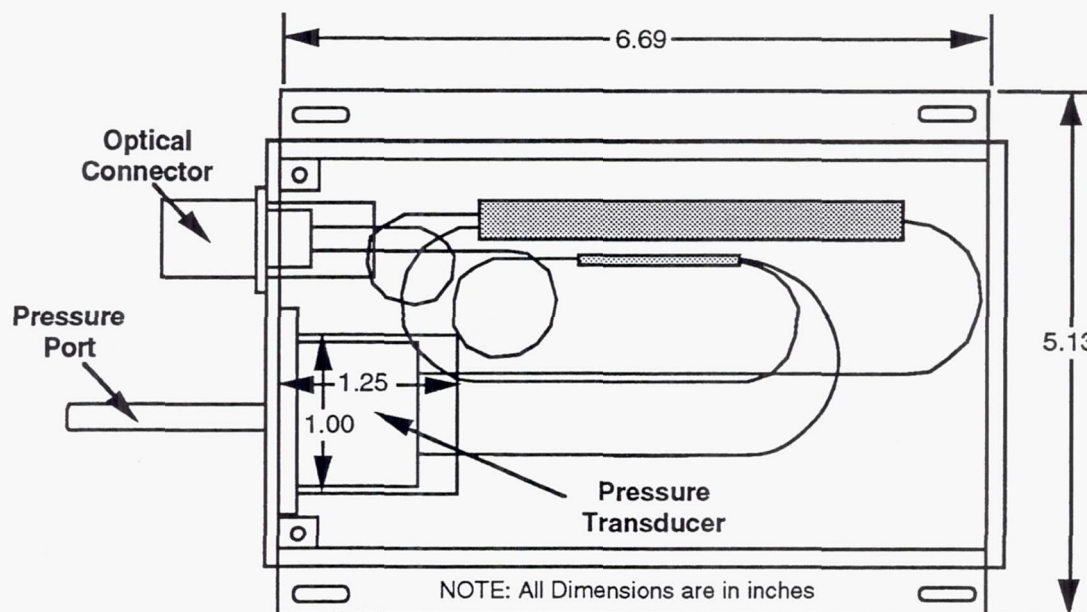
Figure 2.4-12. Air Data Pressure Sensor Mechanical Envelope

In order to meet the stringent accuracy requirement (0.1%) of the existing air data pressure sensor, optical source variation with time had to be very limited, or measured and compensated for by the EOA. Both B&W and Litton believed that meeting the accuracy requirement was possible; however, Litton believed that the source could not be built to operate inherently with the stability that the pressure sensor required. Consequently, the EOA source power would have to be measured and compensated for by the EOA.

One of the major issues of using the microbend type of pressure sensor which B&W proposed was controlling the temperature sensitivity of the pressure sensor. B&W was selected as the pressure sensor supplier, in part, because they recognized that temperature sensitivity could be a problem, and they proposed several possible solutions. Very early in sensor definition, B&W began work on defining the advantages and disadvantages of several methods for measuring the temperature of the pressure sensor.

B&W evaluated several design alternatives to achieve temperature compensation within the sensor itself. It was reported that the need to meet the 0.1% accuracy requirement resulted in a need for a -30 dB limit on cross-talk rather than the -20 dB expected. Such a cross-talk limit would be difficult to meet with current technology and a reasonable insertion loss in the baseline approach, shown in Figure 2.4-13. In the baseline approach, three wavelength channels were used. They were split out in a WDM at the sensor and a separate channel provided for the pressure and temperature sensors and the reference path.
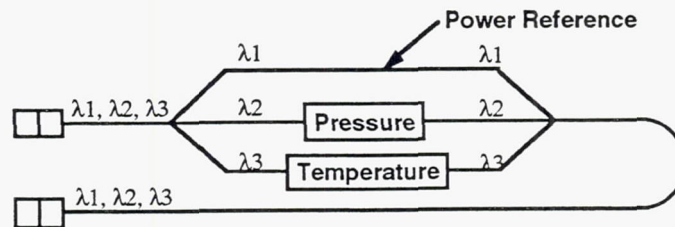
Figure 2.4-13 Baseline Pressure Sensor Approach

Two alternatives to the baseline were evaluated. One used a two channel design on a single port. The other used a two channel design at each of two ports. The two channel and two port approaches are shown in Figure 2.4-14(A) and Figure 2.4-14(B) respectively. The reasons for the differences between the baseline three channel approach and the two alternatives are described below.
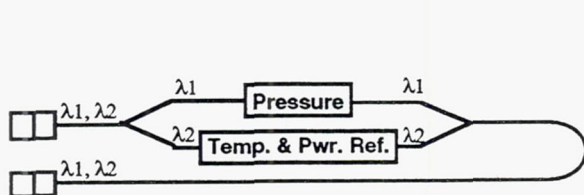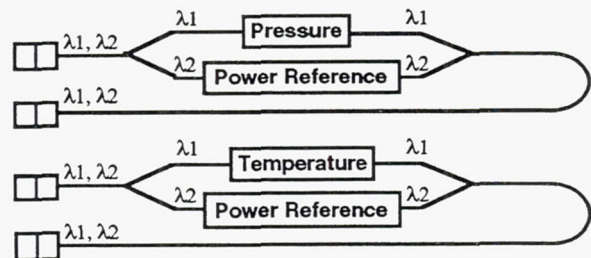
(A) Two Channel Approach   (B) Two Port Approach

Figure 2.4-14 Alternate Pressure Sensor Approaches

The two channel approach, shown in Figure 2.4-14(A), placed the temperature and reference on the same channel. This approach would be feasible if a temperature sensor could be made which has the same response to temperature changes as the pressure sensor. Thus the pressure and reference (containing the temperature sensor) responses would be the same over temperature changes and their ratio would be unchanged. An option to this was that if the pressure sensor could be made to have an opposite response to temperature changes as the temperature sensor, the two sensors could be put in series so that the combined pressure/temperature system would show no reaction to temperature changes over the temperature range of interest. This option would still require a reference leg to allow cancellation of variations in cable and sensor insertion loss.

The two port approach, shown in Figure 2.4-14(B), would be required if the responses of the pressure and temperature sensors to temperature changes could not be related in either of the two desired ways described above. In the two port approach, each port supported a two channel sensor. One port supported a pressure sensor and a reference, and the other supported a temperature sensor and a reference. Correction of the pressure reading for temperature effects would be accomplished by software in the EOA.

Since B&W believed that production of a temperature sensor with the same response as the pressure sensor was possible, the two channel approach shown in Figure 2.2-14(A) was tentatively selected as the preferred approach with the two port approach (Figure 2.4-14(B)) as the alternative. B&W requested that MDA determine the validity of the 0.1% accuracy requirement. MDA withheld approval to proceed with detailed design until B&W could answer questions about their ability to meet the accuracy requirement and questions about the production of a proper vacuum reference for the sensor.

B&W proceeded with production of the temperature reference with the intent of making a selection from the two preferred temperature compensation approaches based upon the characteristics of the temperature sensor produced. For the temperature reference, B&W began production of a temperature sensor made of $100/140$ μm fiber, similar to their existing sensor which was made with fiber of a different size. Testing on a temperature sensor using $100/140$ μm fiber uncovered inconsistencies and non-repeatabilities of data that was eventually traced to poor fiber quality. Further tests were conducted using $150/180$ μm fiber. Test results showed repeatable thermal results which indicated that it should be possible to compensate the microbend pressure sensor to within 0.3% over the required temperature range, but maybe not to 0.1%.

Because of the nature of questions remaining about the compensation and reference, B&W proposed to develop a prototype pressure transducer to demonstrate that satisfactory solutions exist for thermal compensation, aluminum braze materials, and long term vacuum integrity. This prototype was developed with B&W internal research and development funds already in place. While the prototype sensor design was proceeding, microbend sensitivity, thermal drift, and load versus displacement tests were performed on many candidate fibers. An aluminum buffered, $100/110$ μm, 0.20 N.A. fiber gave the most encouraging results. Vacuum testing on the prototype sensor indicated that the final vacuum seal could be made with high temperature epoxy, and that the getter material could be located in a short stand-off tube and activated without heating the entire transducer.

While the tests to characterize sensor fibers were being performed, the first indications of a compatibility problem between the pressure sensor and the EOA arose. Based on the microbend sensitivity, thermal drift, and load versus displacement tests performed by B & W, they concluded that sensor dynamic ranges would need to be less than 6.0 dB to keep thermal sensitivity low enough to assure the required accuracy of 0.1%. Litton responded that with the EOA design being developed, which used a single area CCD array to receive the signal from all the sensors except the TRD, a sensor dynamic range of at least 6.0 dB would be required if the EOA's sensor decoding process were to not degrade the output signal accuracy to worse than 0.1%. Even then, Litton projected that the 0.1% accuracy could be met only under the best of optical system loss conditions. (When the performance of the CCD array was later tested, it was found that a 6.0 dB range for an analog sensor would result in an EOA accuracy closer to 0.25%, not 0.1%.)

MDA notified B&W of Litton's perceived need for a minimum 6.0 dB of sensor dynamic range and requested that B & W determine what the effect on sensor accuracy would be if the sensor were to be required to have a dynamic range of at least 6.0 dB. B&W reported that requiring a sensor dynamic range of 6.0 dB would result in a sensor accuracy of 0.5% of full scale, even if temperature compensation were not a problem. That result was far from the 0.1% thought required and worse than the 0.3% reported earlier as already thought to be achievable. Work with the prototype sensor confirmed these problems.

MDA evaluated the way in which air pressure data was used by the flight control system. MDA determined that though the 0.1% accuracy requirement levied on the air data pressure system was real in the sense that it was the requirement met by the existing air data pressure sensor system, it was not realistic in that the flight control laws did not need 0.1% accurate data. Reducing the accuracy of the data to 0.5% would not affect the flight control system of the aircraft. MDA notified B&W that pressure sensor accuracy could be reduced to 0.5%, but MDA would require B&W to meet a dynamic range of at least 6.0 dB and solve the sensor's thermal stability problem. It was hoped that in this way the accuracy of the combination of the sensor and the EOA operating together would be limited by the sensor accuracy, and would be 0.5% of full scale. This was believed possible, if the system parameters could also be treated so as to assure that the signal from the sensor would have a strength near the top of the EOA's sensitivity range.

The prototype sensor was completed and characterization of the sensor began immediately. The sensor verified the success of the methods B&W chose for mechanical design of the sensor, vacuum seals, and getter materials. Those issues were the purpose for constructing the prototype sensor. However, sensor testing also uncovered a temperature cycle induced hysteresis in the pressure measurement which led to more dynamic range and accuracy problems.

The hysteresis was investigated in the prototype sensor and duplicated in subsystem bench tests. The cause of the hysteresis was found to be the aluminum coating on the fiber. The aluminum coating had not been a source of trouble when the sensor's internal fiber was a 150µm/180µm fiber. However, to reduce the sensor's insertion loss and improve the sensitivity (to provide a dynamic range of 6.0 dB), a 100µm/140µm fiber was substituted. On this thinner fiber, the aluminum coating (which was the same thickness as before) was proportionately thicker. The thick coating received less support by the more compliant 100µm/140µm fiber than it had from the earlier thicker fiber. Consequently, it flowed proportionately more between the teeth of the new sensor. This greater flow caused the aluminum to take a different "set" between the teeth at high temperatures than at low temperatures. This variation in the set of the teeth in the aluminum caused the hysteresis.

Another result of reevaluating the accuracy with which the EOA could interpret signals from analog sensors was the determination that the temperature compensation of the pressure sensor would have to be intrinsic to the sensor. The optical temperature compensation sensors with which B & W was familiar would not be usable as stand-alone sensors operating on a separate port. The reason for this was that the temperature effect was very small, even in relation to the already small signal produced by the pressure sensor. While accurately interpreting the small signal from the pressure sensor would be difficult for the EOA, interpreting the tiny signal from a stand alone temperature sensor which mimics the temperature dependence of the pressure sensor would be impossible. It would have been possible to install an entirely separate temperature sensor in the pressure sensor head to supply temperature information to a correction algorithm in the EOA; however, for B & W to develop a new optical temperature sensor would violate the plan to have no new sensors developed as part of FOCSI. Adding a thermocouple or thermistor would violate the plan that the sensors be optical, and adding another TRD sensor from Rosemount would require another major TRD sensor repackaging effort, since the TRD sensor was also new to flight control and not characterized in that application. Consequently, it was believed that the best approach was to develop an intrinsic temperature compensation method. It was believed that since the required sensor accuracy was now 0.5%, temperature compensation would be easier, and perhaps not required at all, if the new polyimide coated fiber was stable enough.

B&W was informed of the need to maximize accuracy by having the power level of the sensor return be near the maximum the detector could accept. That presented a problem in that the optical loss of the reference leg of the sensor was much less than the optical loss of the sense leg of the sensor, a condition which would lead to saturation of the detector if the sensed signal was forced to be near the saturation limit of the detector. In particular, in the ICD a maximum insertion loss was specified. The insertion loss in the sensor leg was expected to be near the 18 dB maximum loss, but the insertion loss in the reference leg was less than the maximum ($\approx$12 dB). This combination met the requirements of the ICD, but would probably saturate the EOA receiver.

To alleviate this problem, MDA suggested installation of a second set of sensor teeth in the sensor head. Those teeth would be identical to the pressure sensor teeth except that they would be fixed in position. The reference fiber would then be run through the fixed teeth and the temperature compensation loop could be removed from the sensor fiber. The fixed teeth would be set to increase the reference fiber insertion loss by about 3 dB. Removal of the temperature compensation loop from the sensor fiber would reduce its insertion loss by about 3 dB. Thus the two fibers would have similar insertion losses. In theory the fixed teeth would have the same temperature response as the actual pressure sensor teeth, thus the sense and reference signals would suffer the same changes with temperature. Then, even though the EOA could not accurately read the temperature induced signal variation by itself, a ratio of the signals from the sensor and reference fibers could effectively remove the temperature effect from the pressure reading.

This approach also had the advantage of providing good modal balance between the sense and reference fibers, which would make the mode volume in these fibers as similar as possible. Thus, sensitivity to cable bending and variable connector losses would be as small as possible. The weakness of the approach was that the temperature dependence of the signals in the two fibers would not be exactly the same, because the variation with temperature of the sense fiber would be different with different pressures applied by the teeth, a variation which would not occur with the reference fiber with its fixed teeth. However, with this approach, some temperature compensation would still be present, and with the sense and reference optical losses similar, the best part of the EOA receiver's sensitivity range would be used. This combination would allow the system to meet the 0.5% accuracy requirement over nearly all of its temperature range.

Unfortunately for all the above plans, when B&W ordered more of the fiber for more testing, the ordered fiber did not perform as well as the sample of the (supposedly) same fiber. The change in performance was traced back to the manufacturer of the fiber and, eventually, to the manufacturer of the glass preform. It was determined that the numerical apertures (N.A.) of the preforms and the subsequent fibers were different between the sample and the purchased fibers. Unfortunately, the poor behavior of the purchased fiber was due to its having the advertised N.A. of 0.22. The good behavior of the sample fiber was due to its accidentally having an N.A. of 0.28.

Upon learning of the N.A. difference, B&W requested a run of fiber with an N.A. of 0.28. The response from both the fiber and preform manufacturers was that neither of them knew why the sample fiber had the large N.A., but for approximately $100K the preform manufacturer would investigate the matter.

This issue left B&W with three options for the FOCSI sensor. One, B&W could have manufactured the FOCSI sensor with the remainder of the sample fiber with the 0.28 N.A. If this had been done, B&W could have met the FOCSI requirements over most of the temperature range, but could not have made any more sensors like the FOCSI sensor without a fiber research program.

Two, B&W could have manufactured a reflective sensor with 150/180 μm aluminum coated fiber. This would have met the 6 dB range requirement and would have had good thermal properties, because for that fiber the temperature sensitivity did not vary measurably with pressure. However, a reflective sensor would have changed the sensor insertion losses and would have required a major sensor re-design.

Three, a transmissive sensor could have been made with 150/180 μm aluminum coated fiber. This sensor would have had only a 3 dB range, but it would have had good thermal properties. The possible way to use such a sensor would be that, with the EOA accuracy known as a function of optical power, a 3 dB range might be found near the CCD saturation limit which might give almost as good accuracy as a 6 dB range farther from the limit. The unknown issue was control of the EOA source so that the pressure sensor signal would stay near, but not exceed, the CCD saturation limit. MDA agreed to pursue with Litton the possibility of adding automatic gain control to the EOA source to maintain its output in a range which would allow the CCD array to always operate near the upper end of its sensitivity range.

MDA investigated which of the three options identified for the pressure sensor would be the most promising for development and subsequently recommended that B&W concentrate on the 3 dB dynamic range option (Option 3) with fixed reference leg teeth to help match sensor and reference leg losses. Litton believed that with a sensor with perfect temperature characteristics, and the power adjusted so that the 3.0 dB signal would be near the saturation limit of the detector, it would be possible to decode such a sensor with an accuracy of 0.35%. Given the real sensor's likely characteristics, Litton believed the sensor and EOA combination would have an accuracy of 0.5% over most of the sensor's temperature range and an accuracy between 0.5% and 1.0% over the full range. MDA accepted those characteristics as the best that could be obtained in the remaining time and funding, so MDA gave B&W formal authorization to build a 3.0 dB range sensor.

2.4.1.3.2 Fabrication.
Fabrication and assembly of the two pressure sensors was straightforward. Changes to the vacuum sealing procedure were implemented to make the sensor more producible. Gold brazing was eliminated in favor of TIG welding, and the vacuum plug was replaced by a TIG welded pinch tube assembly. These changes resulted in only minor modifications to the sensor hardware. The pressure diaphragms were welded in place. The dynamic ranges of both sets of diaphragms, teeth, and fibers were measured at 850 nm as 2.9 dB, nominal.

Because an analog sensor depends upon filtering broadband light into two wavelength bands, the amplitude of one of which is modulated by the sensor, while the other is not; and because the information is obtained from the signals by forming the ratio of the power in the two bands, it was initially thought that cross-talk of light from each band into the other must be carefully controlled. Numerous approaches, dealing with controlling sources and detectors were evaluated and found to fail at isolating the desired cross-talk signal. Consequently, it was realized that the cross-talk could not be measured on an intact sensor unless the sensor were designed from the start with the optical equivalent of test points. The fact that the cross-talk, as it was defined, could not be measured was simply a supporting argument that cross-talk was not an important parameter.

The analysis done on the cross-talk did point to the correct parameters. In the analysis, the measure of success or failure of the system was the decodability of the sensor by the EOA. The factors that were of most concern to the EOA were found to be the sensor dynamic range and the stability of the reference signal. Dynamic range was already a parameter of the system. The cross-talk studies indicated that reference stability needed to be added as a system parameter, and cross-talk needed to be removed.

Unexpected problems encountered in the development of the pressure sensor exhausted available program funds for sensor fabrication and testing. As a compromise solution, B&W agreed to complete assembly of the two pressure sensors and conduct basic tests to verify their operability. The sensors were then shipped to MDA for environmental testing. The completed Air Data Pressure sensor is shown in Figure 2.4-15.
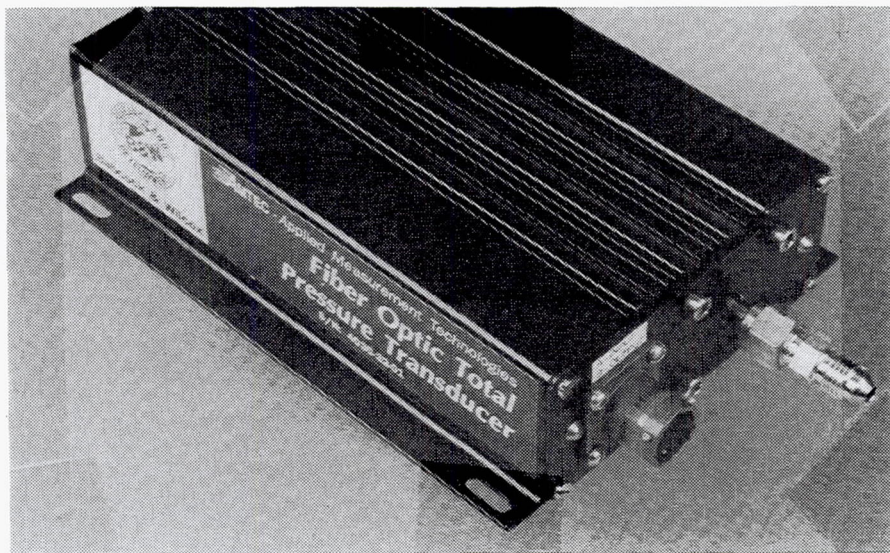
Figure 2.4-15. Air Data Pressure Sensor
(WDM Analog Ratiometric, Babcock & Wilcox)

2.4.1.3.3 Performance Testing and Delivery to MDA.

Functional testing of the second pressure sensor showed that it was non-functional. Preliminary testing traced the cause of the problem to the sense leg of the sensor. Because the optical circuit of the sense leg appeared to be open, MDA authorized destructive inspection of the sensor head for the purpose of determining the cause of the failure for inclusion among the lessons learned about the pressure sensor.

The cause of the failure of the second pressure sensor was identified as a break in the fiber just inside the vacuum seal for the sensor head. The break is suspected to have been caused by unexpected motion of a metal tube which was added to the sensor head to provide strain relief for the fiber. In the sensor design before the strain relief tube was added, the stainless steel body had two fiber access holes (~0.062") for the fiber to enter and exit the head. The fiber was retained and vacuum sealed in the holes with epoxy, which filled the holes completely. That approach was probably sound; but, the designers became worried that with the fiber exiting directly out of the smooth back side of the sensor head, and running for some length (>1") before its next support point, that vibration could break it. Therefore, B&W drilled blind 0.125" holes into the back of the sensor head and fitted 1" long, 0.125" O.D. stainless steel tubes into the holes to limit motion of the fiber. The fiber then ran up the inside of each tube before entering the sensor head itself. When the epoxy was installed, it filled the 0.062" holes around the fiber and filled part of the inside of each stainless steel tube. It appears that sometime in the assembly process after the tubes, fiber, and epoxy were in place, the tube where the fiber exits the head was bumped. When the tube was bumped, it was broken loose in the sensor head. To break the tube loose, the epoxy that filled it from one end had to be broken from the rest of the body of epoxy that filled the fiber access hole. Since the fiber was solidly fixed in the epoxy, breaking the epoxy also broke the fiber. Based on comments from the B&W assembly technician, it is believed that the strain relief tube was loose, and the fiber broken before the sensor head was installed in the sensor enclosure.

The strain relief tube is not expected to cause trouble for the working sensor because that sensor was tested and found to operate after the sensor head and strain relief tube were fixed in place within the enclosure.

B&W shipped the failed sensor head to MDA. However, B&W requested permission to keep the sensor optics (coupler and WDM system) that go in the enclosure with the sensor head, to use as laboratory test equipment.

2.4.1.4. Nose Wheel Steering Position Sensor

2.4.1.4.1 Design.

BEI Motion Systems was selected to construct the Nose Wheel Steering (NWS) Position Sensors, based upon BEI's WDM Analog sensor proposal. As a first step, BEI generated detailed sensor interface requirements which were submitted to the EOA supplier, Litton Poly-Scientific, for review and approval. After approval of the sensor ICD parameters, sensor mechanical design commenced. BEI personnel visited NASA-Dryden to inspect an F-18 aircraft to get sufficient physical information to begin mechanical design of the NWS position sensor. Inspection of the aircraft indicated that installing the NWS sensor would be straightforward. An outline drawing for the FOCSI LEF position sensor is shown in Figure 2.4-16.
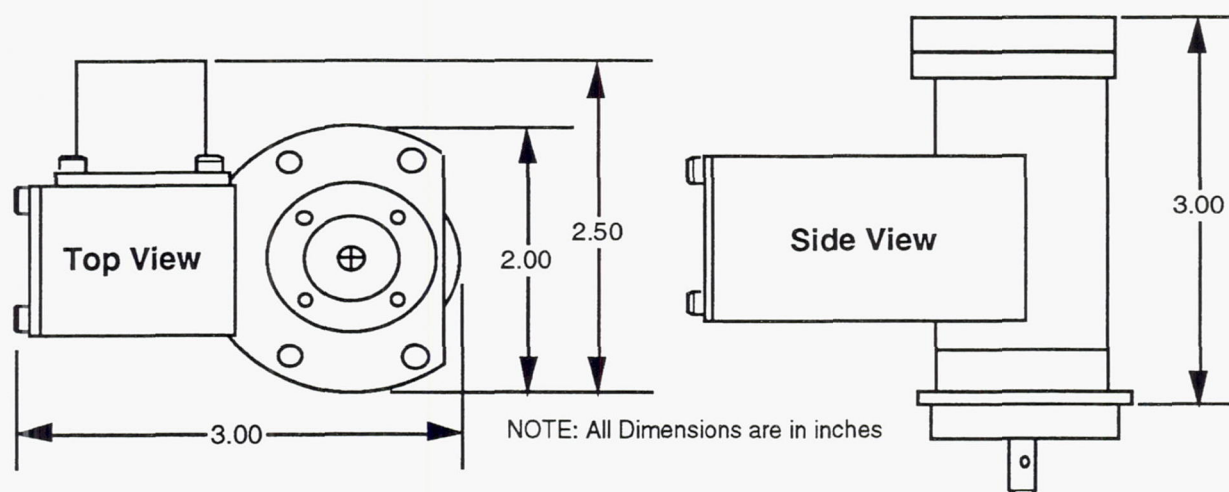
Figure 2.4-16. NWS Sensor Mechanical Envelope

Initial laboratory testing of optical components including couplers, lenses, right angle micro-optics, and optical filters, revealed that it was necessary to increase the insertion loss value from 9 dB to 16 dB. The insertion loss value was later adjusted from 16 dB to 20 dB to accommodate sensor connector losses which BEI had not understood were assigned to the sensor in the optical power budget analysis.

BEI worked with the gradient plate suppliers to develop a minimum contrast ratio value, which fixes the sensor minimum dynamic range. This value was determined to be 15 dB, down from the original 20 dB. Transmissibilities of 1% to 31.6% will give this range and were thought to be reliably producible. BEI reported that they would attempt to raise the maximum transmissibility to 79.4%. The higher maximum transmissibility would allow a dynamic range of almost 19 dB, or it could be used to shift the 15 dB range to greater light intensities at the receiver, which is good for the EOA signal to noise ratio. Higher transmissibilities than 79.4% were not believed to be practical because of nonuniformities of the absorbing material across the area illuminated by the optics at the gradient plate.

As with the analog microbend sensor, It was discovered that the analog code plate sensors would be sensitive to variation of the optical source spectral intensity distribution with time. BEI was asked to supply values for maximum allowable variation, over time, both with and without optical feedback from the source to the receiver. These values were used to modify the ICD. The change required coordination with Litton to add an optical feedback loop to the EOA for optical source stabilization.

Based on the evaluations of NWS sensor detailed designs, BEI was given authority to proceed with sensor fabrication.

2.4.1.4.2 Fabrication.

Fabrication of the NWS sensor was delayed due to problems related to the optical code plates. Repeatability of the neutral density code plates was a problem. BEI began work on an in-house code plate design using very fine lines of variable width and fixed period placed on glass by a divided circle machine. This approach yielded results equivalent to the best results of the neutral density approach, and with good repeatability. BEI determined that the ruled code plates, manufactured by another division of BEI, were likely to give superior performance in the aircraft environment, therefore, they shifted to the ruled code plate design.

During sensor fabrication, BEI was notified by the coupler manufacturer (Gould) that the 95/5 couplers designed into the sensors could not be manufactured, contrary to previous belief. The use of available 50/50 couplers would add another 2.5 dB per coupler to the sensor loss estimates. This splitting loss increase, along with the 0.5 dB excess loss increase, caused the sensor insertion losses to exceed the required maximums by 0.5 dB. The low losses measured by Gould were valid only for the optimized optical launch conditions used during coupler fabrication. However, the larger losses measured by BEI were valid for the optical launch conditions present in the optical sensors. Therefore, the power budget in the ICD was modified to reflect the measured losses.

2.4.1.4.3 Performance Testing and Delivery to MDA

Upon completion of assembly, preliminary performance checks were run on the finished sensors. Two problems were found; the insertion losses were greater than expected, and the dynamic ranges were much less than expected. The insertion loss of each sensor with connectors was specified to be less than 20 dB. Unfortunately, the measured loss without connectors was 20 dB. Another 4 dB was the allowance for the connectors.

Further testing of the NWS sensor showed excessive and highly variable optical losses in the sensor. These losses were traced down to disadvantageous combinations of the tolerances of the machined mechanical parts from the outside

suppliers. As reworking the parts to tighter tolerances was not practical at that stage of the contract, BEI developed an active alignment system for the optics. Applying this alignment system reduced the losses by 4 dB, and the spread of the losses for the two sensors was drastically reduced from 17 dB to 0.7 dB.

In contrast, the dynamic range of the sensors was expected to be 17 dB, well above the 15 dB minimum specified in the ICD. However tests of the assembled sensors yielded dynamic ranges of about 8 dB. Unfortunately, the reduction of the dynamic range could not be corrected. The explanation given for the change was that BEI engineers had misunderstood from the beginning of the program that to calculate optical power in dBs, one uses $10 \log(x)$, not $20 \log(x)$. Consequently the performance had not deteriorated, it had merely been consistently overstated. Fortunately, because of the linear behavior of the EOA receiver, Litton expected the effect of the dynamic range reduction on the decoding of the sensor to be small.

The effect of the reduction in the dynamic range of the sensor was a reduction in the apparent resolution of the sensor. Manufacturers of analog sensors like to claim that the resolution of the sensors is infinite. That is not true. Electrical sensors have quantization effects due to the fact that they are wound of discrete turns of wire. Optical sensors have quantization effects at the light and dark extremes on the code plates because of the unevenness of the deposition of the reflective material on the glass. It is worth repeating here that because of repeatability problems with the code plates, BEI went to a design with lines ruled on the code plate. That forces a quantization, and resolution limit, on the code plate.

The effect of the limited dynamic range is a further reduction of the resolution from the limit imposed by the nature of the code plate. The electronics in the EOA has its own resolution limitations. Some of the limitations come from the CCD detector resolution, and the rest arise from the noise characteristics of the rest of the electronics. As should be expected, reducing the dynamic range of the incoming signal while leaving the noise of the system the same will reduce the resolution of the sensed parameter. Fortunately, the effect was small.

The reason the effect was small is that the main factor component of EOA resolution is the quantization of the CCD detector. The CCD detector is a linear device. Cutting the signal in half in the logarithmic dB scale is worse than cutting the resolution in half. In this case, the drop in dynamic range reduced the resolution from being equivalent to a 10 bit sensor to a 7 or 8 bit sensor.

During the fabrication of the NWS sensor, BEI underwent a major business reorganization which resulted in the loss of all personnel who had been associated with the production of the sensors for the FOCSI program. Sensor final assembly and testing were moved from the Carlsbad, California facility to a facility in Chatsworth, California and taken over by a new group of people from the industrial (electric) sensor division. This reorganization caused some difficulties during testing when, not unexpectedly, problems arose.

Preliminary acceptance testing was performed on the NWS sensors. NWS sensor S/N 001 passed the acceptance test and completed the 200 hour life test.

NWS sensor S/N 002 was tested and found to have a reduced angular span and an anomalous dip in the output signal at positions near one end of its travel. The angular span of NWS sensor S/N 002 was 148.3° instead of the required 150° ($\pm$ 75°) because of an error in bonding the optical heads into the sensor. The heads could not be adjusted without disassembling the sensor. Disassembly would risk damaging the sensor, would have required contracting for a second day for vibration testing at the testing laboratory used by BEI, and would have further delayed contract completion. The anomalous output near the end of travel appears to be due to a flaw in the code plate. Correcting the flaw would require the production of a new code plate. MDA determined that NWS sensor S/N 002 was acceptable for the FOCSI flight test program. The reduced span will only be noticed if the nose wheel is turned right to an angle exceeding 73.3°. That is almost to the stop at 75°. Such hard turns are rarely allowed to occur. The anomalous output will only be seen if the nose wheel is turned to near its stops, and can be accounted for in post flight processing. Since the sensor is not being used for in-the-loop control, neither problem will affect the operation of the aircraft.

The NWS sensors experienced several failures during environmental testing. NWS sensor S/N 002 suffered a failure during thermal testing which prevented it from being ready for altitude and vibration testing at the scheduled time. The failure was of the Gould coupler used in the sensor. The coupler was replaced and testing resumed. At the time the coupler was replaced, the heads in that sensor were realigned, correcting the restricted sensor range which was found earlier Unfortunately, after reassembly it was found that the sensor insertion loss varied from 22 to 26 dB, well in excess of the 20 dB limit in the ICD. Furthermore, the sensor dynamic range was 6 to 7 dB, which was less than the 7 dB required for minimal compatibility with the EOA and specified in the most recent modification to the ICD. MDA requested BEI to rebuild NWS 002 to meet the ICD requirements.

The second failure of an NWS sensor consisted of two broken screw heads on one sensor. It was possible to replace the small screws with larger screws with no redesign of the sensor. Because the optical NWS sensor must support the electrical sensor, it has a thick-walled case which can safely be tapped for larger screws. Originally, a larger size screw had been specified in the sensor design. The original retention screw size had been reduced because of machinists' concerns about drilling the screw holes parallel to the case walls. In practice, the BEI machinists did not have any problems with drilling the larger holes when the sensors were re-worked. The re-worked sensor passed a repeat of the vibration tests.

The final NWS sensor failure occurred during life testing. BEI was performing the cyclic motion life test with rotation in one direction only. MDA instructed BEI to alter the test to include frequent reversal of rotation, thus better simulating actual use. The new cyclic motion life test caused the graphite-filled Teflon seal at the

transformer (upper) end of the NWS sensor to disintegrate, which filled the sensor with debris. The problem appears to have been caused by a misunderstanding between BEI and the seal supplier about the speed at which the shaft would rotate. When the correct rotation speed, with periodic reversals, was specified, the seal supplier stated that the original seals would not have met the requirements; but, they did have available seals which would meet the requirements. BEI obtained new seals, and successfully tested them in a special seal test fixture; whereupon the new seals were installed in the NWS sensors. Both NWS sensors from BEI were shipped to MDA. The completed NWS sensor is shown in Figure 2.4-17.
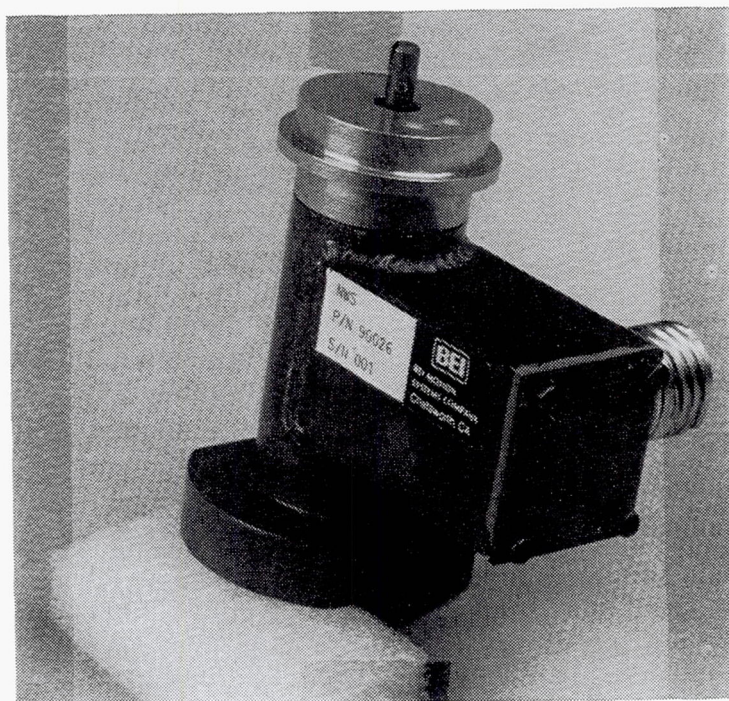
Figure 2.4-17. Nose Wheel Steering Rotary Position Sensor
(WDM Analog Ratiometric, BEI Motion Systems)

2.4.1.5 Aileron/Trailing Edge Flap Position Sensor

2.4.1.5.1 Design.

BEI Motion Systems was originally selected to construct Aileron linear position sensors, based upon BEI's WDM analog sensor proposal. As a first step, BEI generated detailed sensor interface requirements which were submitted to the EOA supplier, Litton Poly-Scientific, for review and approval. After approval of the sensor ICD parameters, sensor mechanical design commenced. BEI personnel visited NASA-Dryden to inspect an F-18 aircraft to get sufficient physical

information to begin mechanical design of the Aileron position sensor. Inspection of the aircraft indicated that space did not appear to be available for adding an optical sensor to the aileron. MDA suggested the possibility of instrumenting the trailing edge flap with an optical sensor, since the Trailing Edge Flap (TEF) linear position sensor and the Aileron have very similar sensors in the same environment, but with more room in the TEF. In addition, the TEF sensor has a greater stroke length than any of the other sensors. This is an advantage for the FOCSI program, since it would allow testing of a long stroke linear position sensor. After discussions with NASA, it was decided to switch to a TEF linear position sensor. This change required minor mechanical re-design to accommodate the longer stroke length of the TEF sensor.

Optical design of the linear TEF sensors progressed identically to that of the rotary NWS sensors described earlier. As with the NWS sensors, problems with repeatability of the neutral density code plates forced the selection of ruled code plates manufactured by BEI.

Mechanical design of the linear TEF sensor focused on the selection of appropriate linear bearings, seals. Based on the calculations of material stresses and vibrationally induced resonances, BEI identified materials for the sensor shaft, housing, and optical heads, as well as bearings, seals, and proposed mounting methods. Remaining mechanical issues involved identifying the preferred mounting approaches within the flight test aircraft.

The initial mechanical design resulted in a linear sensor that was 25 inches long to cover the 8 inch TEF actuator stroke. This presented a problem for installation of the sensor into the aircraft. Efforts to shorten the sensor design from 25 inches to the 14 inches required for acceptable installation clearances were unsuccessful. Mounting of the TEF sensor appeared to require some modification to the aircraft structure regardless of the sensor length. Therefore, a study was begun of the feasibility of other options, including external aircraft mounting locations.

All aircraft modification options, including external mounting, were found to be prohibitively expensive. Mechanical interference problems were finally resolved by changing the TEF sensor from a linear to a rotary sensor. This change had minimal impact on schedule, because BEI was able to modify mechanical packaging of the NWS sensor to make a TEF sensor.

An outline drawing for the FOCSI TEF position sensor is shown in Figure 2.4-18.
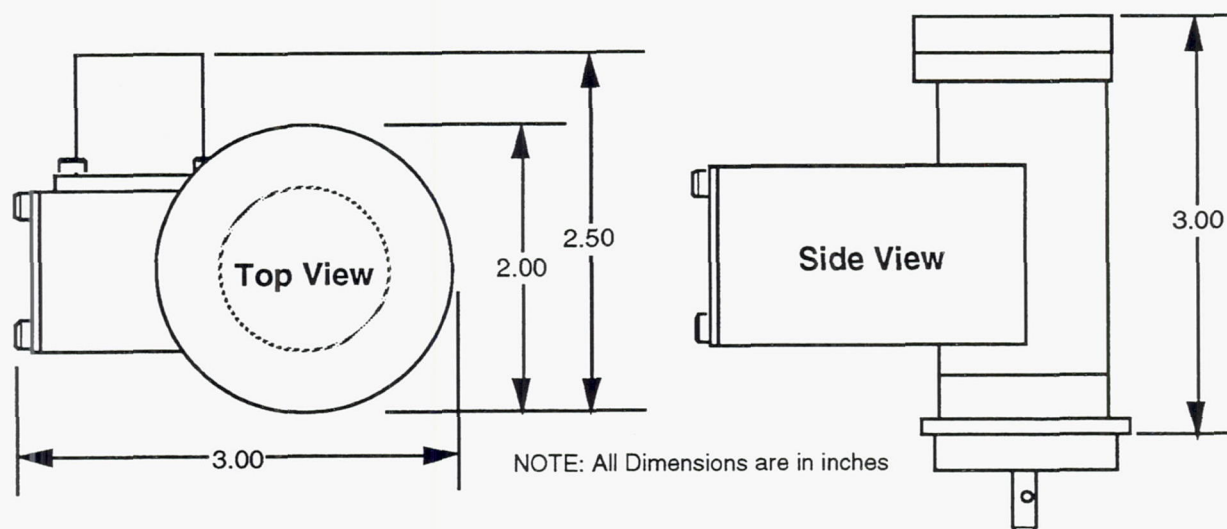
Figure 2.4-18. TEF Sensor Mechanical Envelope

2.4.1.5.2 Fabrication.

During sensor fabrication, a difficulty arose in that converting the long flap stroke into the 150° rotation angle of the present sensor design would requires a large diameter (8 inch) input pulley or a potentially unreliable gear train. Upon visiting NASA-Dryden, MDA mechanical engineers found a way to install the TEF rotary sensor adjacent to the actuator. The sensor would be driven by a pulley and bracket assembly which would convert the linear motion to rotary motion. A gearbox would be placed on the sensor to allow a sensor with 150° of rotation to be used.

The TEF sensor experienced the same problems with code plate and optics that were described for the NWS sensor. After these problems were resolved, assembly of TEF sensors was completed.

2.4.1.5.3 Performance Testing and Delivery to MDA.

The two TEF sensors were assembled and preliminary performance checks were run on the finished sensors. The same increased optical losses and decreased dynamic range that were characteristics of the NWS sensors also appeared in the TEF sensors.

Problems were encountered during environmental testing of the TEF sensors. One TEF sensor was found to have a broken screw after the vibration testing was completed. The screw was one of four which hold the case of the sensor to the base. The broken screw was not sufficient to cause the sensor to fail; however, the potential for breaking screws presented a possible foreign object hazard to the aircraft, as well as increasing the likelihood of failure of the sensor. Full repair of

the broken screw would require some re-working of the sensor. The sensor design had a can-shaped top cover fitting over a (inverted) can-shaped base. The cover screws penetrated the flat top edge of the cover and entered holes drilled into the walls of the base. Those holes were drilled parallel to the wall surfaces. Thus, it was unlikely that larger holes could simply be drilled for larger screws without breaching the walls of the base.

MDA determined that this failure presented no hazard to the aircraft, since there is nothing in the TEF area of the aircraft with which small debris could interfere. In addition, the location is one from which small debris could easily escape completely from the aircraft. In the event of a major failure of the sensor, such as all the retention screws failing, the case can not come loose until after breaking off all the internal cables and optics in the sensor. Even if that were to occur, the sensor base would remain bolted in place, and the case would be retained by the cable connected to it. Therefore, case retention screw breakage was deemed to not be a hazard. Nevertheless, to minimize risk, MDA recommended that the TEF sensor with the broken retention screw (S/N 001) be used only as a backup sensor, or as a source of parts for sensor S/N 002. To prevent contamination of the optical system inside sensor S/N 001, BEI adhesively bonded the screw head in place.

TEF sensor S/N 002 also had some problems. There were no mechanical difficulties associated with sensor SN 002. However, the code plate seems to have suffered some damage during environmental testing. That damage caused three positions on the code plate to have optical signal drop-outs, one of which caused the sensor to not meet the 1.0 % FS linearity requirement of the procurement specification. Since cleaning of the code plate did not correct the problem, it was concluded that the code plate suffered actual damage during testing. Correcting the damage would require production of a new code plate. Rather than contend with the time and expense of replacing the code plate and repeating the environmental testing, MDA decided to accept the TEF sensor in its slightly flawed condition.

Both TEF sensors from BEI Motion Systems were shipped to MDA. The completed TEF sensor is shown in Figure 2.4-19.
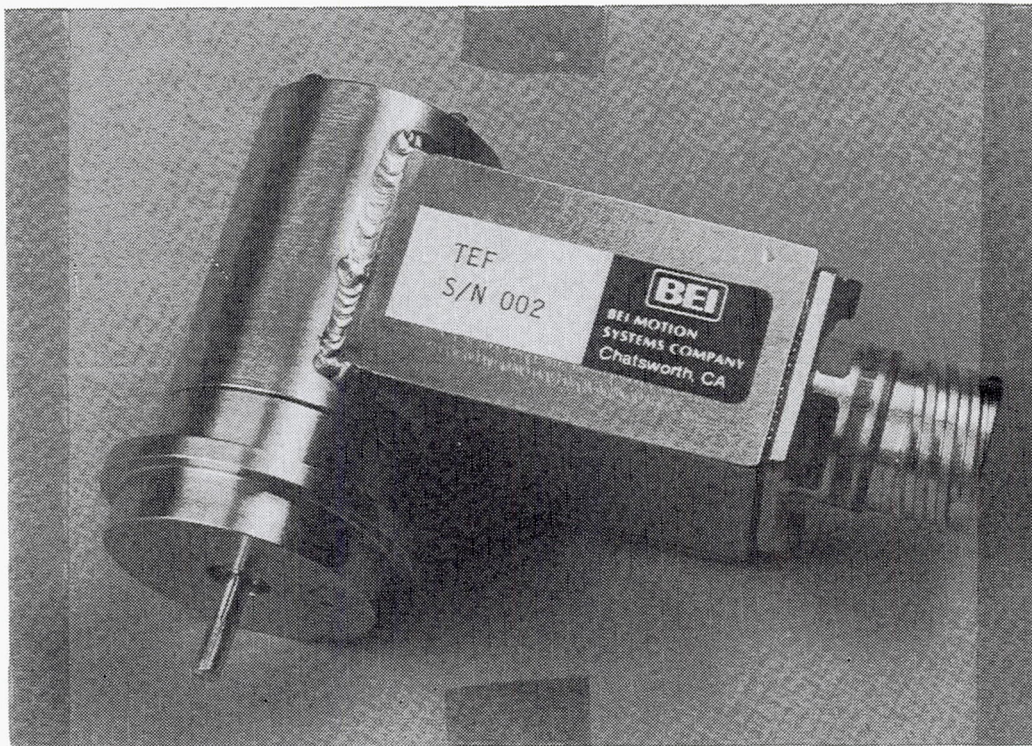
**Figure 2.4-19. Trailing Edge Flap Rotary Position Sensor
(WDM Analog Ratiometric, BEI Motion Systems)**

2.4.1.6 Pitch Stick Position Sensor.

2.4.1.6.1 Design.

BEI Motion Systems was selected to construct two Pitch Stick linear position sensors, based upon BEI's Wavelength Division Multiplexed Analog sensor proposal. As a first step, BEI generated detailed sensor interface requirements which were submitted to the EOA supplier, Litton Poly-Scientific, for review and approval. After approval of the sensor ICD parameters, sensor mechanical design commenced. BEI personnel visited NASA-Dryden to inspect an F-18 aircraft to gather information to begin mechanical design of the Pitch Stick sensor. Inspection of the aircraft indicated that installation of the sensor would be straightforward.

Optical design of the Pitch Stick linear position sensor was identical to that of the rotary NWS and TEF sensors described earlier. As with the rotary sensors, problems with repeatability of the neutral density code plates forced the selection of ruled code plates manufactured by BEI.

Mechanical design of the linear Pitch Stick sensor focused on the selection of appropriate linear bearings and seals. Based on the calculations of material stresses and vibrationally induced resonances, BEI identified materials for the sensor shaft, housing, and optical heads, as well as bearings, seals, and proposed mounting methods. Remaining mechanical issues involved identifying the preferred mounting approaches within the flight test aircraft.

The initial mechanical design resulted in a linear sensor that was 17 inches long to cover the 3 inch Pitch Stick actuator stroke. This presented a problem for installation of the sensor into the aircraft. BEI successfully redesigned the sensor to fit within the 12 inch installation constraint. Included in the redesign was the removal of the integral fiber optic connector and the addition of a fiber "pigtail" which placed the fiber optic connector several feet from the sensor body. An outline drawing for the FOCSI Pitch Stick position sensor is shown in Figure 2.4-20.
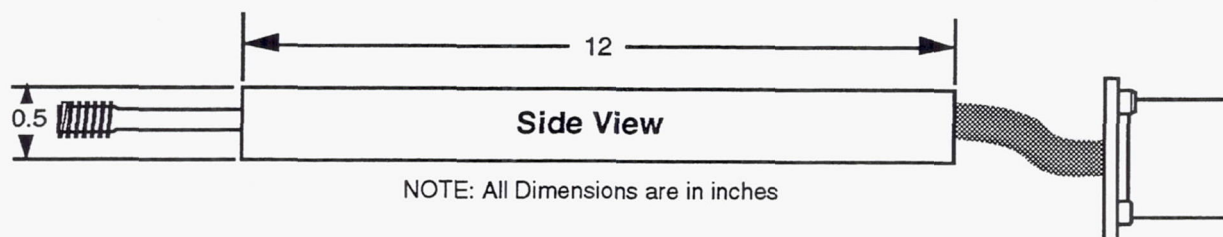
Figure 2.4-20. Pitch Stick Sensor Mechanical Envelope

MDA and BEI mechanical designers discussed potential break-away structures for the pitch stick sensor to assure that the sensor could never jam the pilot's controls. It was determined that a 20 pound breaking force should be greater than any normal friction in the sensor and greater than any likely axial acceleration, but small enough for the pilot to reasonably exert if necessary. Since a 20 pound force would require a wire smaller than 1/32 inch in diameter, a spring loaded ball in a detent for a breakable link was implemented. Such a structure also has the advantages of being potentially adjustable and reusable. A mechanically complete brassboard Pitch Stick sensor was assembled, except for the code plate. No mechanical problems were discovered. Based on the evaluations of Pitch Stick sensor detailed designs, BEI was given authority to proceed with sensor fabrication.

2.4.1.6.2 Fabrication.

BEI personnel visited NASA-Dryden to resolve mounting issues for the Pitch Stick sensor before beginning fabrication. It was discovered that installation of the sensor directly on the pitch/trim system was not practical. However, the sensor could be bolted to the back structural wall of the next bay aft, and the motion picked up from the pitch control arm which enters that bay. Fabrication of the Pitch Stick sensor proceed smoothly.

2.4.1.6.3 Performance Testing and Delivery to MDA.

The Pitch Stick sensors were assembled and preliminary performance checks were run on the finished sensors. The same increased optical losses and decreased dynamic range that were characteristics of the NWS and TEF sensors also appeared in the Pitch Stick sensors.

Optical spectrum analyzer testing of the sensors uncovered a sensor measurement error. The error ranged from +2 to -3% of full scale, which was outside the bounds of the procurement specification. BEI believed the cause of the error was insufficient resolution of the master pattern for the code plates and improper copying of the master onto the code plates. New code plates for the Pitch Stick sensor were ordered, installed in the holder, and promptly broke. BEI then re-designed the holder as a single-piece unit which would not place stress on the code plate. The re-designed holder was successfully tested with the remaining code plate.

While the Pitch Stick sensors were in the testing phase, the sensors were found to have been produced with faulty code plates. The faulty plates were the second set of code plates ordered. They were to have been patterned with half the line spacing of the original plates, thus providing twice the resolution. Instead, the second set of plates was patterned with twice the line spacing of the first set, thus yielding half the resolution. This flaw was apparently not noticed when the plates were received. New code plates were ordered and installed in the sensors. The sensors were completed and acceptance and environmental testing began.

Early mechanical testing showed signs of wear debris from the seals. The seals were replaced with new seals of the same material as the new seals in the rotary sensors. The new seals also shed particles, but only when new; so, BEI modified their assembly procedure to include a separate break-in of the seals prior to installing them in the sensors. Testing of the sensors with the new, broken-in seals indicated that the problem of seal wear debris was solved; however, wear debris from the sliding metal parts inside the sensor was detected after the life tests were completed. The cause of the debris was traced to the Magnaplate low friction coating used on the code plate frame. BEI removed the coating and cleaned the code plate and optics. Cleaning was successful; however, the sensors then had metal-to-metal sliding surfaces without special low friction coatings. BEI did not know if these surfaces would generate more wear debris; so, BEI recommended periodic cleaning of the optics and code plate after every 1000 to 5000 strokes.

BEI shipped both completed Pitch Stick sensors to MDA. Sensor S/N 001 arrived in good condition. Sensor S/N 002 arrived with the sliding shaft bent and the threaded end broken. The broken shaft on Pitch Stick sensor S/N 002 would make installation of the sensor difficult, and the reliability of the connection would be suspect. Therefore, the Pitch Stick sensor S/N 002 was returned to BEI for installation of a new shaft.

The problem with debris generation remained unresolved after the sensors were shipped to MDA. Periodic cleaning every 1000 to 5000 strokes was determined to be unacceptable, as the Pitch Stick sensor would be operated through 1000 strokes in as little as three hours under certain flight conditions. A further question was the rate of production of wear debris, since the possibility existed that debris production was highest for new surfaces, which then burnished with use and ceased producing debris. BEI engineers believed that the most used portions of the sliding surfaces in the sensors burnished quickly and ceased to generate debris. To verify this, BEI agreed to conduct a two hour operational test to determine if the sensor sliding surfaces had burnished during life testing or were still capable of generating debris. Because Pitch Stick sensor S/N 002 was returned to BEI for re-work of the bent shaft, BEI agreed to test the repaired sensor on their existing sensor life testing fixture.

The Pitch Stick sensor (S/N 002) was repaired. However, the two hour debris generation test was not performed before BEI disbanded the sensor group and dismantled the sensor life test stand. Fortunately, BEI located the results of similar tests performed on the variable exhaust nozzle position sensor constructed for GE. BEI had built the sensor and was operating it, when it became necessary to open the sensor for some re-work. After the re-work, the sensor was cleaned and re-assembled. Following that, the sensor was operated with no debris generation seen. Given the completed performance testing, the lack of an operative test stand at BEI, the lack of test personnel at BEI, the lack of debris generation in the GE sensor, and on BEI's apparent declining interest in aerospace optical sensors, MDA requested that BEI ship the repaired sensor to MDA. The completed Pitch Stick sensor is shown in Figure 2.4-21.
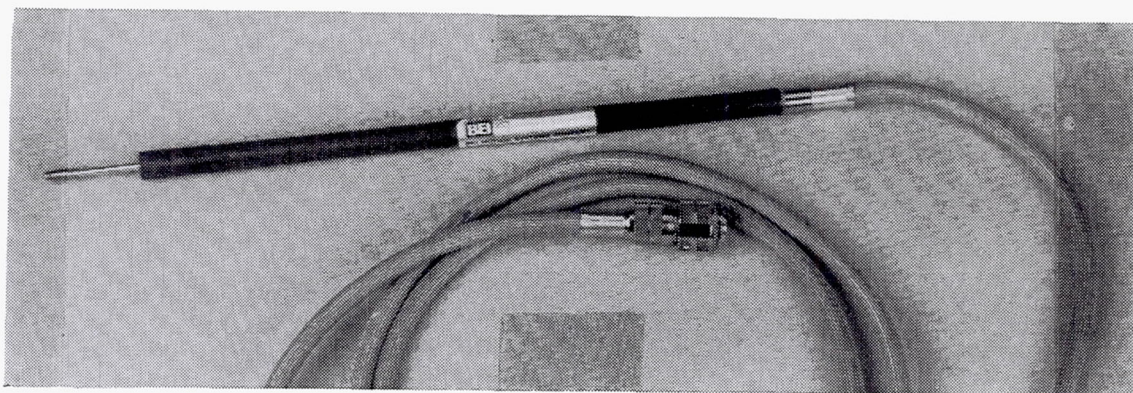
**Figure 2.4-21. Pitch Stick Linear Position Sensor
(WDM Analog Ratiometric, BEI Motion Systems)**

2.4.1.7 Stabilator Position Sensor.

2.4.1.7.1 Design.
Litton Poly-Scientific was selected to build two Stabilator Position sensors based upon their WDM digital sensor proposal. As a first step in the design process, Litton generated detailed interface requirements as part of the sensor ICD. After approval of the ICD parameters, sensor mechanical design commenced. Litton produced a preliminary design for the code plates and opened discussions with code plate manufacturers. The same occurred for bearings and seals, and resulted in the selection of a preliminary design in which a slide mechanism would carry the code plate and optical head. That would be soft-mounted to the external shaft. Sealing for the sensors was by means of a bellows.

Optical designs for the sensors were based upon mature technology developed by Litton for other optical sensor applications which were similar to those in FOCSI. Litton had completed preliminary optical sensor designs and had evaluated some prototype optical hardware in the laboratory. However, some significant changes had been incorporated in the optical sensor designs since the proposal. Originally, each sensor was to have ten optical wavelength bands. Early in analyzing the optical power available, and the specified characteristics of the EOA, Litton determined that each of the ten bands needed to be divided into two sub-bands which always have opposite polarity. Thus, any one band would not just read 0 or 1, but would read 1,0, which is read as 0, or 0,1 which is read as 1. This differential Manchester coding allowed the EOA to work with low contrast ratio signals.

Litton made another change that was similar to a change made independently by AlliedSignal. This was the addition of fixed wavelength reference bands at the short and long wavelength ends of the code plate. These bands made it possible for the EOA to locate the information coded in the wavelengths of the returned broadband signal despite any wavelength changes that might have been caused by temperature or aging effects at the sensors.

Initial mechanical design of the Stabilator sensor resulted in a linear sensor that was >36 inches long to cover the 7 inch Stabilator actuator stroke. This was obviously unacceptable from an aircraft installation standpoint. Litton redesigned the Stabilator sensor to be approximately 17 inches long; however, inspection of the flight test aircraft by MDA showed that the sensor could be no more than 12 inches long and still fit in the required location. To solve this problem, MDA developed the moving case linear sensor concept. In this configuration, the case of the sensor is built much like that of an automotive shock absorber, the outer part of the case moves with the code plate. Since the code plate carries part of the sensor case with it, it is not necessary to make a single case long enough to encompass the full range of motion of the code plate and all the bearings and seals. This allows the sensor length to be shortened from four times the stroke length to slightly more than the stroke length. This was particularly helpful for the Stabilator sensor, which was further reduced in length from 17 inches to 9.6 inches.

Litton subsequently adopted the moving case sensor concept for all their linear sensor designs. The moving case sensor concept is shown in Figure 2.4-22.

Original Linear Sensor Design

"Moving Case" Sensor Design
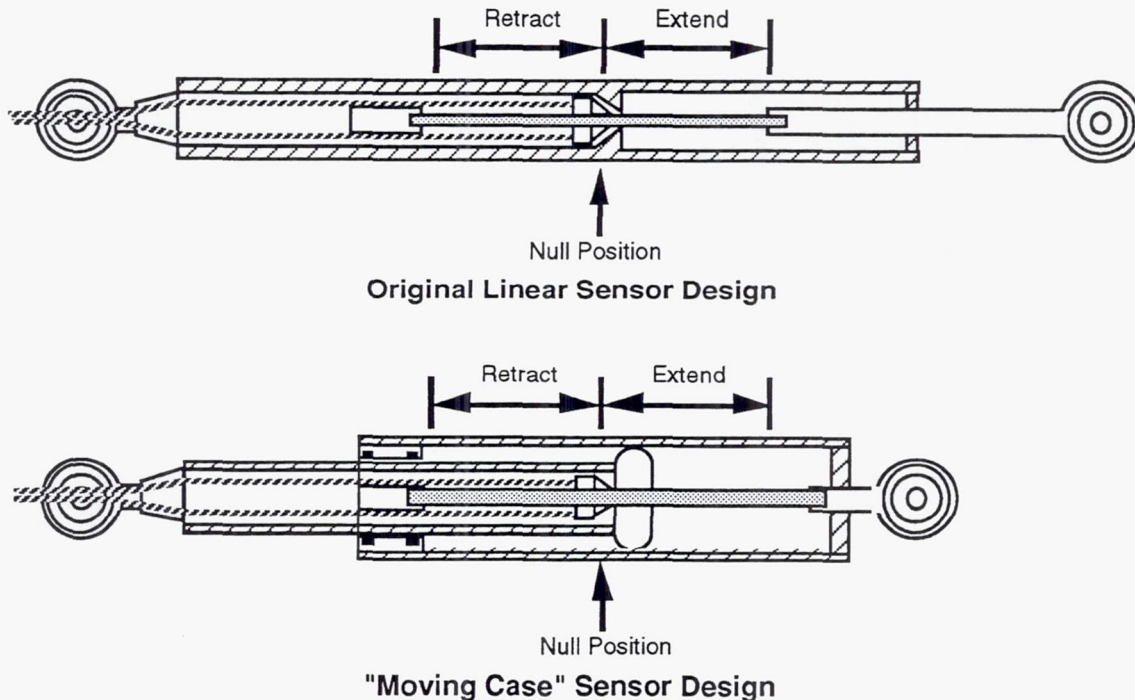
Figure 2.4-22. Compact "Moving Case" Linear Sensor Design Concept

MDA mechanical engineers determined that the 9.6 inch long Stabilator sensor proposed by Litton would fit in the aircraft at the bottom of the left side actuator, and the fibers had to exit from the rod end of the sensor. The moving case design provided the needed fiber exit as well as the required sensor length, and so solved the problem of meeting both requirements.

Litton selected materials for the sensor housings, optical heads, seals, and bearings, and begun construction of a seal test fixture for the short stroke linear sensors. Shaft seal testing was performed on several ground and polished stainless steel shafts. No noticeable wear debris was generated. Based on results of the Stabilator sensor detailed designs, and test fixture results, Litton was granted authority to begin sensor fabrication. An outline drawing for the final FOCSI Stabilator position sensor configuration is shown in Figure 2.4-23.
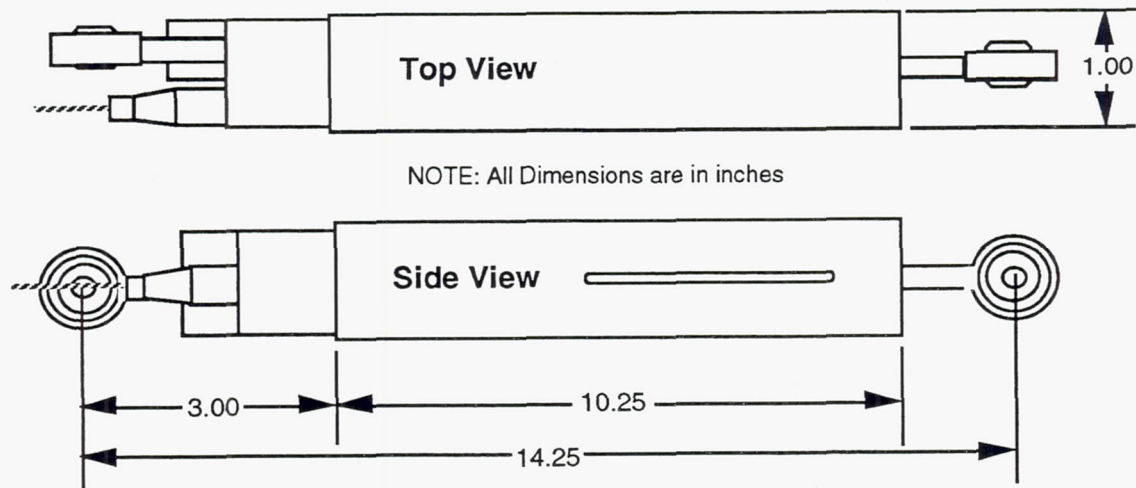
Figure 2.4-23. Stabilator Sensor Mechanical Envelope

2.4.1.7.2 Fabrication.

As the sensor mechanical design was refined and assembly began, further checks were made of the aircraft on which the sensors would be mounted. To develop an installation method for the Stabilator sensor, a Litton engineer joined the MDA engineers at NASA Dryden. They decided the sensor location had to change. The new approach would have the rear mount of the sensor clamped to the cylinder of the Stabilator actuator. The front mount of the sensor would be bolted to the actuator using existing bolts which hold the two halves of the actuator together. NASA Dryden engineers stated that use of those bolts as a support point would be acceptable. The motion for the sensor would be picked up from the travel arm of the follower, located under the Stabilator actuator.

With the mounting provisions fully defined, machining of mechanical parts, including components for supporting the optics, was completed for all sensors. In addition, special adjustment tooling for the optical components was fabricated.

2.4.1.7.3 Performance Testing and Delivery to MDA.

The Stabilator sensors successfully passed initial and post-thermal test functional checks. The thermal testing caused a slight shift in the wavelengths of the signal channels. After thermal testing, the signal channel wavelengths were still within acceptable limits as defined by the ICD; however, the special test receiver is unable to track channel shifts greater than 0.5 nm, so a spectrum analyzer was used for the post-test functional checks.

The use of the spectrum analyzer was fortunate in that it led to the discovery and correction of a subtle error in the optical amplitude peak finding algorithm of the EOA decoding software. That error was corrected immediately.

Shipping of sensors from Litton to MDA began as soon as sensors completed life testing. Both Stabilator sensors were shipped to MDA. Spectrum analyzer plots taken at MDA of the Stabilator sensor outputs after shipping looked good.

The completed Stabilator sensor is shown in Figure 2.4-24.
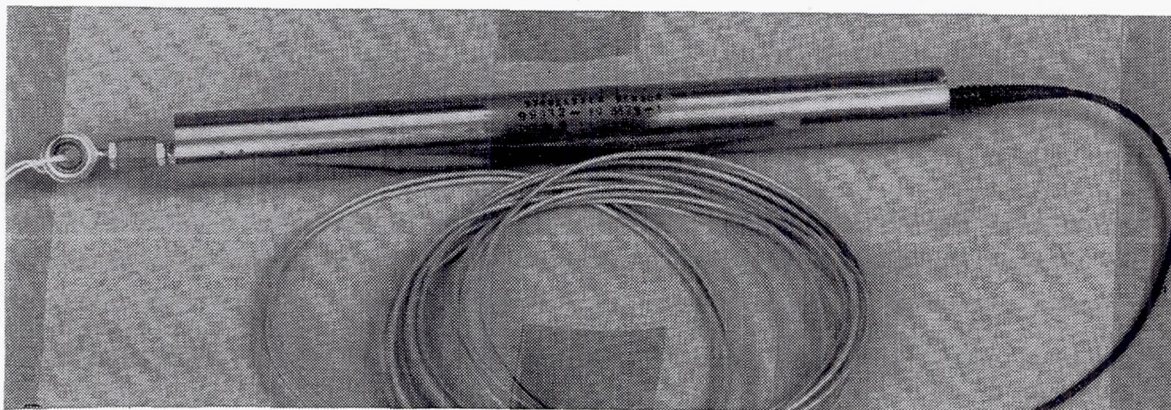
Figure 2.4-24. Stabilator Linear Position Sensor
(WDM Digital Code Plate, Litton Poly-Scientific)

2.4.1.8 Rudder and Rudder Pedal Position Sensor.

2.4.1.8.1 Design.
Litton Poly-Scientific was selected to build two each of Rudder and Rudder Pedal Position sensors based upon their WDM digital sensor proposal. The Rudder and Rudder Pedal sensor development efforts proceeded in parallel because the sensors were so similar as to be essentially identical until the testing phase. As a first step in the design process, Litton generated detailed interface requirements as part of the sensor ICD. After approval of the ICD parameters, sensor mechanical design commenced. Litton produced a preliminary design for the code plates and opened discussions with code plate manufacturers. The same occurred for bearings and seals, and resulted in the selection of a preliminary design in which a slide mechanism would carry the code plate and optical head. That would be soft-mounted to the external shaft. Sealing for the sensors was by means of a bellows.

Optical designs for the Rudder and Rudder Pedal sensors were based upon mature technology developed by Litton for other optical sensor applications which were similar to those in FOCSI. Litton had completed preliminary optical sensor designs and had evaluated some prototype optical hardware in the laboratory. The same changes incorporated into the Stabilator sensor design also appeared in the Rudder and Rudder Pedal designs. These consisted of the shift from simple to differential coding in the optical tracks and the addition of fixed wavelength reference bands at the short and long wavelength ends of the code plate.

Page 89

Litton selected materials for the sensor housings, optical heads, seals, and bearings, and began construction of a seal test fixture for the short stroke linear sensors. Shaft seal testing was performed on several ground and polished stainless steel shafts. No noticeable wear debris was generated.

The initial mechanical design of the rudder sensor revealed that it was short enough to fit the proper location, but was too large in diameter (approximately 2 x 2 inches square). The possibility existed that the rudder access panel could be modified to accommodate the wide sensor. MDA determined that the cost of modifying the aircraft to accept the larger sensor would be cost prohibitive. As a lower cost option it was determined that if the rudder sensor could be reduced to a 1.5 by 1.5 inch cross section, it would fit in the aircraft at the base of the rudder left side without the need for modifications to the aircraft skin.

The Rudder and Rudder Pedal sensors were each totally redesigned using the "moving case" designs previously developed for the Stabilator sensors. The new Rudder and Rudder Pedal designs fit within a 1 inch diameter cylinder. Although the overall sensor lengths were increased slightly, the reduced diameters allowed them to fit into the flight test aircraft. This diameter is smaller than the earlier 1.5 inch maximum and enhances the likelihood of being able to apply these sensors in other applications. It also eliminated the need to alter the orientation of the Rudder Pedal sensor. An outline drawing for the final FOCSI Rudder/Rudder Pedal position sensor configuration is shown in Figure 2.4-25.
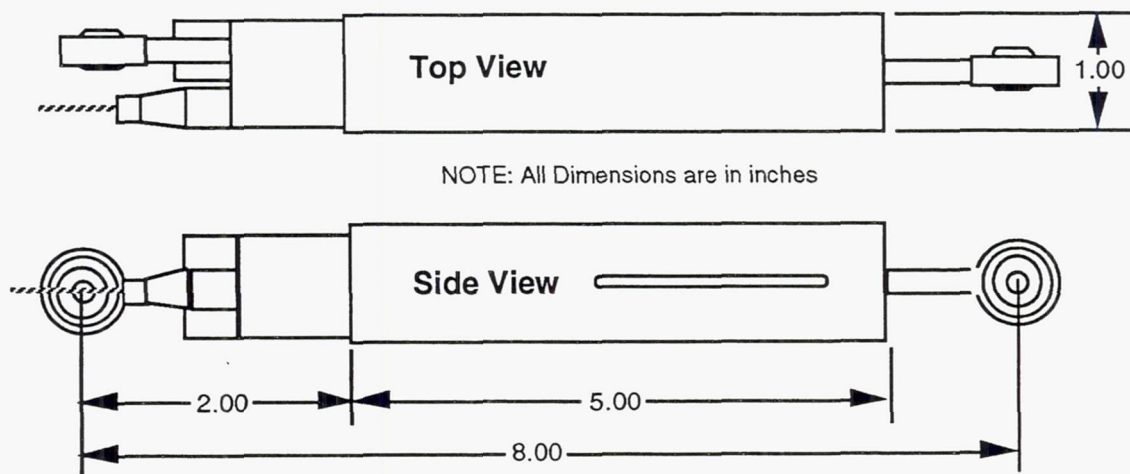
Figure 2.4-25. Rudder/Rudder Pedal Sensor Mechanical Envelope

Sensor prototype test parts were coated with an amorphous diamond-like coating and assembled for run-in testing at Litton. However, during assembly, the substrate was damaged. The cause of the damage was traced to insufficient substrate surface preparation prior to coating. Mechanical design changes were incorporated into the sensors to allow the contacting surfaces to be adequately polished in the future. Re-coated parts were received and tests of the re-coated parts were successful.

The run-in tests of the Rudder and Rudder Pedal sensor inner and outer housings were completed, and no abnormal effects were observed at either 100% or 2% stroke. In addition, sample code plates successfully passed performance tests, so the code plate supplier was instructed to start fabrication of the final plates.

Based on the successful tests of sensor parts, Litton was granted authority to proceed with fabrication of the Rudder and Rudder Pedal sensors.

2.4.1.8.2 Fabrication.

Assembly of the prototype Rudder and Rudder Pedal sensor mechanical components uncovered some mechanical fit problems with the gratings. Fixtures to allow a change in the angle of the gratings were fabricated and corrected the problem. A test article was assembled and successfully completed the full set of vibration and temperature tests. However, problems appeared when life tests were performed. In those tests, the test article was found to generate wear debris which floated to surfaces in the sensors. This debris was traced to the sliding spring edge (which would not remain flat) in the test article which served to hold the code plate carrier in position transverse to its direction of motion in a high vibration environment. The problem had not shown up in previous run-in tests of prototype parts because the spring was not installed. This problem was solved by redesigning the spring so as to cause it to remain flat. According to Litton, that change reduced the generation of debris to an acceptable level. (Note that the generation of debris may not have been totally eliminated. This is a factor in the conclusion that linear optical sensors are harder to build than rotary optical sensors, and may be harder to use reliably in the field.)

In addition to mechanical design and assembly, work continued to reduce the optical loss of the sensor read heads. The effort concentrated on two problems. The first was that the specified wavelengths of light were not appearing at the predicted locations on the CCD array. The second was that the demux optics had greater loss than expected. Litton believed that a 2% to 3% shrinkage of materials in the grating/prism assembly as it cured was causing the wavelength positions to shift. This problem was solved with a minor tooling change.

Litton believed that the higher than expected loss in the demux optics was due to the fact that the couplers were built with 100 μm core fibers using a technique developed for 50 μm fibers. Litton revised the coupler manufacturing method, which reduced the optical losses of the sensor optics to levels within the ICD limits.

During fabrication and testing, Litton made numerous changes to the number of wavelength bands used by the sensors. The changes Litton made repeatedly increased the number of wavelength bands, and therefore the number of code tracks on the code plate, to assure that the EOA would be able to read the sensor accurately and reliably. As a result, the Litton sensors originally intended to have identical optical characteristics ended the program all different.

Another problem was a defect in the sensor optics coating. New optics were made and shipped to the supplier for proper dielectric coating. Final assembly of all the sensors was delayed by lack of properly coated optics. After receipt of the new optics, assembly of both Rudder and Rudder Pedal sensors was completed.

2.4.1.8.3 Performance Testing and Delivery to MDA.

Environmental testing of the Rudder sensors in October uncovered a sensor failure mechanism. During vibration testing, cracks formed in the clevis structure which attaches to the moving portions of the sensor. The Rudder and Rudder Pedal sensors were identical in design, but tested to different vibration levels. The Rudder sensor vibration level is more severe than that of the Rudder Pedal sensor. Litton rebuilt the damaged Rudder sensor, and redesignated both Rudder sensors as Rudder Pedal sensors. The redesignated sensors were then successfully tested to Rudder Pedal sensor requirements. This was done to minimize the impact of the failure on the test schedule. While the redesignated sensors were being tested as Rudder Pedal sensors, the Rudder sensor parts were redesigned with titanium shafts to prevent breakage when exposed to Rudder sensor vibration levels and built into the old Rudder Pedal sensors, which were in assembly. The modified Rudder Pedal sensors were then declared to be Rudder sensors. Unfortunately, the rebuilt Rudder sensors again failed vibration testing. Those sensors had been built with titanium shafts incorporating turnbuckles. Litton could not increase the shaft strength without eliminating the turnbuckle. Litton installed new, stronger shafts lacking turnbuckles, on the Rudder sensors, and tested those. One of the Rudder sensors, without turnbuckles, passed environmental and life testing. The other sensor was found to have excessive optical loss during testing. It was returned to the assembly area for repair, and successfully completed.

The second Rudder sensor entered environmental and life testing after its optics had been re-worked and successfully passed environmental and life testing. The Rudder Pedal sensors were then shipped to MDA. Spectrum analyzer plots of the sensor outputs after shipping indicated that the sensors did not meet the contrast ratio specified in the ICD to guarantee that the EOA could decode the sensors. Litton investigated the question and concluded that the apparent failure was due to differences in the resolutions of the spectrum analyzers used at Litton and MDA.

High resolutions make the contrast ratios appear better. However, the time required for a high resolution spectrum analyzer measurement is much greater

than the time available to the EOA for each sensor reading. Therefore, the critical issue was, could the EOA decode those sensors? Testing at Litton indicated that the EOA was able to decode the Rudder Pedal sensors, even with the possibly lower than expected sensor contrast ratios.

The completed Rudder/Rudder Pedal sensor is shown in Figure 2.4-26.
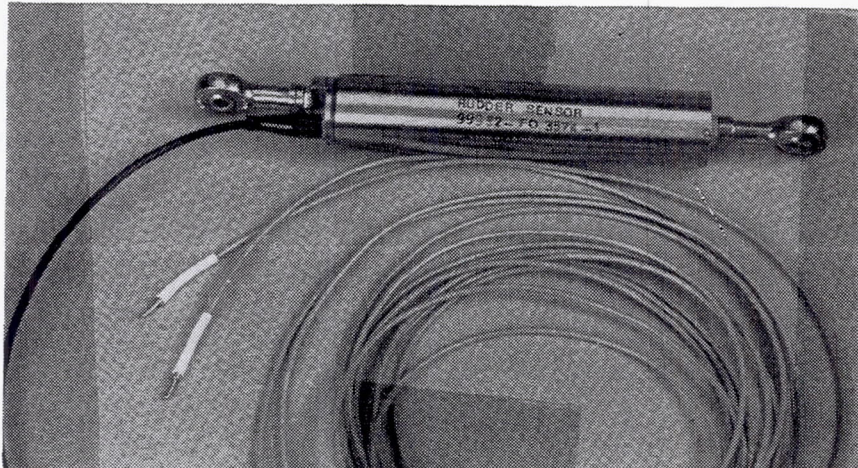
Figure 2.4-26. Rudder/Rudder Pedal Linear Position Sensor (WDM Digital Code Plate, Litton Poly-Scientific)

2.4.1.9 Power Lever Control Position Sensor

2.4.1.9.1 Design.

Litton Poly-Scientific was selected to build two Power Lever Control (PLC) rotary position sensors based upon their WDM digital sensor proposal. As a first step in the design process, Litton generated detailed interface requirements as part of the sensor ICD. After approval of the ICD parameters, sensor mechanical design commenced. Litton produced a preliminary design for the code plates and initiated discussions with code plate manufacturers. The same occurred for bearings and seals, and resulted in the selection of a preliminary design in which a mechanism would carry the code plate and optical head.

Optical designs for the PLC position sensors were based upon mature technology developed by Litton for other optical sensor applications which were similar to those in FOCSI. Litton had completed preliminary optical sensor designs and had evaluated some prototype optical hardware in the laboratory.

Work progressed slowly because many questions arose concerning mounting the sensors into the aircraft and rigging and nulling procedures. A simple mock up of the sensor was fitted into an aircraft at MDA and confirmed the availability of sufficient space for mounting the sensor.

MDA mechanical designers submitted PLC mechanical design and mounting information to engineers at the GE-Lynn facility for review and approval. Minor recommendations were made and the overall design approved. In addition, engineers at GE were able to identify the thermal environment near the PLC sensor. The ambient temperature range near the PLC is -65°F to +335°F. The existing PLC sensor itself is fuel cooled and is specified to operate over a temperature range of -20°F to +275°F. The Litton PLC sensor was to be made of titanium, therefore the additional temperature differential did not pose a problem.

Based on results of the PLC sensor detailed designs, Litton was granted authority to begin sensor fabrication. An outline drawing for the final FOCSI PLC position sensor configuration is shown in Figure 2.4-27.
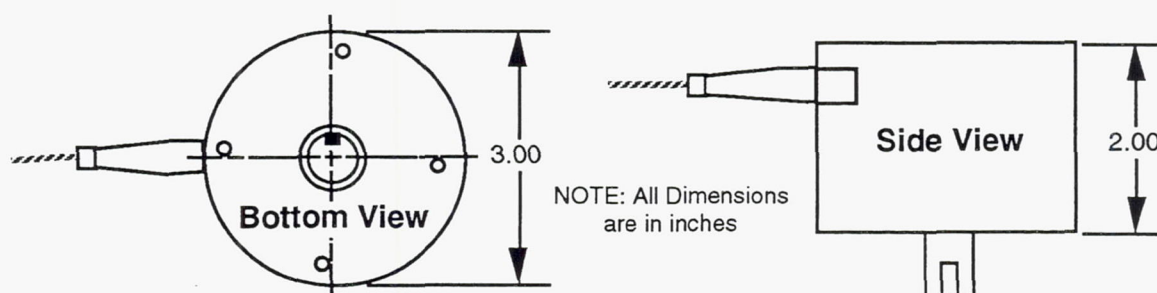
Figure 2.4-27. PLC Sensor Mechanical Envelope

2.4.1.9.2 Fabrication

Final assembly of the sensors was delayed by lack of properly coated optics. After receiving new optics, sensor assembly resumed. Completion of one PLC sensor was further delayed when some epoxy accidentally got into one of the sensor's bearings. The epoxy could not be removed, so a new bearing was ordered. With installation of the new bearing, both PLC sensors were successfully completed.

2.4.1.9.3 Performance Testing and Delivery to MDA.

PLC sensor S/N 001 failed during vibration testing. Inspection of the sensor showed that improperly tightened bearings inadequately supported the code plate. The code plate broke during vibration testing. A test bearing and code plate assembly was built and vibration tested to determine proper bearing tighteness. Those tests were successful. A new bearing set was ordered for PLC sensor S/N 001. The new bearings and code plate were installed, completing re-assembly.

After completion of the tests on the bearing and code plate assembly, PLC sensor S/N 002 was checked. Its bearings were found to have been installed properly. Both PLC sensors then successfully completed environmental and life testing.

PLC sensor S/N 001 was shipped to MDA. However, Litton personnel requested that they be allowed to keep the PLC S/N 002 and Rudder S/N 002 sensors to use in checking the EOA. MDA agreed to that request, as MDA already had the first of each sensor for use in integration testing.

The completed PLC sensor is shown in Figure 2.4-28.
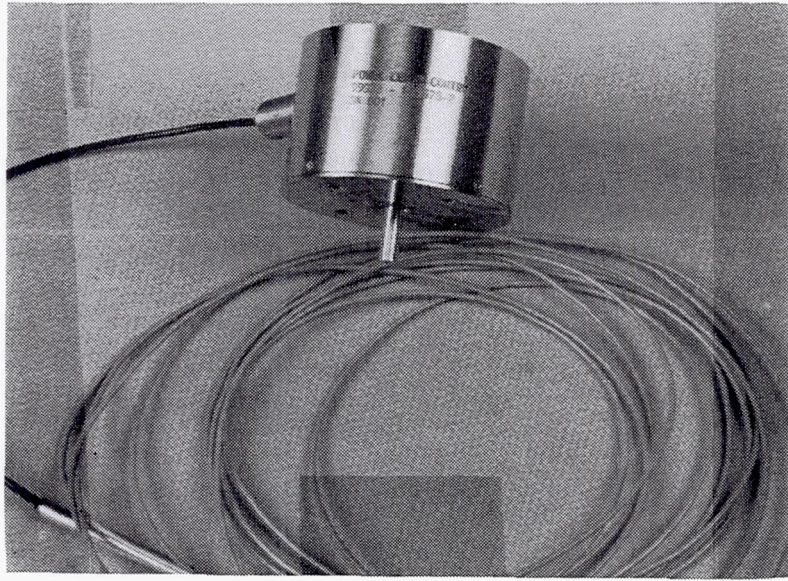
Figure 2.4-28. PLC Rotary Position Sensor
(WDM Digital Code Plate, Litton Poly-Scientific)

2.5 Lab Integration and Test

The final step in the FOCSI program, as highlighted in Figure 2.5-1, involved laboratory integration and testing of the FOCSI hardware components. This step was crucial to verify that the hardware operated as specified, and that it would not pose a safety problem when installed in the flight test aircraft.
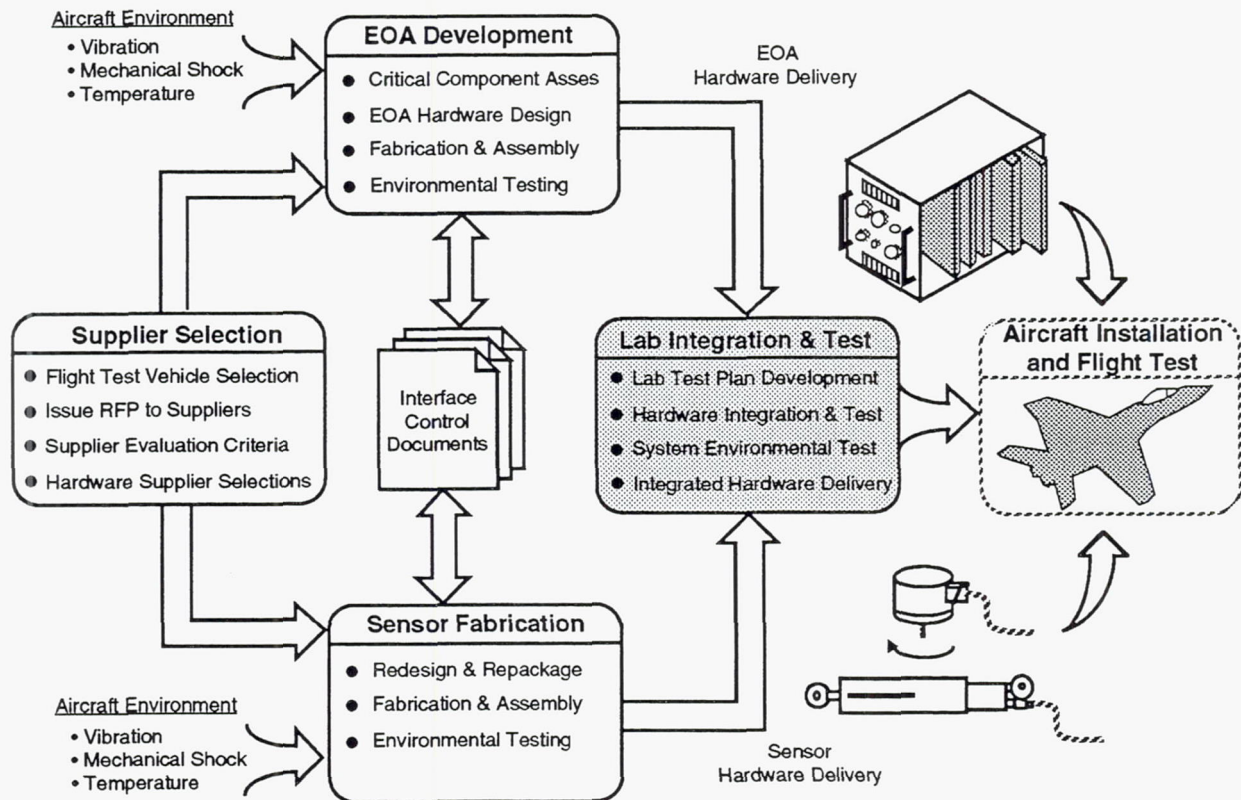
Figure 2.5-1. FOCSI Program Roadmap - Laboratory Integration and Test

Results of laboratory acceptance, integration, and environmental testing are described in the following paragraphs. Acceptance testing consisted of optical testing to verify compliance with the ICD. Integration testing consisted of integrating the sensors to the EOA and verifying performance of the system. Environmental testing consisted of temperature, altitude, vibration, and EMI testing.

2.5.1 Acceptance Test Results

2.5.1.1 EOA CCD Array and TRD Sources and Receivers

The optic test results reflect the mixed successes and failures of EOA performance. The data in Table 2.5-1 shows that the sources and receivers of EOA #1 and EOA #2 had only minor differences in optic performance. However, EOA #2 does perform better than EOA #1 as explained in section 2.5.1.1.1.3.

WDM CCD SOURCE	SPEC.	EOA #1	P/F	EOA #2	P/F
Allowed Power Variation with Wavelength & Temp	≤ 6.0 dB	4.75 dB	P	2.4 dB	P
Allowed Power Variation with Wavelength & Time	≤ 6.0 dB	1.75 dB	P	0.75 dB	P
Repeatability	≤ 8.0 dB	0.50 dB	P	1.125 dB	P
Power Spectral Density (PSD)	≥ -38.0 dBm/nm	-46.4 dBm/nm (max. is -41.3)	F	-45.6 dBm/nm (max. is -43.375)	F
Wavelength Range	≤ 750nm ≥ 900nm	None of the spectrum meets the PSD	F	None of the spectrum meets the PSD	F
Excitation Off Leakage	≥ 20 dB	19.1 dB	F	17.0 dB	F
Repetition Rate	$100 +/- 1$ pulses/sec	100 pulses/sec	P	100 pulses/sec	P
Source Duty Factor	$90 +/- 1\%$	89.6%	P	89.6%	P
Required Rise Time	< 100nsec	20.0 µsec	F	28.0 µsec	F
Required Fall TIme	< 100nsec	28.0 µsec	F	28.0 µsec	F
WDM TRD SOURCE					
Peak Power	≥ -17.5dBm	-37.8 dBm	F	-34.0 dBm	F
Wavelength Range	> 650 nm < 675nm	650nm to 1000nm. None of the spectrum meets the PSD	F	650nm to 1000nm. None of the spectrum meets the PSD	F
Repetition Rate	≤ 1000 pulses/sec	996 pulses/sec	P	990 pulses/sec	P
Source Modulation Depth	≥ 15 dB	0.2dB of normal variation	N/A	source adjustment not possible	N/A
WDM CCD RECEIVER		EOA #1 and EOA #2 (Test results are the same)			
Saturation Level	≥ -60 dBm/nm	CCD array pixel value of 910 (actual value from sensor displays)			
Dark Current Level	≤ -86 dBm/nm	CCD array pixel value of 30 (value obtained from Litton)			
Dynamic Range (at room temperature only)	≥ 26 dB	29.5 dB (This is the calculated range, and it only applies at room temperature.)			
WDM TRD RECEIVER - Tests not possible: no source adjustment or receiver display.					

Table 2.5-1. Optic Test Results for WDM CCD Array and TRD Source / Receiver

2.5.1.1.1 EQA CCD Array Source

2.5.1.1.1.1 Specification Failures

The power spectral density failure results in sensor return signals that are lower than expected which can cause problems depending upon the signal range. Fortunately, the CCD array receiver is able to receive lower power signals than originally expected, however, signals in the lower part of the receiver bandwidth are affected by receiver noise. These signals also have less resolution when fed to an analog to digital converter than signals in the upper portion of the receiver range due to the logarithmic internal workings of the CCD array. For sensors with high insertion loss, the failure of the source to meet power spectral density requirements results in a degraded ability to decode the sensors

The wavelength range failure is due to the failure to meet the power spectral density requirements. The maximum power of the source spectrum is within the correct wavelength range, however this test records the wavelength range covered by the spectrum which meets or exceeds the minimum power spectral density. This is not a serious failure.

The excitation off leakage allowed failure may result in corrupted sensor signals. The area CCD array requires the source to be off when it shifts out its information, otherwise, the optic signals will be exciting the CCD array as the information in the array is being moved through the array. The leakage failure of the source is not serious for two reasons: the sources only failed by 0.9dB and 2.0dB, and the method of measurement is questionable. Since the source is pulsed, an optic to electric converter had to be use to compare the source on and off levels. This converter had a large gain which may have introduced an error causing the leakage to appear greater than actual.

The required rise and fall time failures are due to the vertical bandwidth sensitivity (or resolution) of the oscilloscope. During the test, different scale factors resulted in different rise and fall times. As the resolution increased, the rise and fall times decreased. The resolution could not be made small enough to accurately measure the rise and fall times.

2.5.1.1.1.2. Specification Successes

These successes contribute greatly to successful sensor decoding. Meeting power variation with wavelength prevents a sensor signal which covers too much of the receiver range thus allowing the receiver dynamic range to vary with temperature and still receive the entire sensor signal. Meeting power variation with time prevents a sensor signal from varying too much and allowing returned signals to drift out of the receiver dynamic range. The power variation with time was observed to be very slow which is important to properly decode analog sensors since the effects of the source must be removed. A slowly varying source ensures that the source spectrum which the processor uses to condition the sensor signal is the same

spectrum which excited the sensor. Meeting repeatability creates sensor signals which consistently fall within a certain receiver power range. This allows consistent sensor decoding since it minimizes the effects of the receiver having better resolution at the higher power levels than at the lower power level. It also helps to keep the sensor signal in the receiver range at all times.

2.5.1.1.1.3. Performance Notes
The performance of the CCD array source and receiver in decoding the analog and digital sensors differs between the EOAs. EOA #2 is able to decode more sensors than EOA #1 because of a slightly different placement of an optical block which is used to reduce optical reflections. The effect of the optical block was strongest at the long wavelengths for both EOAs, but its effect in EOA #2 was more evenly distributed over wavelength than in EOA #1. Because of the shape of the power spectrum, the effect of the optical block causes EOA #2 to have a smaller power variation over wavelength, a higher power spectral density, and more power at the 900nm wavelength. These differences allow EOA #2 to better decode sensors which vary to the extremes within their optical specifications.

2.5.1.1.2. EOA TRD Source
The peak power and wavelength range failures caused difficulty in decoding the temperature TRD sensor. The failure of the source to meet the minimum peak power results in a weak sensor signal which is more susceptible to corruption. The wavelength range failure of the source caused source wavelengths to overlap the sensor signal wavelengths which corrupted the sensor signal. The peak power of source spectrum is from 650nm to 700nm, but the source has significant power extending to 1000nm. The sensor signal range is from 700nm to 900nm.

The source modulation depth could not be measured since the power level of the source could not be adjusted. The small source variation during normal operation aids sensor decoding because it helps provide a consistent sensor signal.

2.5.1.1.3. EOA CCD Array Receiver
The expected and actual results of these tests are in different units so the results are limited in value. The CCD receiver display relates power levels to CCD array pixel values instead of dBm, and a pixel value cannot be translated to dBm. The difference between pixel values, however, can be converted to dB so the range was calculated by this method. The calculated range is only good for room temperature since the noise and saturation levels change with temperature.

2.5.1.1.4. EOA TRD Receiver
These tests are not possible since there is no source power level adjustment or display.

2.5.1.2. Sensors

The optic sensor test results reflect the mixed success and failure of the sensors performance. In general, the digital and TRD sensors performed well, but the analog sensors performed poorly. The data in Tables 2.5-2 through 2.5-5 shows the large variance in the code plate characteristics of similar sensors. Large differences even occur between the two sensors of the same type. These differences point to problems in the manufacturing process of the code plates.

2.5.1.2.1. Digital Sensors

The digital sensors meet most of the specifications, and the specifications which are not met did not prevent the EOA from decoding the sensors. However, those failures increased the difficulty of decoding the sensors. The sensor decoding algorithms had to be modified for the sensors with the worst optic failures so the EOA could decode them. Digital sensor data is summarized in Tables 2.5-2 and 2.5-3.

DIGITAL SENSORS	INSERTION LOSS (dB)			CONTRAST RATIO (dB)			WAVELENGTH RANGE (nm)		
	SPEC.	MEAS-URED	P/F	SPEC.	MEAS-URED	P/F	First Channel	Last Channel	P/F
Stabilator 1	≤ 24.0	21.0	P	≥ 6.0	6.8	P	758.6	861.8	P
Stabilator 2	≤ 24.0	16.6	P	≥ 6.0	9.0	P	759.0	864.6	P
Rudder 1	≤ 24.0	17.1	P	≥ 6.0	3.1	F	759.4	873.4	P
Rudder 2	≤ 24.0	17.6	P	≥ 6.0	6.6	P	758.6	867.4	P
Rudder Pedal 1	≤ 24.0	17.2	P	≥ 6.0	8.2	P	759.4	867.0	P
Rudder Pedal 2	≤ 24.0	21.7	P	≥ 6.0	5.4	F	765.8	867.0	P
Power Lever Control 1	≤ 24.0	22.5	P	≥ 6.0	4.8	F	753.0	877.4	P
Power Lever Control 2	≤ 24.0	19.0	P	≥ 6.0	5.9	F	760.2	885.0	P
Leading Edge Flap 43	≤ 28.0	29.4	F	≥ 6.0	5.4	F	778.6	886.6	P
Leading Edge Flap 45	≤ 27.0	22.6	P	≥ 5.0	1.6	F	777.8	888.6	P

Table 2.5-2. Optic Test Results for Digital Sensors (part 1 of 2)

DIGITAL SENSORS	NUMBER OF CHANNELS	CHANNEL WIDTHS (nm)				GUARDBAND WIDTHS (nm) (expect 2.5nm)	
		SPEC.	Smallest	Largest	P/F	Smallest	Largest
Stabilator 1	12	8.5 +/- 0.5	8.0	8.8	P	2.2	7.2
Stabilator 2	12	8.5 +/- 0.5	8.0	8.8	P	1.8	5.8
Rudder 1	13	8.5 +/- 0.5	8.0	8.8	P	2.2	3.8
Rudder 2	13	8.5 +/- 0.5	7.6	8.4	F	2.0	3.6
Rudder Pedal 1	13	8.5 +/- 0.5	7.6	8.8	F	2.0	3.8
Rudder Pedal 2	13	8.5 +/- 0.5	7.8	8.8	F	1.8	3.6
Power Lever Control 1	15	8.5 +/- 0.5	7.2	9.2	F	2.0	2.8
Power Lever Control 2	15	8.5 +/- 0.5	7.6	9.2	F	2.0	4.0
Leading Edge Flap 43	13	8.5 +/- 0.9	7.6	9.6	P	N/A	N/A
Leading Edge Flap 45	13	8.5 +/- 0.9	7.6	10.8	F	N/A	N/A

Table 2.5-3. Optic Test Results for Digital Sensors (part 2 of 2)

The contrast ratio failures of 5dB and below are the failures which make decoding the sensors difficult. The sensors with failures of 5dB or less - rudder 1, leading edge flap (LEF) 43 and 45, and power lever control (PLC) 1 - needed their decoding algorithms fine tuned to their optic spectrum in order for the EOA to be able to decode them. (The algorithm for PLC 1 was never revised because the optic code plate was found to be out of alignment, and it needed to be fixed before changing the algorithm. PLC 1 was not repaired.) Contrast ratio failures between 5dB and 6dB did not affect the ability of the EOA to decode those sensors.

The insertion loss failure of LEF 43 contributes to effects of its contrast ratio failure. The high insertion loss causes the sensor signal to be near the receiver noise level so the sensor signal is easily corrupted by receiver noise.
The wavelength range results for all of the sensors meet the specified range of 750nm to 900nm.

The channel width failures are either not large enough to effect sensor decoding or the widths of the channels are not an important factor in sensor decoding because the results of the channel width test do not correlate with the ability of the EOA to decode the sensors.

The guardband width results are not important. After most of the testing was completed, Litton revised their sensors' interface control documents and eliminated the specification for guardband width. This is permissible since the results do not correlate with the ability of the EOA to decode the sensors, and the locations of the guardbands in the sensor spectrums are not clear and were arbitrarily chosen during testing. The guardbands were originally specified so the EOA could easily distinguish between channels.

2.5.1.2.2. Analog Sensors

The analog sensors meet most of the specifications, and the specifications which were not met only slightly increased the difficulty of decoding the sensors. The fact that the analog sensors are noisy when decoded is mostly due to the EOA, however the sensor dynamic range factors into the problem. Analog sensor data is in Table 2.5-4 and Table 2.5-5.

The reference integrity failures slightly increase the noise of the sensors during decoding, but they do not account for the poor integration test results. The pitch stick sensors will be used as an example. Pitch Stick 1 passes the reference integrity test by a large margin while Pitch Stick 2 fails the test by a significant margin, however, Pitch Stick 1 only performs slightly better than Pitch Stick2 in the integration tests in Table 2.5-10. The integration data contains the effects of internal EOA noise as well as the reference integrity failure effects, and the amount of noise attributed to each cannot be determined.

ANALOG SENSORS	INSERTION LOSS (dB)			DYNAMIC RANGE (dB)			REFERENCE INTEGRITY (dB)		
	SPEC.	MEAS-URED	P/F	SPEC.	MEAS-URED	P/F	SPEC.	MEAS-URED	P/F
Pitch Stick 1	≤ 20.0	15.7	P	≥ 7.5	8.0	P	≤-26.0	-67.1	P
Pitch Stick 2	≤ 20.0	20.2	F	≥ 7.5	8.2	P	≤-26.0	-13.3	F
Trailing Edge Flap 1	≤ 20.0	16.8	P	≥ 7.5	6.8	F	≤-26.0	-7.6	F
Trailing Edge Flap 2	≤ 20.0	11.1	P	≥ 7.5	9.9	P	≤-26.0	-19.4	F
Nose Wheel Steering 1	≤ 20.0	13.6	P	≥ 7.5	19.5	P	≤-26.0	-14.5	F
Nose Wheel Steering 2	≤ 20.0	19.1	P	≥ 7.5	10.6	P	≤-26.0	-1.6	F
Total Pressure 4030-32-01	≤ 17.5	16.8	P	≥ 2.7	2.9	P	≤-30.0	-59.4	P

Table 2.5-4. Optic Test Results for Analog Sensors (part 1 of 2)

ANALOG SENSORS	NUMBER OF CHANNELS	CHANNEL WIDTHS (nm)				WAVELENGTH CENTER (nm)	
		SPEC.	Reference	Signal	P/F	Reference	Signal
Pitch Stick 1	2	≤ 75	51.4	50.2	P	776.2	874.6
Pitch Stick 2	2	≤ 75	45.8	50.0	P	771.8	885.0
Trailing Edge Flap 1	2	≤ 75	50.6	49.8	P	777.0	875.4
Trailing Edge Flap 2	2	≤ 75	51.0	49.0	P	776.2	875.4
Nose Wheel Steering 1	2	≤ 75	50.2	49.8	P	777.4	875.4
Nose Wheel Steering 2	2	≤ 75	49.8	50.2	P	775.0	875.8
Total Pressure 4030-32-01	2	≤ 75	63.8	60.2	P	779.6	885.0

Table 2.4-5. Optic Test Results for Analog Sensors (part 2 of 2)

The dynamic range results are good, however, there are problems concerning dynamic range which include the variations between sensors. The specification of ≥7.5dB is half of the original interface control document value of 15dB. Reducing the dynamic range reduces the signal to noise ratio thus creating noisier sensor decoding. Even though the pressure sensor exceeds the specified dynamic range, the range is so small that the sensor value is greatly affected by small amounts of noise in the EOA decoding process. The pressure sensor vendor does not have this problem since they have an EOA and decoding algorithm tailored to the sensor.

The dynamic range variations between sensors resulting from an inability to produce a repeatable analog code plate is another problem affecting the sensor decoding. The trailing edge flap and nose wheel steering sensors' analog code plates were made the same yet the dynamic range varies widely. As a result, the EOA decoding algorithms were modified to work with the dynamic range of a specific sensor. This would not be necessary if the dynamic range were consistent or larger.

The insertion loss results are good except for the large variation between sensors. The only insertion loss failure, Pitch Stick 2, is very close to passing and is not a concern. The variation of insertion losses shows the inconsistency in the manufacturing process, but does not affect EOA decoding since the largest difference in insertion losses is 9.1dB which is much smaller than the ~30dB range of the EOA receiver.

The results of the number of channels, the channels widths, and the wavelength centers are satisfactory.

The rotary analog code plates of the trailing edge flap and nose wheel steering sensors all have anomalies on the ends of the optic tracks, however, the anomalies seemed to be just outside of the sensors' operational range so they are not a concern. Each end of an optic track is different, but the reference and signal tracks are genarally not consistent. In some cases, the reference is not a constant power level while the signal track is constant. In other cases, the signal track varies too much.

2.5.1.2.3. TRD Sensors

The TRD sensors pass the optic tests, and are the best sensors for providing duplicate results. The data for the TRD sensors is in Table 2.5-6.

The signal duration success is the key characteristic in determining that the sensors are performing properly. The duration of the sensor florescent time decay signal varies with temperature and determines the phase shift between the signal and the source. The EOA examines the phase shift between the signal and source signals to determine the temperature.

The power conversion efficiency for both temperature sensors actually passes if the entire sensor signal is taken into account instead of just the peak of the sensor spectrum. The test was conducted with just the peak of the source and signal spectrums and reflects a failure as a result. The test was performed this way due to the misunderstanding that the TRD receiver uses only the peak spectrum values. The TRD receiver actually uses the entire signal spectrum.

TRD SENSORS	SIGNAL DURATION(μsec) (@ room temp.)			POWER CONVERSION EFFICIENCY (dB)			CHANNEL CHARACTERISTICS		
	SPEC.	MEAS URED	P/F	SPEC.	MEAS URED	P/F	# of Chan.	Channel Width	Channel Center
Total Temperature 2	175 +/-	280	P	≥ -28	-49.7	F	1	36.0 nm	753 nm
Total Temperature 3	125	270	P	≥ -28	-48.0	F	1	36.0 nm	753 nm

Table 2.5-6. Optic Test Results for TRD Sensors

2.5.2. Integration Test Results

2.5.2.1. EOA

EOA #1 passed all of the functional tests. These were used to provide a quick test of EOA operation. The data is summarized in Table 2.5-7. The EOA chassis is able to thermally dissipate approximately 100 Watts without cooling air so it will be able to dissipate 65.4 Watts easily. The optic functions and the electrical data bus performed as expected. The optic to electric conversion and the sensor value decoding were not checked in the functional tests.

EOA FUNCTIONAL TEST	EOA FUNCTIONAL TEST RESULTS		
	Expected	Actual	P/F
Power Dissipation	≤ 76.5 Watts	65.4 Watts	P
1553 Multiplex Bus	No errors in transmission and good data transfer.	Good data transfer. A nuisance error is reported, but it does not affect the data transfer. Suspect the test equipment is the source of the problem since the problem has been seen on other non-FOCSI tests.	P
EOA Spectrum Analyzer Mode	Source and all sensors (except temp. sensor) visible on display.	Source and all sensors except the temperature sensor are visible on the display. Digital sensors show a good digital pattern, and the analog sensors show the reference and signal channels. The attenuation for each sensor was adjusted so all sensors fell within the receiver range.	P

Table 2.5-7. Integration Test Results for EOA

EOA #2 performs better than EOA #1 by decoding sensors with less noise and by operating reliably. This is due in part to optical differences explained in section 2.5.1.1.1.3. EOA #1 also has had the 1553 bus stop updating on many occasions including the altitude test, the vibration test, and when EOA #1 was powered for long periods of time with no tests being performed. This seems to be due to software halting in the decoding processor module. The root cause may be internal EOA noise which could be generated by many sources, several high frequency clocks, high frequency 1553 data transfers, power supply switching, or decoding modules activity. A similar problem was present before the data acquisition card's printed wiring board (PWB) was re-laid out to use better methods of electrical PWB lay out. The solution to the loss of EOA #1 1553 updates is to turn off power to EOA #1 and then turn on power; EOA #1 always returns to normal operation. EOA #2 has never had this problem. This is probably due to EOA #2's decoding modules being less susceptible to internal noise. This may also explain why EOA #2 decodes sensors with less noise than EOA #1.

EOA decoding noise is dependent on the environment and may be high frequency noise affecting the CCD optic receiver. The receiver operates with very low power levels and is therefore more susceptible to noise than other electronics. Decoding noise is not as pronounced when the modules are on the vendor's development backplane as it is when the modules are in the EOA chassis. On vendor backplane, the modules are not as close to each other, the 1553 data bus does not run next to the modules, and an inherently noisy switching power supply is not used. The confined EOA chassis is a different environment than the open development backplane so it is not unusual that the modules operate a little differently in the two environments.

2.5.2.2. Digital Sensors

The EOA performs very well in decoding digital sensors that can be decoded, however a small amount of noise does cause a few failures. EOA decoding noise is discussed in section 2.5.2.1. Good performance is expected since the EOA vendor also made the digital sensors except for the leading edge flap sensor which could not be decoded. Digital sensor test results are summarized in Tables 2.5-8 and 2.5-9.

2.5.2.2.1. Stabilator Sensor
The EOA decodes the Stabilator sensor fairly well. The decode value is quite stable, although there is some intermittent noise which causes the failures in the null offset and resolution tests. The overall results are good.

2.5.2.2.2. Rudder Sensor
EOA #1 cannot decode rudder 1, and EOA #2 has difficulty decoding rudder 1. This is probably due to the optical contrast ratio of less than 5.0dB. With EOA #2, the sensor output looks noisy which is reflected in the integration data, although, rudder 1 still performs fairly well. When rudder 1 was returned to the vendor for testing, the decoding algorithm was changed so that rudder 1 performed very well, however rudder 2 cannot use the same algorithm. The flight EOA rudder decoding algorithm is dependent on which rudder is flying. The EOA decodes rudder 2 sensor very well. The decode value is quite stable, although there is some intermittent noise which causes the failure in the null offset test. The overall results are good. The rudder and rudder pedal sensors are the same, and the decode algorithms are only slightly different.

2.5.2.2.3. Rudder Pedal Sensor
The EOA decodes the rudder pedal sensors better than any other sensor. The range and resolution results are excellent, the linearity results are almost perfect, and there is hardly any noise in the decoded sensor signals. The only failure, by rudder pedal sensor 2, is very close to passing and is not a concern. The rudder pedal and rudder sensors are the same, and the decode algorithms are only slightly different.

2.5.2.2.4. Power Lever Control Sensor

Neither EOA can decode power lever control 1. This is probably due to an optical contrast ratio of less than 5.0dB, or the sensor may have been damaged before the integration tests. When this sensor was returned to the vendor for testing, it was reported that the sensor was broken. The code plate was shifted, and the shaft did not turn as freely as it should. The sensor may have been damaged before the integration tests were performed.

EOA #2 decodes power lever control 2 very well while EOA #1 cannot. This is due to the different optics in the EOAs explained in section 4.1.1.3. Power lever control 2 has its last channel at a wavelength of 885nm which is close to the limit of 900nm. EOA #1 does not receive signals as well as EOA #2 at this end of the spectrum, and the performance of power lever control 2 is proof.

2.5.2.2.5. Leading Edge Flap Sensor

The EOA decoding algorithms could not decode either leading edge flap sensor. Both sensors had optic failures which contributed to the decoding problem; see the optic test results in section 2.5.1.2.1. However, the main reason was due to the wide variation of the wavelength of the first channel on the code plate as the sensor was moved through its full stroke. The decoding algorithm searched for each channel, and because the location varied so much, the algorithm needed more time than the EOA update rate would allow.

The decoding algorithms were changed after integration tests were performed at McDonnell Douglas so the leading edge flap sensors could be decoded. The algorithms were written to find the data channels at specific wavelengths. As a result, the algorithms would not decode the sensors if the data channels move from their initial locations. This occurs if the code plate shifts even slightly.

DIGITAL SENSORS	NULL OFFSET (inches unless specified)			RESOLUTION (inches unless specified)		
	Specified	Measured	P/F	Specified	Measured	P/F
Stabilator 1	≤ +/-0.018	+/- 0.045	F	≤ +/-0.018	0.002	P
Stabilator 2	≤ +/-0.018	+0.052, -0.073	F	≤ +/-0.018	0.022	F
Rudder 1	≤ +/-0.0032	+0.007, -0.011	F	≤ +/-0.0032	0.001	P
Rudder 2	≤ +/-0.0032	+/-0.002	P	≤ +/-0.0032	0.002	P
Rudder Pedal 1	≤ +/-0.0045	+/-0.001	P	≤ +/-0.0045	0.002	P
Rudder Pedal 2	≤ +/-0.0045	+0.004, -0.005	F	≤ +/-0.0045	0.002	P
Power Lever Control 1	≤+/-0.325deg	Not Decoded		≤+/-0.325deg		
Power Lever Control 2	≤+/-0.325deg	+/-0.064deg	P	≤+/-0.325deg	0.079 deg	P
Leading Edge Flap 43	≤ +/-0.30deg	Not Decoded *		≤ +/-0.30deg		
Leading Edge Flap 45	≤ +/-0.30deg	Not Decoded *		≤ +/-0.30deg		

Table 2.5-8. Integration Test Results for Digital Sensors (part 1 of 2)

DIGITAL SENSORS	RANGE (inches unless specified)			LINEARITY				
	Spec.	Measured	P/F	Slope	Con-stant	Standard Deviation Specified	Meas.	P/F
Stabilator 1	+/- 3.56	+/- 3.56	P	0.996	0.008	≤+/-0.0356	0.034	P
Stabilator 2	+/- 3.56	+/- 3.56	P	0.989	-0.009	≤+/-0.0356	0.051	P
Rudder 1	+/-0.665	+/- 0.665	P	0.986	-0.004	≤+/-0.0033	0.014	P
Rudder 2	+/-0.665	+/- 0.665	P	0.996	0.002	≤+/-0.0033	0.008	P
Rudder Pedal 1	+/-0.750	+/- 0.750	P	0.999	0.001	≤+/-0.0019	0.002	P
Rudder Pedal 2	+/-0.750	+/- 0.750	P	1.000	0.001	≤+/-0.0019	0.004	P
Power Lever Control 1	0.000 to			Not Decoded		≤ +/- 0.175		
Power Lever Control 2	130.000 degrees	0.000 to 130.000	P	0.993	-0.539	≤ +/- 0.175	0.563	P
Leading Edge Flap 43	+36, -7			Not decoded*		≤ +/- 0.675		
Leading Edge Flap 45	degrees			Not decoded*		degrees		

* Before the decoding algorithms were changed at the EOA vendor.

Table 2.5-9. Integration Test Results for Digital Sensors (part 2 of 2)

2.5.2.3. Analog Sensors

The EOA performs poorly in decoding analog sensors for several reasons: the EOA decoding noise discussed in section 2.5.2.1., poor optical reference integrity test results slightly increase the decoding noise, and the decoding algorithms are dependant upon a consistent dynamic range (which did not occur) for the similar analog sensors. The last reason is due to the fact that the EOA vendor did not have the sensors to work with when writing the decoding algorithms so the algorithms were not tailored to the specific dynamic range of the sensors. Analog sensor test results are summarized in Tables 2.5-10 and 2.5-11

2.5.2.3.1. Pitch Stick Sensor

Pitch stick 2 broke during integration testing so the linearity data was not obtained. A small amount of strain was applied to the sensor and it broke apart. The mechanical design was very poor in that the two halves of the sensor were butt coupled and held together only by glue.

The EOA decoding of the pitch stick sensors is the best of the analog sensors, however a slightly incorrect expected dynamic range caused the range and linearity results to fail. The decoding noise does not affect these sensors as much as the other analog sensors, but the noise does cause the null offset results to fail.
After the decoding algorithm was tailored to the correct dynamic range, the pitch stick sensor performs fairly well. EOA noise still prevents this sensor from providing excellent performance.

2.5.2.3.2. Trailing Edge Flap Sensor and Nose Wheel Steering Sensor

The nose wheel steering and trailing edge flap sensor code plates were made the same, and the decoding algorithms are only slightly different, yet the decoded performance of the sensors varies widely due to the wide variation in dynamic range. Only trailing edge flap 1 is decoded over the entire range of shaft movement with any accuracy. The other decoded sensor values either fail to relate to the shaft movement or only a portion of the shaft movement is decoded.

After the decoding algorithms were tailored to the dynamic ranges of these sensors, the decoded sensor performance improved, but the overall decoded performance is still poor. The decoded values are very noisy, and the sensors' linearity is poor.

2.5.2.3.3. Total Pressure Sensor

The EOA decoding algorithms could not decode the pressure sensor because the equation for the sensor signal received from the sensor vendor did not fit the location and dynamic range of the sensor as seen by the EOA CCD receiver. Modified algorithms enabled the decoded sensor value to wok over a portion of the pressure sensor range, but not enough to do integration tests on the sensor.

The decoding algorithms were changed after integration tests were performed at McDonnell Douglas so the pressure sensor could be decoded over its full range. The algorithms were written for linear operation of the pressure sensor even though the sensor vendor used a third order equation to approximate the sensor response and get the desired accuracy from the sensor. The person writing the decoding algorithm felt that there was less error in using the linear method.

ANALOG SENSORS	NULL OFFSET (inches unless specified)			RESOLUTION (inches unless specified)		
	Specified	Measured	P/F	Specified	Measured	P/F
Pitch Stick 1	≤ +/-0.010	+0.030, -0.039	F	≤ +/-0.010	0.003	P
Pitch Stick 2	≤ +/-0.010	+0.047, -0.053	F	≤ +/-0.010	0.004	P
Trailing Edge Flap 1	≤ +/-0.049in	+/- 0.123 in	F	≤+/-0.898deg	0.567deg	P
Trailing Edge Flap 2	≤ +/-0.049in	+0.075,-0.076in	F	≤+/-0.898deg	0.099deg	P
Nose Wheel Steering 1	≤ +/- 0.186 degrees	+2.273, -2.419 degrees	F	≤ +/- 0.186 degrees	0.265 degrees	F
Nose Wheel Steering 2	≤+/-0.186deg	+/- 0.953 deg	F	≤+/-0.186deg	0.773deg	F
Total Pressure 4030-32-01	Neither EOA #1 nor EOA #2 could decode the pressure sensor at the time of the integration testing at McDonnell Douglas.					

Table 2.5-10. Integration Test Results for Analog Sensors (part 1 of 2)

ANALOG SENSORS	RANGE (inches unless specified)			LINEARITY				
	Spec.	Measured	P/F	Slope	Con-stant	Standard Deviation		P/F
						Specified	Meas.	
Pitch Stick 1	+2.02 -1.01	+1.950 ** -0.763 **	F	0.976	0.047	≤+/-0.0202	0.087	F
Pitch Stick 2	+2.02 -1.01	+2.02 -0.783 **	F	Pitch Sensor 2 broke before the linearity data was taken.				
Trailing Edge Flap 1	+/- 4.05	+/- 4.05	P	1.219	-0.075	≤+/-0.0405	0.719	F
Trailing Edge Flap 2	+/- 4.05	+4.05 -0.820 **	F	-0.386	-2.558	≤+/-0.0405	0.046	F
Nose Wheel Steering 1	+/-75.00 degrees	+/-75.000 degrees *	F	0.992	18.749	≤ +/-0.188	18.383	F
Nose Wheel Steering 2	+/-75.00 degrees		F	1.067	0.459	≤ +/-0.188	7.721	F
Total Pressure 4030-32-01	Neither EOA #1 nor EOA #2 could decode the pressure sensor at the time of the integration testing at McDonnell Douglas.							

*   Even though the full range is covered, the measured value has no relationship with the reference.
** These measured values are before the decoding algorithms were changed at the EOA vendor.

Table 2.5-11. Integration Test Results for Analog Sensors (part 2 of 2)

2.5.2.4. TRD Temperature Sensors

The conventional platinum resistance thermometer (PRT) elements performed well, but the optic temperature sensor decoding performed poorly as shown in the data summarized in Table 2.5-12. The accuracy of the PRT elements, tested in an ice bath, were very stable; the results were so good that a second test point was not needed. Comparing the tracking of the decoded optic sensor value to the PRT element revealed the optic decoding was not working between $360°R$ and $410°R$, and the error was as much as $36°R$ from $410°R$ to $580°R$.

The poor range of the optical temperature decoding is probably due to the decoding algorithms being fine tuned to a different Rosemount optical sensor than is used in the integration tests. The decoding algorithms were later fine tuned to the optical sensors used in integration testing.

The noise and poor tracking of the optical temperature sensor is probably due in part to the optic source used to excite the fluorescent sensor. This is due to the fact that the source wavelengths overlap the sensor signal wavelengths. Even though an optical filter was used to block the source at the sensor signal's peak wavelengths, much of the sensor signal is blended with the source. The small section of the sensor signal that is unaffected by the source may not be enough for the optic receiver to obtain a consistent signal.

TRD SENSORS	PRT ELEMENT RESISTANCE (@ 32°C)				GEN. THERMAL. DIFFERENCE BETWEEN PRT & TRD				INITIAL CHECKOUT		
	Spec.	PRT 1	PRT 2	P/F	Spec.	Max.	Min.	P/F	Spec.	Measured	P/F
Total Temperature S/N 2	50.00 +/- 0.05Ω	49.992 ohms	49.995 ohms	P	≤ +/- 0.50°F	No optical tests performed due to poor performance of S/N3.			≤ 2.0°F	Unstable and noisy. Much	F
Total Temperature S/N 3	50.00 +/- 0.05Ω	50.038 ohms	50.008 ohms	P	≤ +/- 0.50°F	36°R	1°R	F	≤ 2.0°F	greater than 2.0°F.	F

Table 2.5-12. Integration Test Results for TRD Sensors

2.5.2.5. Sensor Results After Decoding Algorithms Changed

The LEF, temperature, and analog sensor decoding algorithms were changed by the EOA vendor after the integration tests at McDonnell Douglas. The LEF sensors were able to be decoded, and their performance appeared to equal the performance of the other digital sensors. The temperature sensor algorithms were tuned to the individual sensors so the specified temperature range was met, but the temperature sensors are still much too noisy. The Pitch Stick, trailing edge flap, and nose wheel steering sensor algorithms were changed so those sensors met the range specifications. Their linearity performance was improved but not enough to meet the specifications. Null offset and resolution performances were not improved.

2.5.3. Environmental Test Results

2.5.3.1. Pressure Sensor

The pressure sensor was environmentally tested at MDC since Babcock & Wilcox did not complete environmental testing. The pressure sensor survived all environmental testing: temperature, altitude, and vibration. The environmental test profiles are the same as the EOA environmental profiles.

2.5.3.2. EOA

2.5.3.2.1. Temperature Test
EOA #2 survived the thermal test chamber temperature range of -30°C to 75°C, however, the EOA did not decode all of the sensors over that range. The test results summarized in Table 2.5-13 show the EOA's success in decoding digital sensors and the EOA's difficulty in decoding analog sensors.

SENSOR	SENSOR VALUE	SENSOR IS SUCCESSFULLY DECODED OVER EOA#2 TEMPERATURE RANGE OF:	
Digital Sensors			
Power Lever Control 2	97.5 deg.	Full Range of -30°C to 75°C	
Rudder Pedal 2	0.293 in.	Full Range of -30°C to 75°C	
Stabilator 2	-3.212 in.	Full Range of -30°C to 75°C	
Rudder 2	-0.496 in.	Rudder is sometimes decoded throughout full range.	
Leading Edge Flap 43	Not Decoded	EOA unable to decode LEF sensor during thermal test.	
Analog Sensors			
		Successful Decoding Over EOA#2 Temp. Range Of:	Direction of Temperature Change
Pitch Stick 1	~-0.330 in.	26°C to -30°C+5minutes	Decreasing
		10°C to 60°C	Increasing
		none	Decreasing
Trailing Edge Flap 1	~1.2 in.	26°C to -10°C	Decreasing
		30°C to 55°C	Increasing
		25°C+10min. to 25°C+15min.	Decreasing
Nose Wheel Steering 2	~26 deg.	26°C to -5°C	Decreasing
		none	Increasing
		none	Decreasing
Total Pressure	Not Connected	EOA software is not able to decode the pressure sensor at room pressure during thermal test.	
TRD Sensor			
Temperature	Not Connected	EOA software is not able to decode the temperature sensor at room temperature during thermal test.	

Table 2.5-13. EOA Thermal Test Results

The EOA performance with the digital sensors during the thermal test was excellent. The digital sensors were decoded over the full EOA temperature range, and the sensor values were steady. The two exceptions, rudder and leading edge flap (LEF), were due to problems not related to the thermal test, the rudder connection to the EOA and the EOA decoding algorithm for the LEF. The ability of the EOA to decode the digital sensors is independent of the EOA temperature.

The EOA performance with the analog sensors during the thermal test was poor. The sensors were decoded over very little of the EOA temperature range, and the sensor values were noisy which is normal even at room temperature. The pitch stick was decoded over 50% of the EOA temperature range, the trailing edge flap 29%, and the nose wheel steering 14%. These results agree with the EOA vendor tests which show the EOA has decreasing dynamic range for receiving analog sensors as the EOA temperature approaches the extremes, and at the extremes, there is zero dynamic range. The ability of the EOA to decode the analog sensors is very dependent on the EOA temperature.

The reasons for the poor performance of the EOA decoding the analog sensors are that analog sensor decoding is power level dependent, and the shape of the LED output power spectrum changes with temperature. The decoding algorithms were written to try to take out the effects of the source spectrum shape but were not totally successful since the analog sensor decoding is very EOA temperature dependent.

2.5.3.2.2. Altitude Test

EOA #1 survived the altitude test chamber range of room altitude to 50,000 feet. Room pressure was 743 Torr or 29.3 in Hg. The chamber temperature range was 23.7°C to 32.5°C, and the internal EOA temperature range was 24.1°C to 41.5°C. The EOA stopped updating the 1553 bus during a portion of the test, however this failure was not related to the altitude test. The test results summarized in Table 2.5-14 show the EOA's success in decoding all of the sensors during the altitude test.

EOA #1 performance during the altitude test was acceptable. The noisy sensor values and the loss of 1553 bus updates tarnished the results, but these problems were not a result of the altitude test. The ability of the EOA to decode the sensors is independent of the EOA altitude. Since the sensors were decoded equally well throughout the test, and in normal operation EOA #1 reports noisy sensor values much more than EOA #2, the noisy sensor values are not a failure of the altitude test. The loss of 1553 updates is also not a failure of the altitude test and is explained in 2.5.2.1.

SENSOR	SENSOR VALUE	SENSOR IS SUCCESSFULLY DECODED OVER EOA#1 ALTITUDE RANGE OF:
Digital Sensors		
Power Lever Control 2	Not Connected	The Power Lever Control Sensor was not available for the altitude test.
Rudder Pedal 2	~0.121 in.	Full Range of 743 Torr to 50,000 feet
Stabilator 2	-2.210 in. & -2.161 in.	Full Range of 743 Torr to 50,000 feet. The position was changed during test as part of troubleshooting.
Rudder 2	~-0.118 in.	Full Range of 743 Torr to 50,000 feet
Leading Edge Flap 43	Not Decoded	EOA unable to decode LEF sensor during altitude test.
Analog Sensors		
Pitch Stick 1	~1.2 in.	Full Range of 743 Torr to 50,000 feet
Trailing Edge Flap 1	~1.4 in.	Full Range of 743 Torr to 50,000 feet
Nose Wheel Steering 2	~41 deg.	Full Range of 743 Torr to 50,000 feet
Total Pressure	Not Connected	EOA software is not able to decode the pressure sensor at room pressure during altitude test.
TRD Sensor		
Temperature	Not Connected	EOA software is not able to decode the temperature sensor at room temperature during altitude test.

Table 2.5-14. EOA Altitude Test Results

2.5.3.2.3. Vibration Test

EOA #1 survived the vibration tests, and the vibration did not affect the sensor decoding, however, there were failures that were corrected and re-tested and one failure that was not corrected. The vibration testing consisted of a sinusoidal resonance survey, a random performance test, and a minimum structural rigidity test in each of the three axes.

The failure that was not corrected occurred on an already environmentally qualified power supply supplied by the Navy Standard Hardware And Reliability Program (SHARP). The failure was not corrected and retested since all of the performance tests had been completed, and the failure occurred during the structural rigidity test which is not required by NASA Ames-Dryden Flight Research Facility Process Specification No. 21-2 Environmental Testing of Electronic and Electromechanical Equipment. An examination of the power supply revealed the leads of a transformer had sheared because of inadequate support. (Adequate support was provided in later models of the power supply.)

The purpose of the three vibration tests is to determine if the EOA will survive the aircraft vibration environment. The resonance survey locates the frequencies at which the EOA is vulnerable. The performance test requires the equipment operate during the vibration profile and shows the equipment will survive at least fifty flight hours. The minimum structural rigidity test does not require the equipment to operate and verifies the equipment is structurally sound.

The first failure occurred during the vertical axis performance test. The 1553 bus stopped updating, and the failure was isolated to one of the two 1773/1553 converter modules. A loose nut and two washers were found inside the chassis, and a screw was found outside the chassis. The two converter modules were removed, and the 1553 data bus line was jumpered to bypass the 1773/1553 converter modules. The loose mounting hardware was replaced and secured with Locktite. Testing continued without the converter modules. The 1773/1553 converter module failure was attributed to an electrical short caused by the loose mounting hardware.

The second failure occurred during the vertical axis minimum structural rigidity test. The 1553 bus again stopped updating, and the failure was isolated to 1553 bus controller module. An oscillator chip had sheared at the leads. Also, several capacitors had sheared off of the optic receiver module. None of the sheared parts had glue attaching them to the printed wiring board (PWB). The modules were repaired, and on all modules, all of the components which were not glued to the PWBs were glued. This improvement was implemented on the set of flight modules. Testing continued.

The vibration testing continued through the lateral axis and through the longitudinal axis sinusoidal and performance tests without failure, however, two anomalies occurred. The first was not related to vibration testing. The 1553 bus stopped updating several times during and between vibration tests. Turning the

power to the EOA off and then on always restored normal operation. This is the same anomaly explained in section 2.5.2.1. The other anomaly may have been related to the minimum structural vibration test since it occurred during part of both the vertical and longitudinal axes minimum structural vibration tests even though it did not occur during the lateral axis minimum structural vibration test. It dealt with the optic spectrums reported by the EOA CCD array receiver. A new method of monitoring the sensors was used after the last failure. Instead of monitoring the sensor positions, the raw optical sensor data was monitored. For a portion of the minimum structural rigidity tests, the optic data power levels jumped around quite a bit but maintained their shapes unless they saturated the receiver. The anomaly was not a concern since the equipment did not need to operate during the minimum structural rigidity test, and the spectrum shapes were stable.

The last failure occurred during the longitudinal minimum structural rigidity test, and has already been discussed. The power supply failed during the test.

2.5.3.2.4. Electromagnetic Interference (EMI) Test

EOA #1 failed to meet the conducted and radiated emission limits in MIL-STD-461 Part 2 due to spikes in the data; the majority of the conducted and radiated emissions data meets those limits. EMI experts examined the test data and did not feel that the EOA poses an EMI threat to the aircraft since the outages are few and the majority of the outages are small.

EOA #1 was a good EMI test article since it probably has more emissions than EOA #2 based on the performance of the two EOAs. EOA #2 has never failed while EOA #1 has stopped updating the 1553 bus. This was probably due to internal EOA emissions causing errors in the optic decoding modules.

The antennae types used in this test are: rod for 14kHz to 25MHz, biconical for 25MHz to 200MHz, log spiral for 200MHz to 1GHz, and a different size log spiral for 1GHz to 10GHz. The data plots in the EMI section of the Environmental Test Plan contain narrowband and broadband data for each frequency. The data taken with the biconical antenna includes horizontally and vertically polarized antenna data.

3. Discussion Of Results

The performance of the EOA and sensors is good considering that one EOA decodes several types of sensors which vary widely in their optic characteristics. However, the performance of the EOA and sensors is poor when compared to the performance of traditional electrical aircraft sensors and flight control computers. The performance of the EOA with digital sensors is very close to the performance of the traditional electrical sensors, while the performance of the EOA with analog and Time Rate of Decay (TRD) sensors is far below the performance of the traditional electrical sensors.

The EOA produces consistent and stable results when decoding digital sensors. EOA decoding of digital sensors is little affected by noise, is able to overcome some variations in optical code plates, and is not affected by temperature, altitude, or vibration. However, the EOA produces noisy and varied results when decoding analog sensors. EOA decoding of analog sensors is sensitive to variations in power levels, is sensitive to noise, is sensitive to some variations in code plates, and is sensitive to EOA temperature changes. Analog sensor decoding is not affected by altitude or vibration. The EOA produces noisy results when decoding the TRD sensor due to a poor optic source design.

Finally, the EOA fails to meet the electromagnetic interference (EMI) emission limits due to spikes in the data, but the EOA is not an EMI threat to the aircraft since the data outages are few and the majority of the outages are small.

4. Lessons Learned Summary

Electro-Optic Architecture Lessons Learned:

- Need a Flexible EOA Interface Specification, But a Rigid Optical Sensor Interface Specification
- Use a Linear Charge Coupled Device (CCD) Detector Array to Optimize EOA Receiver Speed, Sensitivity, and Decoding Accuracy
- An Optical Spectrum Analyzer with a Digital Signal Processor (DSP) is the Most Efficient and Versatile EOA Approach
- Maximize the Use of "Off-The-Shelf" Hardware

Fiber Optic Sensor Lessons Learned:

- Rotary Optical Sensors are Easier to Build and Use Than Linear Sensors.
- Digital Optical Sensors are Easier to Manufacture Repeatably and Decode Than Analog Sensors
- Repackaging Commercial Sensors for a Military Aircraft Environment is Non-Trivial

The original procurement constraint of "no new technology development" which was levied upon the sensor suppliers, made it impossible for the individual suppliers to agree upon a common ICD format. This resulted in an EOA ICD that was extremely broad in scope in order to accommodate the various existing sensor technologies. The EOA ICD was so broad that it was almost impossible to develop a common EOA implementation using today's technology. Design of the EOA turned out to be one of the most challenging parts of the FOCSI program. This is partly because the EOA was the only component which did not exist in some form prior to the advent of the FOCSI program. The requirement that it deal with wide parameter value ranges greatly increased the difficulty of the EOA development process. In future development programs, the EOA operating parameters should be established **first** and then used to define a single interface specification. Sensor manufacturers have demonstrated great flexibility in tailoring their manufacturing process to accommodate a variety of different optical interfaces.

Digital optical sensors are easier to manufacture repeatably and decode accurately than analog sensors. In every case, the digital sensors were easier to design and build than analog sensors. Testing of the analog sensors showed that they had trouble meeting the specified accuracy requirements. Even the often advertised "infinite resolution" of analog sensors was of no value. First, the resolution is not actually "infinite". Second, the resolution gets lost in the inaccuracies Analog sensor accuracy is only as large as the signal to RMS noise ratio. These problems did not occur for digital sensors. Even where the contrast ratio of digital sensors was a problem, the root of the problem was an incompatibility between the sensor and the EOA. The problem was not inherent in the digital sensor concept.

Rotary optical sensors are easier to build and use than linear sensors for several reasons. The primary reason is that it is easier to design reliable mechanical systems with simple, well characterized, rotary bearings from a catalogue than to design and build custom sliding systems. A second advantage of rotary sensors is that since their internal volume does not change as they operate, the seals to exclude contamination can be very simple. A third advantage is that since rotary sensors do not have any one dimension that is vastly larger or smaller than the other two, they are easier to fit into an aircraft, and they have less trouble with vibration.

Sensor repackaging for military aircraft environment is non-trivial. Numerous difficulties were encountered by the sensor and EOA manufacturers during design, fabrication and assembly to withstand the harsh aircraft environment. Experienced mechanical engineers, even those with limited optics background, seemed to have little trouble understanding that environment and learning the design rules that go with optics. They then had little trouble bridging between the aircraft environment and the optics world. However, experienced optical engineers, even those with experience in mechanics for laboratory optics, had some trouble designing for the aircraft environment. Problems arose in unexpected areas for them, such as designing a case that would retain loose parts in the event of a failure.

5. Summary Of Results

Hardware and software were developed for an optically implemented version of the feedback side of the flight control system of an F-18 aircraft. This development included the design and production of 10 passive optical sensors and associated multiplexed Electro-Optic Architecture (EOA) hardware based on Wavelength Division Multiplexed (WDM) technology. A variety of sensor types (rotary position, linear position, temperature, and pressure) incorporating a broad range of sensor technologies (WDM analog, WDM digital, Analog Microbend, and Fluorescent time rate of decay) were obtained from different manufacturers and functionally integrated with an independently designed EOA. The sensors were built for installation in a variety of aircraft locations, placing the sensors in a variety of harsh environments. The sensors and EOA were designed and built to have the resulting devices be as close as practical to a production system. The integrated system was delivered to NASA for flight testing on a NASA-owned F-18 aircraft.

The Fiber Optic Control Systems for Advanced Aircraft program has been a considerable success at advancing the state of the art for Fly-by-Light technologies, despite the technical problems encountered in building the sensors and EOA. A vast amount of information has been generated concerning the viability of various sensor types for aircraft applications. In addition, considerable knowledge has been generated in how to build systems to operate the sensors. Perhaps the greatest benefit of this program is that at least three of the five contractors have the expertise and are prepared to go ahead with further Fly-by-Light efforts. In addition, one of the remaining contractors is exploring industrial applications of technologies developed as part of the Fiber Optic Control Systems for Advanced Aircraft program.

To summarize the technical results, we determined that rotary optical sensors are easier to build and operate than linear optical sensors; the reverse of what is true with electrical sensors. In addition, we determined that WDM digital sensors are easier to build and operate than WDM analog sensors. Both these results affect the design and use of the EOA as part of the system. In the EOA itself, it has now been shown that a WDM EOA could be built and used, based on technologies available three to four years ago. Progress identified in optical sources, detectors, and digital processors since then will clearly make the task of building an EOA simpler while reducing the cost, size, and weight, and increasing the reliability and performance.

Development and integration testing of the system provided valuable information as to which sensor types were simplest to design and build for a military aircraft environment and which types were simplest to operate with a multiplexed EOA. Not all sensor types met the full range of performance and environmental requirements. Issues in development of the EOA and its limitations in operating the sensors provided information on directions to pursue in future Fly-by-light flight control development programs.